

USNTPS-I-No.3

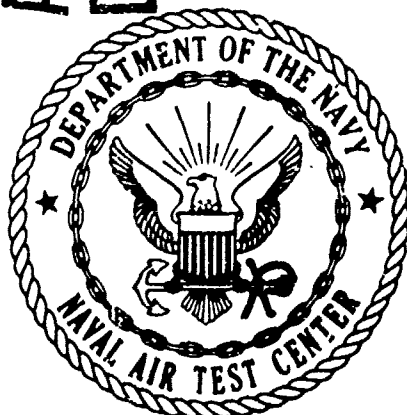
September 1970

(Revised May 1978)

AD No. _____

DDC FILE COPY

AD A 056158

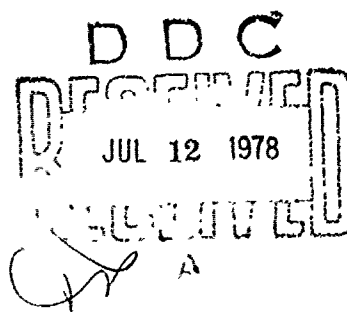


NAVAL TEST PILOT SCHOOL TEXTBOOK

PRINCIPLES OF JET ENGINE OPERATION

BY

JOHN A. MORRISON



DISTRIBUTION STATEMENT A

Approved for public release;
Distribution Unlimited

NAVAL AIR TEST CENTER
PATUXENT RIVER, MARYLAND

78 06 23 510

UNCLASSIFIED

SECURITY CLASSIFICATION OF THIS PAGE (When Data Entered)

REPORT DOCUMENTATION PAGE		READ INSTRUCTIONS BEFORE COMPLETING FORM	
1. REPORT NUMBER	2. GOVT ACCESSION NO.	3. RECIPIENT'S CATALOG NUMBER	
USNTPS-T-No. 3 (14)	USNTPS-T-3		
4. TITLE (and Subtitle)		5. TYPE OF REPORT & PERIOD COVERED	
(C) Principles of Jet Engine Operation, /			
7. AUTHOR(s)		6. PERFORMING ORG. REPORT NUMBER	
(10) John A. Morrison			
9. PERFORMING ORGANIZATION NAME AND ADDRESS		8. CONTRACT OR GRANT NUMBER(s)	
U. S. Naval Test Pilot School Naval Air Test Center Patuxent River, Md 20670		(11) 7-4-71	
11. CONTROLLING OFFICE NAME AND ADDRESS		10. PROGRAM ELEMENT, PROJECT, TASK AREA & WORK UNIT NUMBERS	
Head of Academics U. S. Naval Test Pilot School		(12) 147p.1	
14. MONITORING AGENCY NAME & ADDRESS (if different from Controlling Office)		12. REPORT DATE	
		September 1970	
		13. NUMBER OF PAGES	
		154	
		15. SECURITY CLASS. (of this report)	
		Unclassified	
		15a. DECLASSIFICATION/DOWNGRADING SCHEDULE	
16. DISTRIBUTION STATEMENT (of this Report)			
Approved for public release; distribution unlimited.			
17. DISTRIBUTION STATEMENT (of the abstract entered in Block 20, if different from Report)			
18. SUPPLEMENTARY NOTES			
Revised May 1978			
19. KEY WORDS (Continue on reverse side if necessary and identify by block number)			
Aircraft Engines Jet Engines Thermodynamics			
20. ABSTRACT (Continue on reverse side if necessary and identify by block number)			
<p>This manual is primarily a guide for pilots, Naval Flight officers, and engineers attending the U. S. Naval Test Pilot School. The purpose of this manual is to present the concepts underlying the gas turbine engine, to develop the component characteristics, and to combine the components into an "operating" engine. The configurations considered are the turbojet, the by-pass and the turbo-prop engines.</p>			

8 06 23 510

UNTPS-T-No. 3

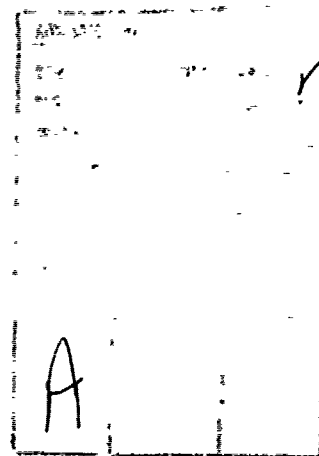
PRINCIPLES OF JET
ENGINE OPERATION

by

JOHN A. MORRISON

September 1970

U. S. NAVAL TEST PILOT SCHOOL TEXTBOOK
NAVAL AIR TEST CENTER



CONTENTS

<u>SUBJECT</u>	<u>PAGE</u>
Introduction	0.1
Cycle Analysis	1.1
Ideal Engine Cycle Analysis	1.1
Component Efficiencies	1.23
Actual Jet Engine Thermodynamic Cycle	1.41
Afterburner Cycle	1.47
Component Performance	2.1
Inlets	2.1
Compressors	2.15
Combustors	2.33
Turbines	2.43
Nozzles	2.49
The Complete Engine	3.1
Matching	3.1
Engine Performance	3.23
Thrust Determination	3.27
Afterburner Operation	3.29

SECTION 0

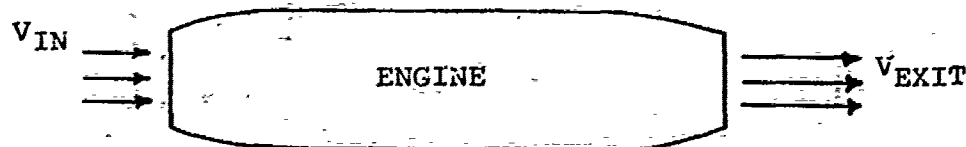
INTRODUCTION

The gas generator has replaced almost completely the internal combustion engine as a source of propulsive power in military aircraft. A basic understanding of the principles of operation of the gas generator and the other elements of the aircraft propulsive system is essential to proper understanding of test techniques and results. The purpose of this manual, therefore, is to present the underlying concepts of the turbine engine, to develop the component characteristics, and to combine the components into an "operating" engine.

For purposes of this text, aircraft turbine power plants are grouped into three general categories: the pure turbojet, the turbo-prop, and the by-pass engine. Basically, thrust is produced by these engines as follows.

Pure Jet

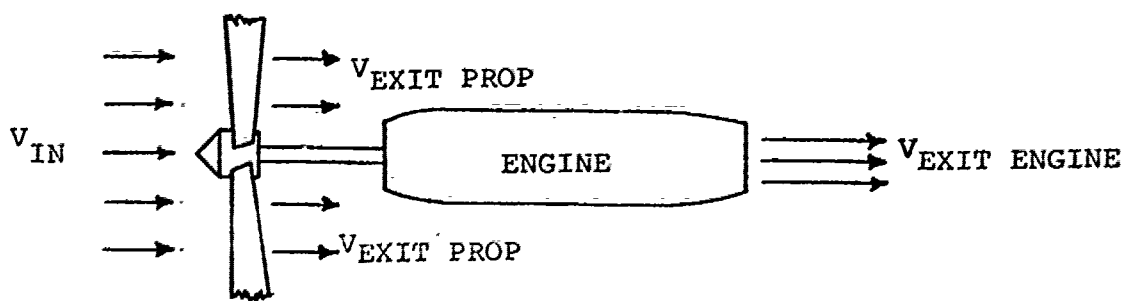
In the pure jet, depicted in Figure 0.1, air is admitted at some velocity and discharged at a velocity higher than that at which it entered. This change in velocity (momentum) produces a thrust. The mechanism within the engine produces the change and, by means of a fuel control, the pilot controls the engine.



PURE JET ENGINE
FIGURE 0.1

Turbo-Prop

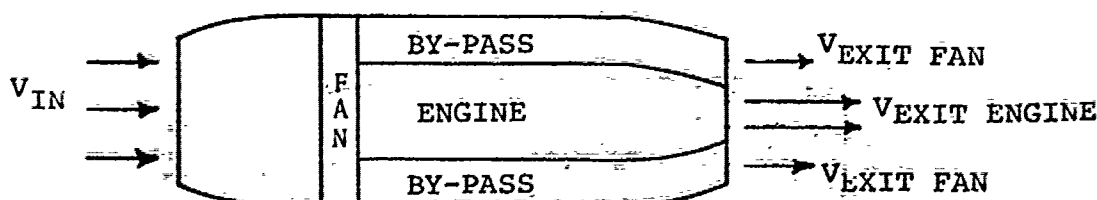
Figure 0.2 shows a typical turbo-prop. Air enters the engine at some energy level and emerges at a higher energy level much like the pure jet. Some of the energy, produced by burning fuel within the engine, is extracted and used to drive the propeller. Thrust is produced, not only by changing the momentum of the air through the engine, but also by increasing the momentum of the air through the propeller. The thrust produced by the propeller is approximately 90% of the total thrust.



TURBO-PROP ENGINE
FIGURE 0.2

By-Pass

The by-pass engine configuration can take several shapes; one of which is shown by Figure 0.3.



BY-PASS ENGINE
FIGURE 0.3

The by-pass engine (sometimes referred to as a turbofan) can be considered a ducted turbo-prop. The engine once again increases the velocity of the main air stream and also drives a "fan" which increases the velocity of the by-pass air. Once again the pilot has control over the magnitude of the velocity increases.

Common to all three power plants is the gas generator, the compressor-combustor-turbine. In order to understand the operation of these engines, the analysis will focus on the development of the simple turbojet from which the turbo-prop and turbofan engines evolve. The principles of turbojet operation are then easily extended to the other two engines. This application, however, will not be covered in this manual.

The basic analysis will assume two dimensional, steady, compressible flow. Most engine operation occurs under steady flow conditions, however,

transients will be considered and discussed where appropriate. An understanding of basic thermodynamics is assumed. The equations to be utilized from this discipline are listed in Appendix AI along with the assumptions. Reference to these equations will be made from time to time.

Section I will concern itself with the jet engine thermodynamic cycle. From this analysis will emerge a glimpse as to how a design engineer looks at the engine. Part of this section will be devoted to component efficiencies which will then permit a comparison of the ideal process to an actual cycle, based on arbitrarily chosen component efficiencies. Ideal, as used in this text, permits variable specific heats with no losses.

Following the cycle analysis, will be a detailed discussion on the design of inlets, compressors, combustors, turbines and nozzles. The main concern of Section II is to show that each component has an optimum operating condition or design point, and that, in order to maintain adequate operation throughout its operating range, the engine may require special devices such as variable geometry or pressure bleed valves. It is not intended for this section to be design oriented but rather a presentation of the basic design philosophy so that, for example, the use of a compressor with bleed valves or a nozzle that converges then diverges become logical consequences.

Following in Section III, all the components will be combined to produce a matched engine. This is probably the single most important concept to understand, because it is here that the mysticism of the jet engine is eliminated. After this procedure, the subject of engine control will be discussed along with performance calculations.

To summarize then, the main purpose of this manual is to present, to test pilots, the operation of the components of a turbojet engine such that the combined operation is logical and easily analyzed. The thermodynamic cycle analysis is presented only to show the effects of the main design variables.

SECTION 1

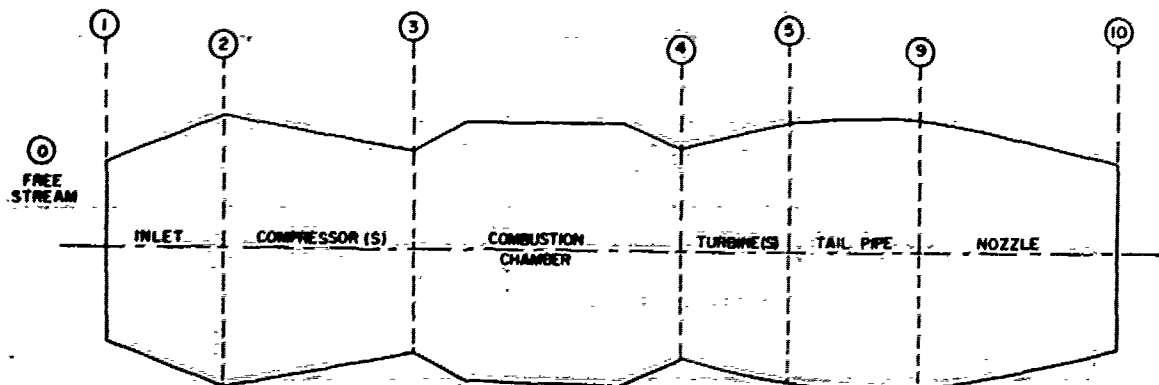
CYCLE ANALYSIS

1.1 IDEAL ENGINE CYCLE ANALYSIS

The purpose of this section is to present the ideal thermodynamic cycle of a pure turbojet engine. From this analysis will come the main variables which affect the engine performance. It will be seen that these are the design variables for the basic jet engine.

All of the equations that will be utilized have been presented in the Thermodynamics course. To understand the operation of a turbojet engine, it is imperative that the basic equations are thoroughly understood since the jet engine operating equations are merely an orderly combination of the basics.

Figure 1.1 shows the engine station terminology that will be used throughout this text. It is the designation normally utilized for a single spool (single compressor-single turbine) turbojet engine. Using this Figure and the equations derived in Thermodynamics, Table 1.1 can be formulated. This table lists the functions of each engine component along with the thermodynamic equation representing each component. From this table, the jet engine cycle is graphically constructed and is shown by the h-s plots for non-afterburning (Figure 1.2a) and afterburning (Figure 1.2b) engines.



NOTE:

THE STATION NUMBERS SHOWN ARE THOSE GENERALLY GIVEN FOR A SINGLE SPOOL TURBOJET

ENGINE STATION DESIGNATIONS

FIGURE 1.1

TABLE 1.1

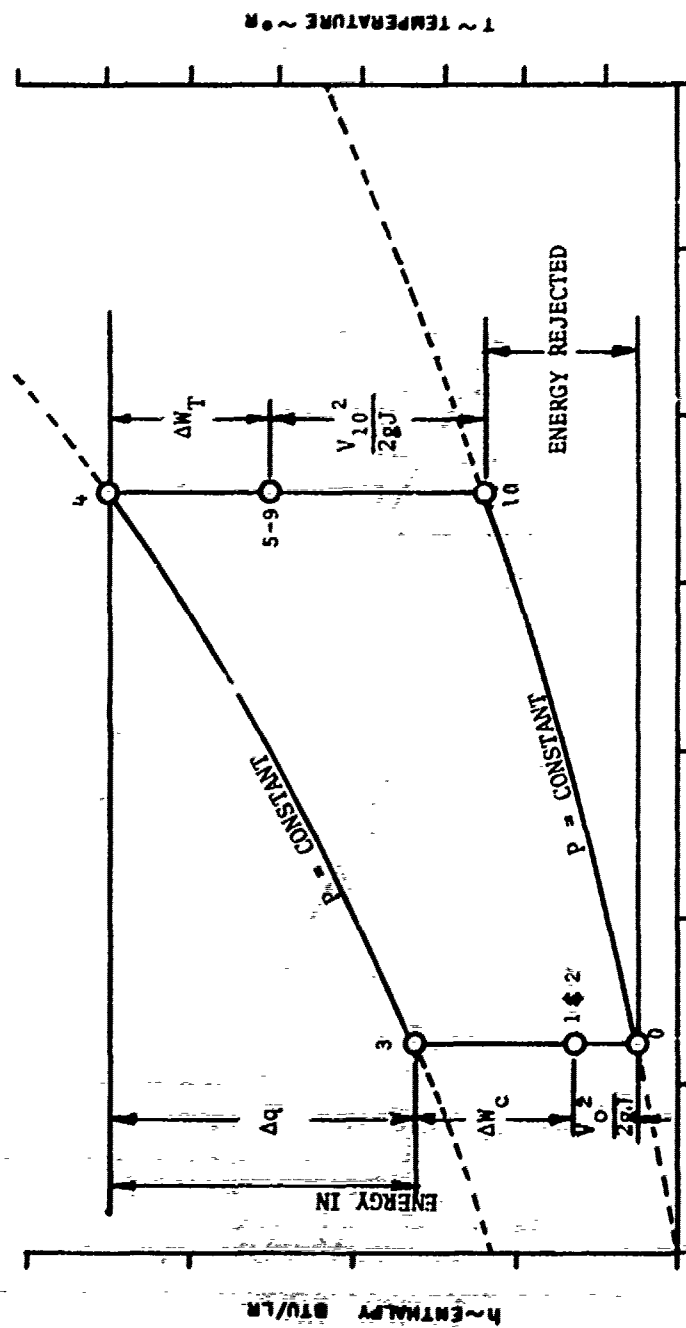
IDEAL TURBO JET COMPONENT PROCESSES AND EQUATIONS

STATION NUMBER	NAME	PURPOSE	IDEAL PROCESS	IDEAL EQUATIONS (1)
0	FREESTREAM			
0-1	AERODYNAMIC INLET	ACCEL. OR DECEL. AIR TO VELOCITY AT INLET FACE	ISENTROPIC NO WORK	$h_{T_0} = h_{T_1}$ $h_0 + \frac{V_0^2}{2gJ} = h_1 + \frac{V_1^2}{2gJ}$
1	INLET FACE			
1-2	GEOMETRIC INLET	ACCEL. OR DECEL. AIR TO VELOCITY AT COMPRESSOR FACE	ISENTROPIC NO WORK	$h_{T_1} = h_{T_2}$ $h_1 + \frac{V_1^2}{2gJ} = h_2 + \frac{V_2^2}{2gJ}$
2	COMPRESSOR FACE			
2-3	COMPRESSOR	INCREASE THE TOTAL PRESSURE OF THE FLOW	ISENTROPIC WITH WORK	$h_{T_2} = h_{T_3} + \Delta w_c$ $h_2 + \frac{V_2^2}{2gJ} = h_3 + \frac{V_3^2}{2gJ} + \Delta w_c$
3	COMBUSTOR FACE			
3-4	COMBUSTOR	INCREASE THE TOTAL ENERGY OF THE FLOW	CONSTANT PRESSURE COMBUSTION	$h_{T_3} + \Delta q = h_{T_4}$ $h_3 + \frac{V_3^2}{2gJ} + \Delta q = h_4 + \frac{V_4^2}{2gJ}$
4	TURBINE INLET			
4-5	TURBINE	EXTRACT WORK TO DRIVE THE COMPRESSOR (2)	ISENTROPIC WITH WORK	$h_{T_4} = h_{T_5} + \Delta w_T$ $h_4 + \frac{V_4^2}{2gJ} = h_5 + \frac{V_5^2}{2gJ} + \Delta w_T$
5	TAILPIPE ENTRY			
5-9a	TAILPIPE (NON-A/B)	DELIVER GAS TO THE NOZZLE	ISENTROPIC NO WORK	$h_{T_5} = h_{T_9}$
5-9b	TAILPIPE AFTERBURNER	INCREASE THE TOTAL ENERGY OF THE FLOW	CONSTANT PRESSURE COMBUSTION	$h_{T_5} + \Delta q = h_{T_9}$ $h_5 + \frac{V_5^2}{2gJ} + \Delta q = h_9 + \frac{V_9^2}{2gJ}$
9	NOZZLE ENTRANCE			
10	NOZZLE DISCHARGE	INCREASE KINETIC ENERGY OF GAS	ISENTROPIC EXPANSION TO AMBIENT PRESSURE NO WORK	$h_{T_9} = h_{T_{10}}$ $h_9 + \frac{V_9^2}{2gJ} = h_{10} + \frac{V_{10}^2}{2gJ}$

NOTES:

- (1) REFER TO APPENDIX A1-1
 (2) IN AN ACTUAL ENGINE THE TURBINE ALSO MUST DRIVE ACCESSORIES.

IDEAL TURBO JET ENGINE CYCLE H-S DIAGRAM (NON-AFTERBURNING)



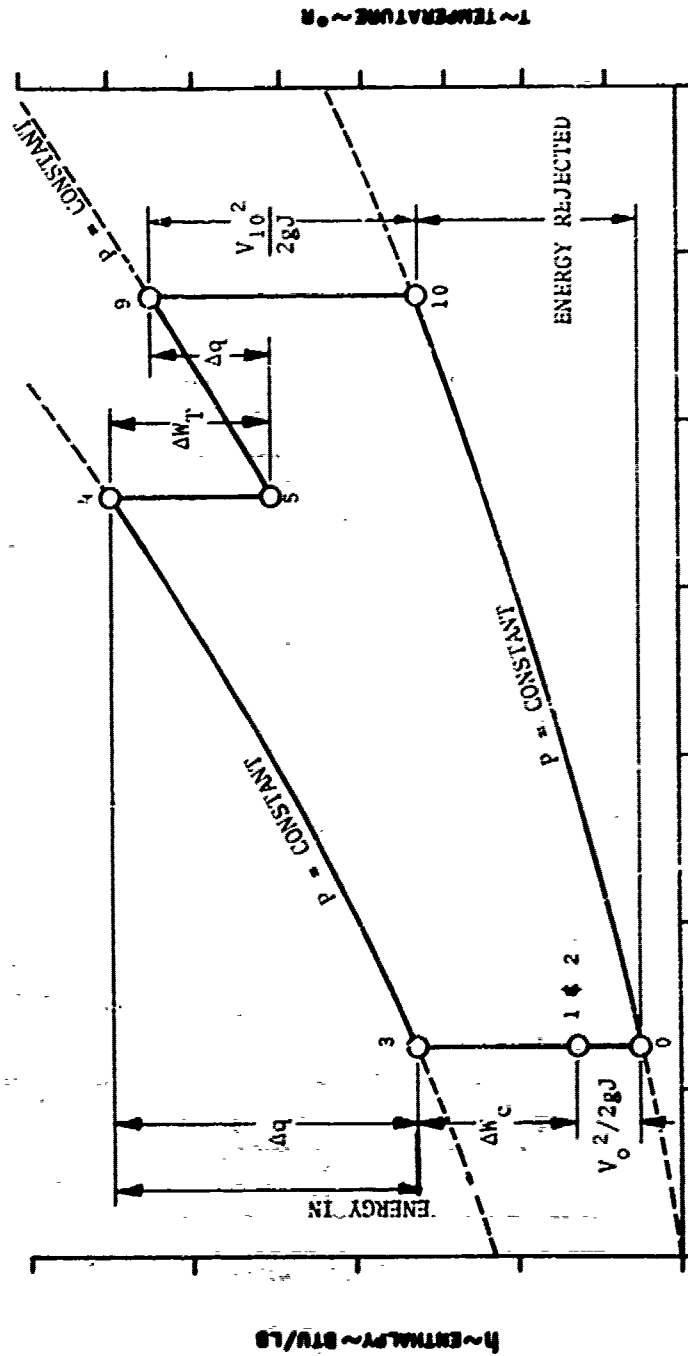
s ~ ENTROPY ~ BTU/LB °R

NOTE: NUMBERS INDICATE ENGINE STATION NUMBER

FIGURE 1.2a

IDEAL TURBO JET ENGINE CYCLE H-S DIAGRAM

(AFTERSBURNING)



$s \sim \text{ENTROPY} \sim \text{BTU/LB} \cdot \text{R}$

NOTES: NUMBERS INDICATE ENGINE STATION NUMBER

ΔW_T AND $V_{10}^2/2gJ$ REPRESENT ENERGY OUT

FIGURE 1.2b

CYCLE THERMAL EFFICIENCY

The non-afterburning thermal efficiency of the ideal jet engine cycle is defined as follows:

$$\eta_{TH} \equiv \frac{\text{ENERGY IN} - \text{ENERGY OUT}}{\text{ENERGY IN}}$$

From Figure 1.2a:

$$\eta_{TH} = \frac{(h_{T_4} - h_{T_3}) - (h_{10} - h_0)}{(h_{T_4} - h_{T_3})} = 1 - \frac{h_{10} - h_0}{h_{T_4} - h_{T_3}} \quad (1.1)$$

If C_p is assumed constant (perfect gas) to illustrate prime variables:

$$\eta_{TH} = 1 - \frac{T_{10} - T_0}{T_{T_4} - T_{T_3}} \quad (\text{ref. A1-2})$$

Factoring out T_0 and T_{T_3} yields:

$$\eta_{TH} = 1 - \frac{T_0}{T_{T_3}} \frac{\left(\frac{T_{10}}{T_0} - 1\right)}{\left(\frac{T_{T_4}}{T_{T_3}} - 1\right)} \quad (1.2)$$

The process from freestream to the entrance to the combustor is isentropic as is the process from the turbine inlet to the nozzle exit. Thus, the following can be written:

$$\left(\frac{P_{T_3}}{P_0}\right)^{\frac{\gamma-1}{\gamma}} = \frac{T_{T_3}}{T_0} \quad \text{and} \quad \left(\frac{P_{T_4}}{P_{10}}\right)^{\frac{\gamma-1}{\gamma}} = \frac{T_{T_4}}{T_{10}} \quad (\text{ref. A1-3})$$

But $P_{T_4} = P_{T_3}$ and $P_{10} = P_0$ for the ideal cycle, thus:

$$\frac{T_{T_3}}{T_0} = \frac{T_{T_4}}{T_{10}} \quad \text{or} \quad \frac{T_{10}}{T_0} = \frac{T_{T_4}}{T_{T_3}}$$

Substituting into (1.2):

$$\eta_{TH} = 1 - \frac{1}{T_{T3}/T_0} = 1 - \frac{1}{\left(P_{T3}/P_0\right)^{\frac{\gamma-1}{\gamma}}} \quad (1.3)$$

For a perfect gas ($C_p = \text{constant}$), the ideal thermal efficiency is solely a function of the cycle pressure ration, P_{T3}/P_0 . Now the cycle pressure ratio can be written as:

$$\frac{P_{T3}}{P_0} = \left(\frac{P_{T3}}{P_{T2}}\right) \left(\frac{P_{T2}}{P_{T0}}\right) \left(\frac{P_{T0}}{P_0}\right)$$

Where: P_{T3}/P_{T2} is the compressor ratio,

P_{T2}/P_{T0} is the total pressure ratio across the inlet (unity for the ideal cycle),

P_{T0}/P_0 is uniquely a function of the Mach number (A1-4).

Therefore, (1.3) can be written as:

$$\eta_{TH} = 1 - \frac{1}{\left(\frac{P_{T3}}{P_{T2}} \times \frac{P_{T0}}{P_0}\right)^{\frac{\gamma-1}{\gamma}}} \quad (1.4)$$

The significance of this equation is that the thermal efficiency is now shown to be a function of two design variables, compressor pressure ratio and Mach number. The efficiency increases with an increase in either parameter. Figure 1.3 shows this variation for two altitudes and two Mach numbers. These plots were computed using (1.1) which accounts for the variation in C_p with temperature (no adjustment was made for the variation of C_p with fuel air ratios). The calculation was performed on a digital computer, using the outline in Appendix 2. Because (1.1) was used to compute Figure 1.3, turbine inlet temperature (T_{T4}) had to be specified to compute enthalpy. Turbine inlet temperature, like compressor pressure ratio, is a design variable. It is seen that the thermal efficiency decreases slightly with increasing turbine inlet temperature. Table 1.2 summarizes the Figure.

IDEAL TURBO JET THERMAL EFFICIENCY

MACH No. = 0 HP = SEA LEVEL

STANDARD DAY

TURBINE INLET
TEMPERATURE

2000°R
3000°R

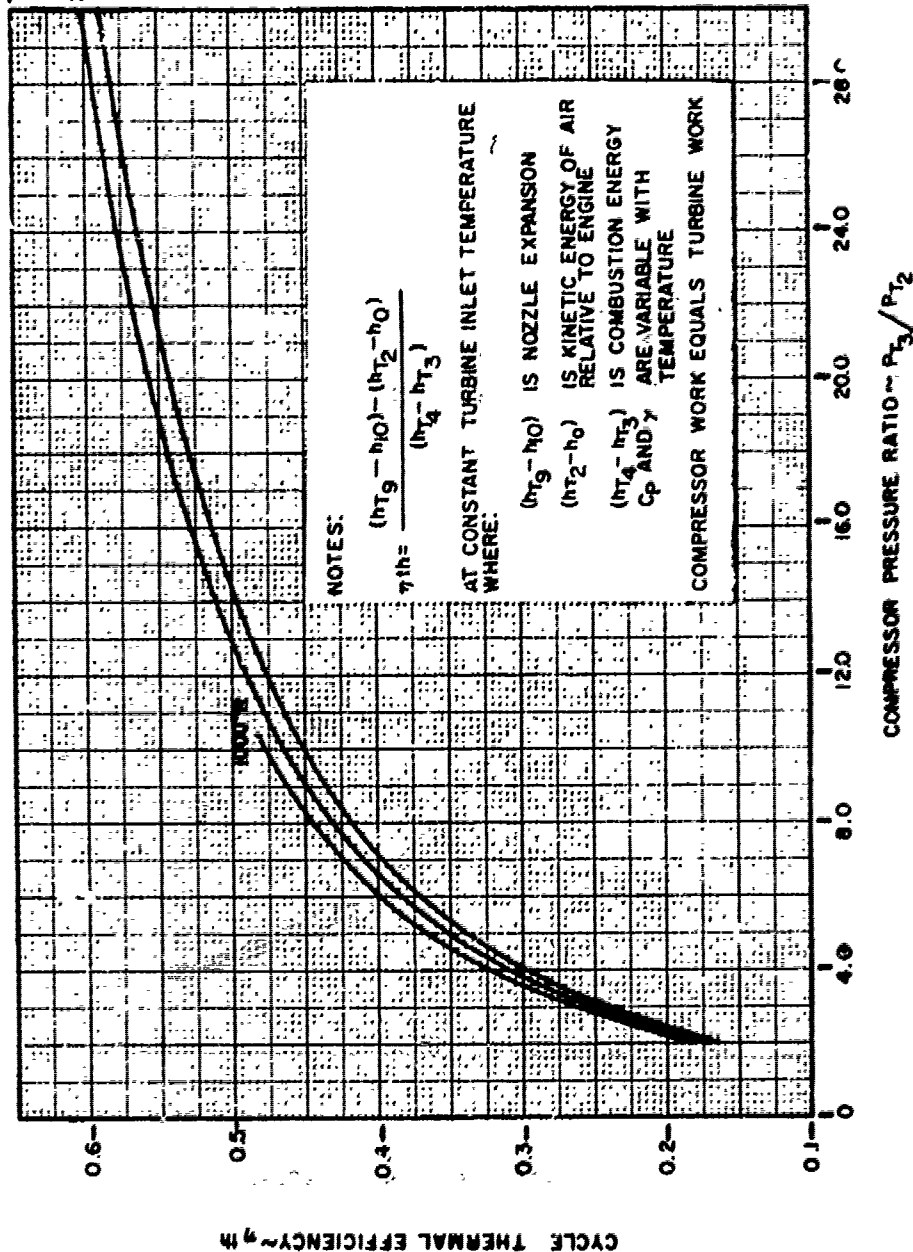


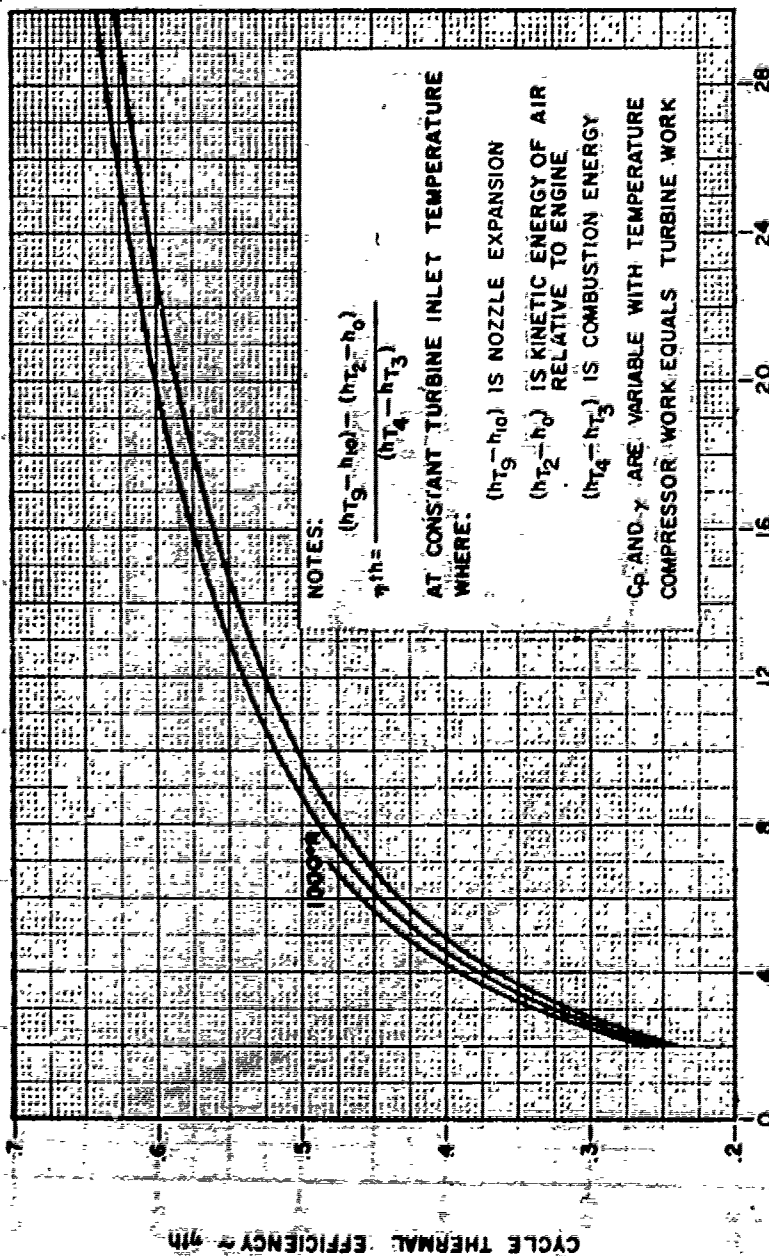
FIGURE 1.3a

IDEAL TURBO JET THERMAL EFFICIENCY

MACH No = 0.75 HP = SEA LEVEL

STANDARD DAY

TURBINE
INLET
TEMP
2000°R
3000°R



COMPRESSOR PRESSURE RATIO ~ PT3/PT2

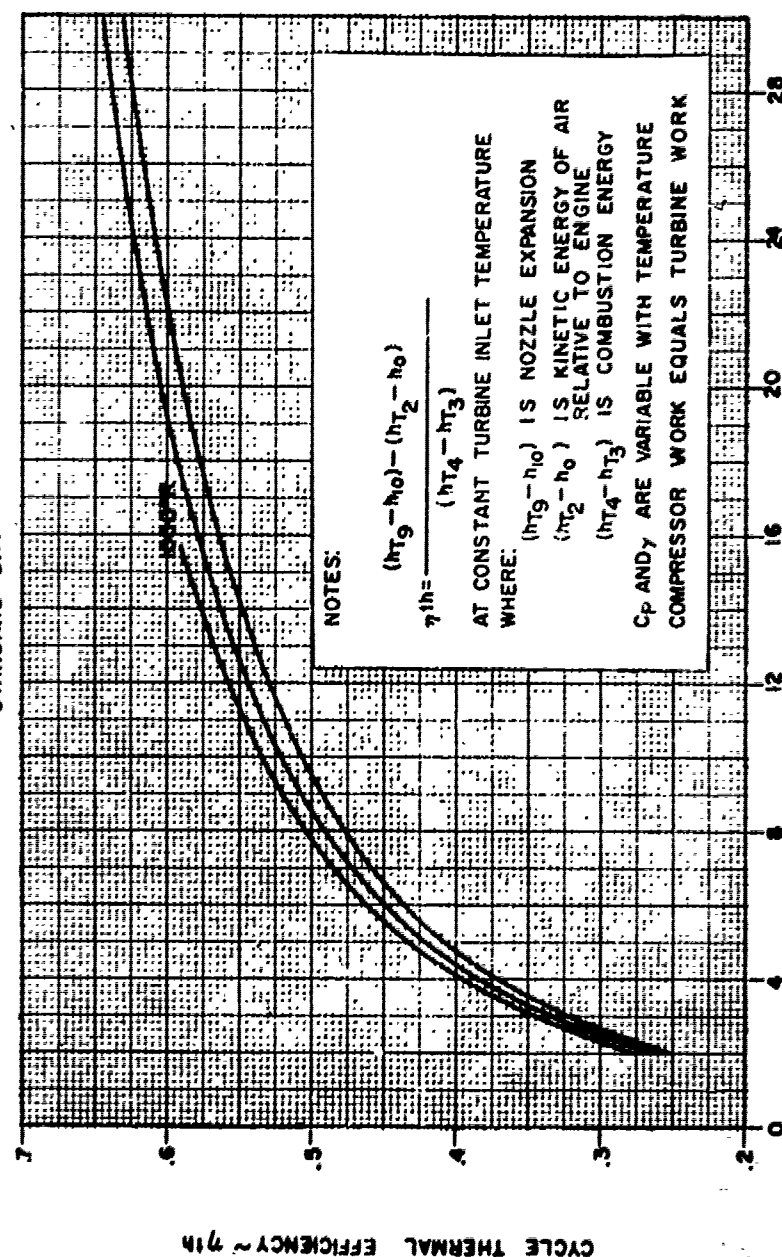
FIGURE 1-3b

IDEAL TURBO JET THERMAL EFFICIENCY

MACH $M_0 = 0.75$ $h_P = 30,000$ FT

STANDARD DAY

TURBINE
INLET
TEMP
2000°R
3000°R



COMPRESSOR PRESSURE RATIO $\sim P_{T3}/P_{T2}$

FIGURE 1.5c

TABLE 1.2

SUMMARY OF FIGURE 1.3

Variable (1)	η_{TH}
INC P_{T_3} / P_{T_2}	INC
INC T_{T_4}	DEC (Slightly) ⁽²⁾
INC M	INC
INC ALTITUDE (DEC T_0)	INC (Slightly) ⁽²⁾

Notes: (1) All other variables constant.

(2) This effect is due only to the effect of C_p being a function of temperature.

It is seen on Figure 1.3 that the equation for thermal efficiency is:

$$\eta_{TH} = \frac{(h_{T_9} - h_{10}) - (h_{T_2} - h_0)}{h_{T_4} - h_{T_3}} \quad (1.5)$$

This equation is identical to (1.1) since:

$$W_c = W_T$$

$$h_{T_3} - h_{T_2} = h_{T_4} - h_{T_5} = h_{T_4} - h_{T_9}$$

Substituting this into (1.1) and rearranging yields (1.5). The significance of (1.5) is that $(h_{T_9} - h_{10})$ is the kinetic energy of the exiting gasses ($V_{10}^2/2gJ$) and $(h_{T_2} - h_0)$ is the kinetic energy of the approaching air ($V_0^2/2gJ$). Thus the thermal efficiency is a measure how the heat energy is transformed into a change in the kinetic energy of the air.

The afterburning cycle will be presented in Section 1.3.

NET THRUST PER UNIT MASS FLOW

The ideal net thrust of a turbojet engine is given by:

$$F_N = \frac{W_a}{g} (V_{10} - V_0) \quad (A1-5)$$

$$\text{or } F_N / \frac{W_a}{g} = V_{10} - V_0 \quad (1.6)$$

$$\text{Since } \frac{(V_{10}^2 - V_0^2)}{2gJ} = (h_{T_9} - h_{10}) - (h_{T_0} - h_0) \quad (1.7)$$

$$\text{and } h_{T_9} = h_{T_5} \text{ (Non A/B),}$$

$$h_{T_2} = h_{T_0} \quad \text{and}$$

$$W_T = (h_{T_4} - h_{T_5}) = (h_{T_3} - h_{T_2}) = W_C$$

$$\text{Then } \frac{(V_{10}^2 - V_0^2)}{2gJ} = (h_{T_4} - h_{10}) - (h_{T_3} - h_0)$$

$$\text{or } V_{10} = \left\{ [2gJ] \left[(h_{T_4} - h_{10}) - (h_{T_3} - h_0) \right] + V_0^2 \right\}^{1/2}$$

Substituting this into (1.6) yields:

$$F_N / \frac{W_a}{g} = \left\{ [2gJ] \left[(h_{T_4} - h_{10}) - (h_{T_3} - h_0) \right] + V_0^2 \right\}^{1/2} - V_0 \quad (1.8)$$

If $C_p = \text{constant}$ and T_{T_4} and T_0 are factored out,

$$F_N / \frac{W_a}{g} = \left\{ [2gJ C_p] \left[T_{T_4} \left(1 - \frac{T_{10}}{T_{T_4}} \right) - T_0 \left(\frac{T_{T_3}}{T_0} - 1 \right) \right] + V_0^2 \right\}^{1/2} - V_0$$

$$\text{But } \frac{T_{T_4}}{T_{10}} = \left(\frac{P_{T_4}}{P_{10}} \right)^{\frac{\gamma-1}{\gamma}} \quad (\text{Isentropic})$$

$$\frac{T_{T_3}}{T_0} = \left(\frac{P_{T_3}}{P_0} \right)^{\frac{\gamma-1}{\gamma}} \quad (\text{Isentropic})$$

$$\text{and } P_{T_3} = P_{T_4} \quad (\text{ideal process})$$

$$P_0 = P_{10} \quad (\text{ideal process})$$

Substituting these into the above yields:

$$F_N / \frac{W_a}{g} = \sqrt{2gJ C_p \left\{ T_{T_4} \left[1 - \left(\frac{P_0}{P_{T_3}} \right)^{\frac{\gamma-1}{\gamma}} \right] - T_0 \left[\left(\frac{P_{T_3}}{P_0} \right)^{\frac{\gamma-1}{\gamma}} - 1 \right] \right\} + V_0^2 - V_0^2} \quad (1.9)$$

For the ideal cycle,

$$\frac{P_{T_3}}{P_0} = \frac{P_{T_3}}{P_{T_2}} \times \frac{P_{T_0}}{P_0} \quad (\text{see page 1.3})$$

It is seen, therefore, that the net thrust per unit mass flow is a function of turbine inlet temperature, altitude (through T_0), compressor pressure ratio and Mach number (through P_{T_0}/P_0 and V_0). All of the above parameters are those which would be at the control of the design engineer. Figure 1.4 shows the variation of net thrust per unit mass flow for each of the control variables. Consistent with the way the thermal efficiency was presented (variable C_p), (1.8) was utilized for the calculation (Appendix 2). Table 1.3 summarizes the effects:

TABLE 1.3

SUMMARY OF FIGURE 1.4

Variable	$F_N / \frac{W_a}{g}$
INC P_{T_3} / P_{T_2}	OPTIMUM
INC T_{T_4}	INC
INC M	DEC
INC ALTITUDE (DEC T_0)	INC

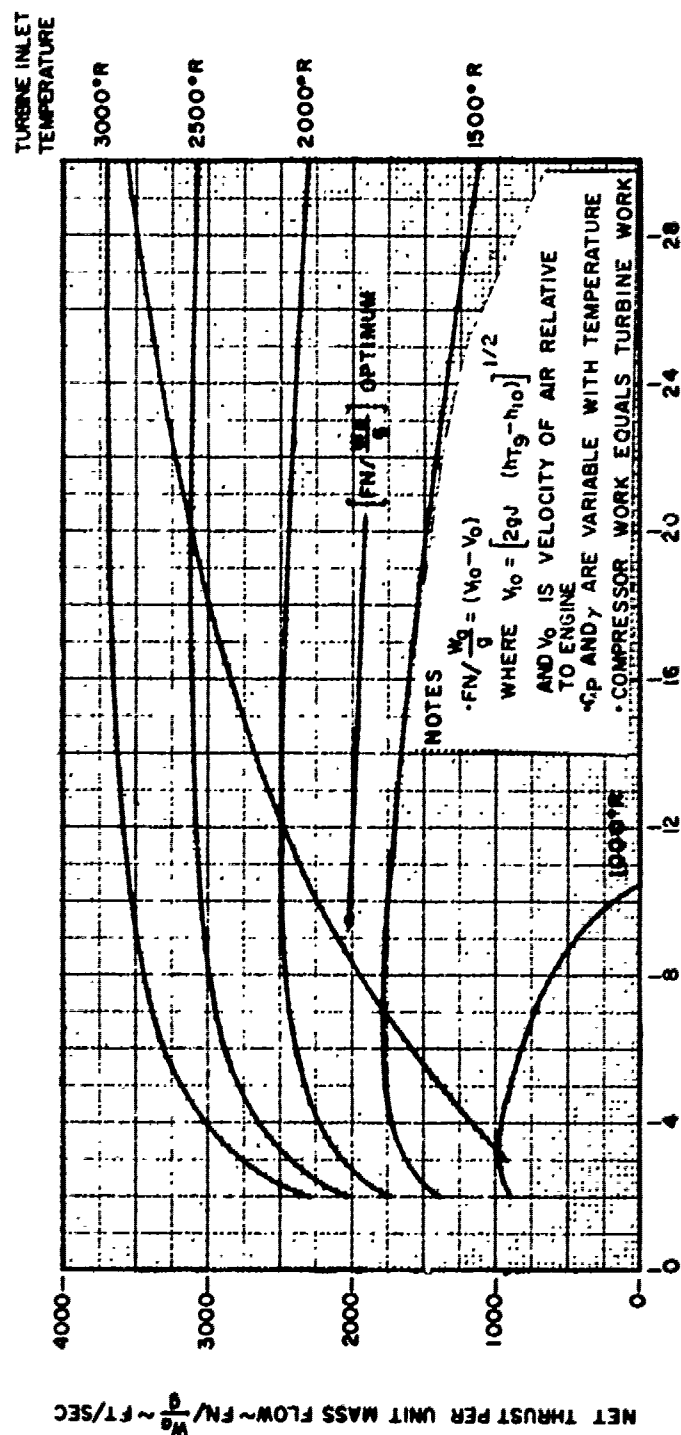
To fully appreciate the results, it must be understood that the variations tabulated above are valid only with all other variables held constant. Thus, the increase in $F_N / \frac{W_a}{g}$ with altitude does not mean an increase in net thrust. The net thrust actually decreases with increasing altitude because the airflow through the engine decreases.

A particular variable of interest is Mach number; the decrease in $F_N / \frac{W_a}{g}$ with increasing M_0 , is primarily due to the increase in V_0 which is the ram drag per unit mass flow. If this term is deducted from the $F_N / \frac{W_a}{g}$, the gross thrust per unit mass flow would result. This term will increase with increasing Mach number.

IDEAL TURBO JET NET THRUST

MACH No=0 HP=SEA LEVEL

STANDARD DAY



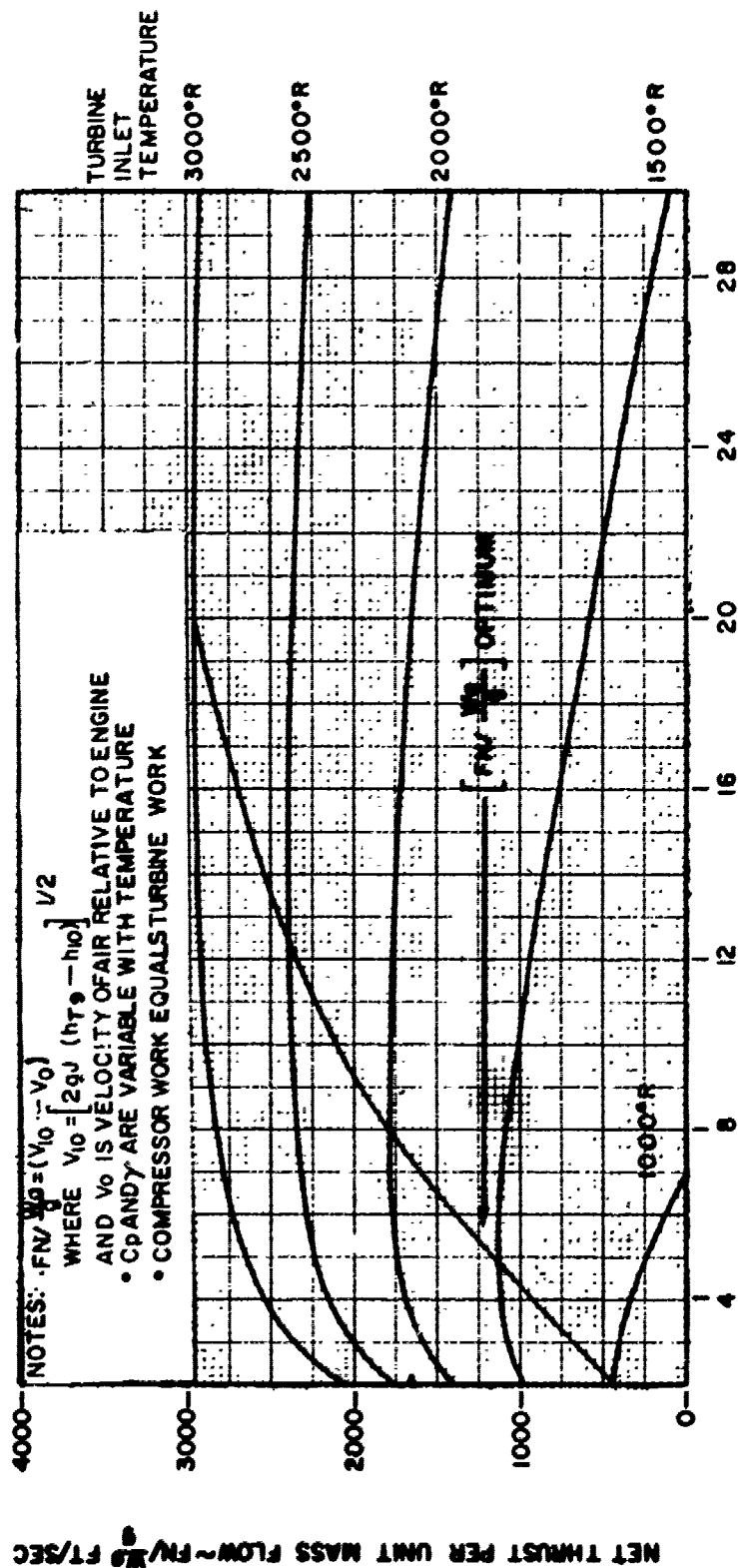
COMPRESSOR PRESSURE RATIO~PT3/PT2

FIGURE 1.4a

IDEAL TURBO JET THRUST

MACH No. = 0.75 HP = SEA LEVEL

STANDARD DAY



COMPRESSOR PRESSURE RATIO ~ PT3/PT2

FIGURE 1.4b

IDEAL TURBO JET THRUST

MACH No. = 0.75 NP = 30,000 FT

STANDARD DAY

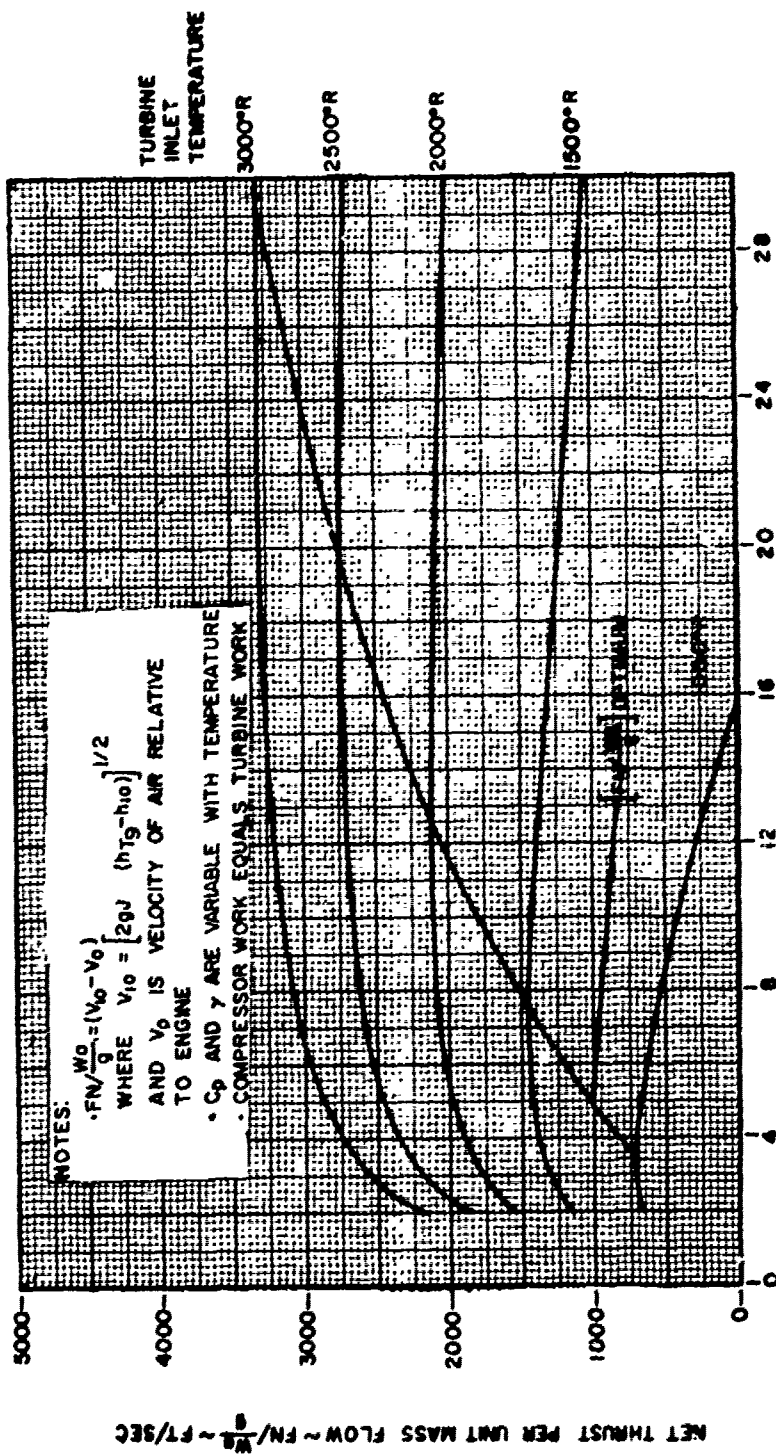


FIGURE 1.4c

THRUST SPECIFIC FUEL CONSUMPTION - TSFC (or SFC)

The fuel consumption of an engine is usually given in terms of the amount of fuel required to produce a given amount of thrust. It is the key parameter for comparing engines. For example, a specific flight condition for any given aircraft produces a drag which the engine(s) must overcome. If at the same flight conditions, engine "A" has better SFC (lower) than engine "B", it will give better range, or require less fuel than engine "B", since both engines must develop the same thrust.

Thrust specific fuel consumption is defined as:

$$\text{TSFC} \equiv \frac{W_f}{F_N} \quad \frac{\text{LBS/HR}}{\text{LB}} \quad (1.10)$$

To expand this (refer to Table 1.1 and Figure 1.2a)

$$h_{T_4} - h_{T_3} = \Delta q \sim \frac{\text{BTU}}{\text{LB (gas)}}$$

$$\Delta Q = \Delta q (W_a + W_f) \sim \frac{\text{BTU}}{\text{SEC}}$$

Thus

$$\Delta Q = (h_{T_4} - h_{T_3}) W_a \left(1 + \frac{W_f}{W_a} \right)$$

Now

$$\frac{W_f}{W_a} < .02 \text{ for most jet engines.}$$

Thus

$$\Delta Q \approx (h_{T_4} - h_{T_3}) W_a \quad (1.11)$$

The heating value (H.V.) of the fuel is the amount of thermal energy released per pound of fuel consumed. Therefore:

$$\Delta Q = \text{H.V.} (W_f) \sim \frac{\text{BTU}}{\text{SEC}}$$

Equating this to (1.11):

$$(h_{T_4} - h_{T_3}) W_a = \text{H.V.} (W_f)$$

or

$$\frac{W_f}{W_a} = \frac{h_{T_4} - h_{T_3}}{\text{H.V.}} \quad (1.12)$$

Dividing the right-hand side of (1.10) by W_a/g yields:

$$\text{TSFC} = \frac{W_f / (W_a/g)}{F_N / (W_a/g)} \times 3600$$

or

$$\text{TSFC} = \frac{(h_{T_4} - h_{T_3}) g}{\text{H.V. } F_N / (W_a/g)} \times 3600 \quad (1.13)$$

If $C_p = \text{constant}$

$$\text{TSFC} = \frac{C_p (T_{T_4} - T_{T_3}) g}{\text{H.V. } F_N / (W_a/g)} \times 3600 \quad (1.14)$$

From (1.14), it is seen that TSFC is a function of the same variables as $F_N / (W_a/g)$ since the total compressor discharge temperature is established by compressor pressure ratio, altitude, and Mach number. The effects of these variables on TSFC, shown in Figure 1.5, were calculated from (1.13) which assumes a variable C_p (Appendix 2).

Figure 1.5 appears to be an inverse of thermal efficiency (Figure 1.3). Upon examination of the equations, the reason for this inverse similarity becomes apparent. The numerator of (1.13) is identical to the denominator of (1.5) and the denominator of (1.13) is a function of the quantity $(V_{10} - V_0)$ while the numerator of (1.5) is a function of $(V_{10}^2 - V_0^2)$. This similarity is also evident in comparing Table 1.2 with Table 1.4 below.

TABLE 1.4

SUMMARY OF FIGURE 1.5

Variable	TSFC
INC P_{T_3} / P_{T_2}	DEC
INC T_{T_4}	INC
INC M	INC (SLIGHTLY)*
INC ALTITUDE (DEC T_0)	DEC (SLIGHTLY)

*This effect is not the inverse of η_{TH} , due to the difference in $(V_{10} - V_0)$ terms.

Comparing Figure 1.4 with Figure 1.5 shows that increasing thrust by increasing turbine inlet temperature increases the TSFC (lower efficiency). Further, the optimum compressor pressure ratio for maximum thrust is lower than the optimum for TSFC. The point to be made is that the selection of an operating point is a compromise. In fact, each design point of every engine component is a compromise within itself. This sometimes produces problems which must be overcome. Section 2 will discuss off design operation in detail.

Digressing to Figure 1.3, it is seen that the thermal efficiency curve for a turbine inlet temperature of 1000°R terminates at some pressure ratio. Looking at Figure 1.4, the terminal pressure ratio corresponds to a net thrust of zero. A check of the cycle on an h - s diagram will show that the compressor discharge temperature is 1000°R and fuel flow is zero. Thus the value of η_{TH} shown on Figure 1.3 is the limiting case as both numerator and denominator approach zero. A fictitious efficiency could be computed above this pressure ratio but the thrust would be negative and $T_3 > T_4$.

There is one remaining observation worthy of recognition. Looking at Figure 1.4 (a & b), the optimum compressor pressure ratio (turbine inlet temperature constant) for maximum thrust decreases for increasing Mach number. The limiting case is $P_{T3}/P_{T2} = 1.0$. This engine is called a ram jet.

Further ideal cycle analysis is not warranted to satisfy the purpose of this manual. Additional detailed discussion on these and other efficiencies can be obtained from numerous references to which the reader is referred.

IDEAL TURBO JET THRUST SPECIFIC FUEL CONSUMPTION

MACH No. = 0 MP = SEA LEVEL
STANDARD DAY

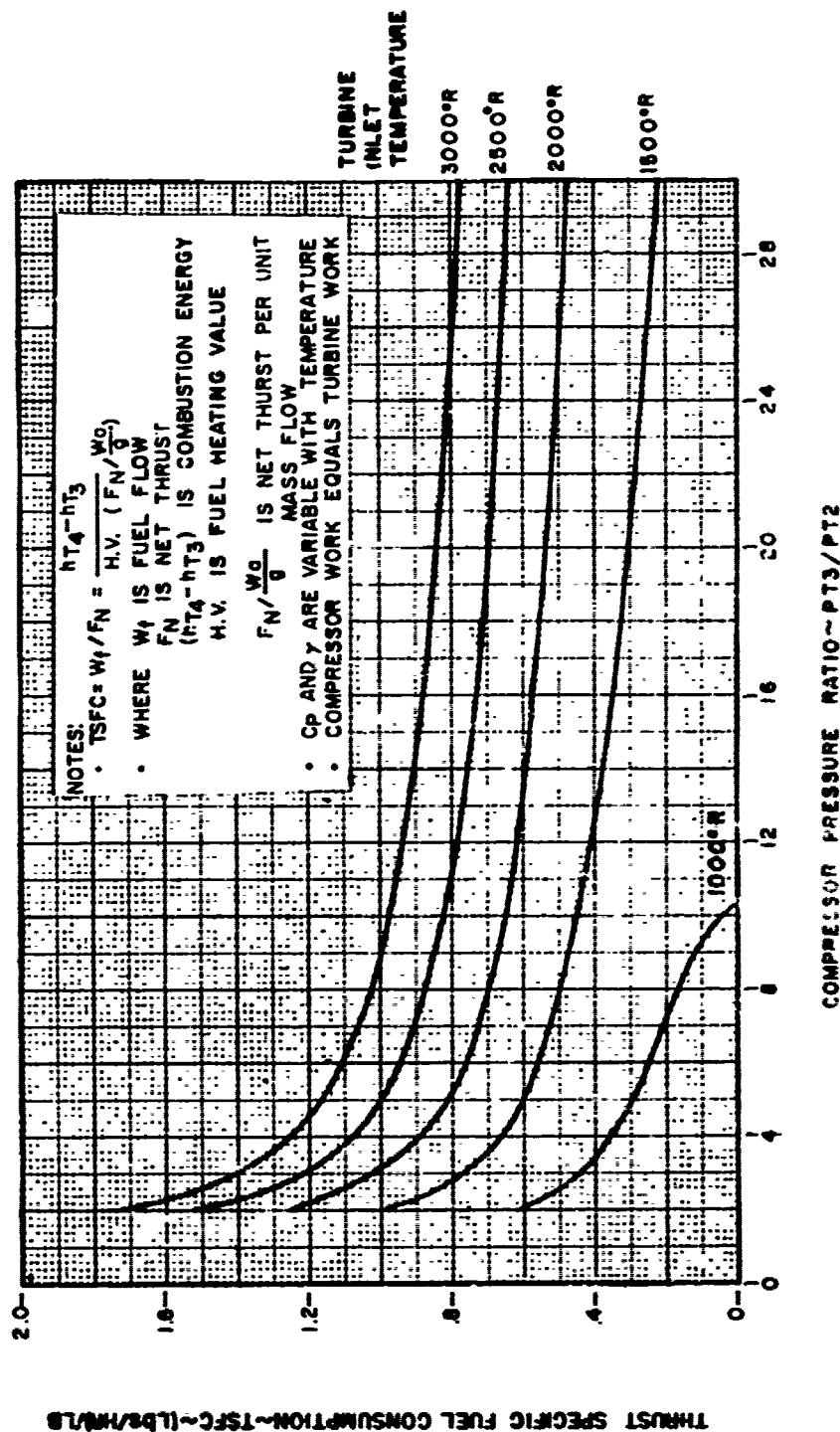


FIGURE 1.5a

IDEAL TURBO JET THRUST SPECIFIC FUEL CONSUMPTION

MACH No. = 0.75 HP = SEA LEVEL

STANDARD DAY

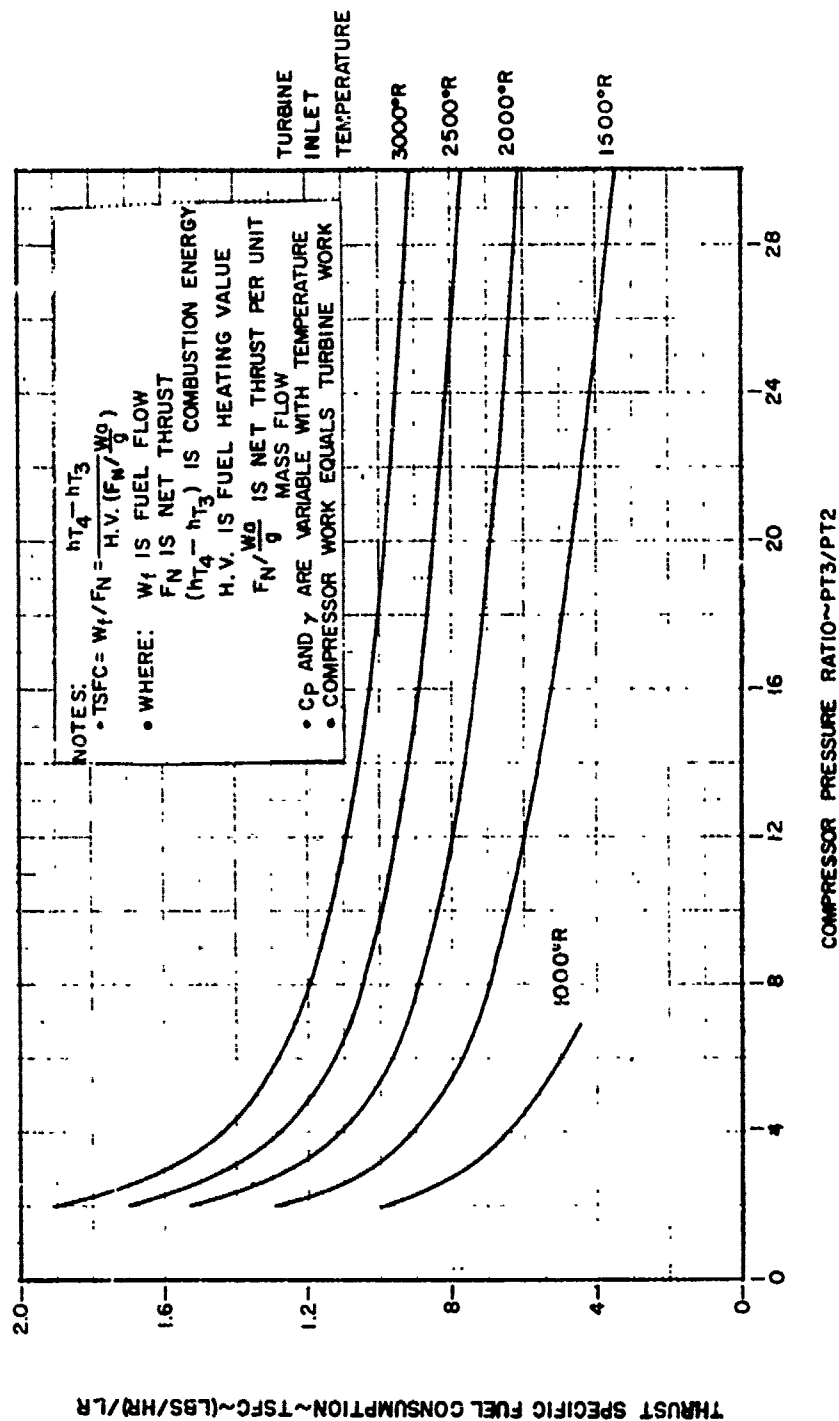


FIGURE 1.5b

IDEAL TURBO JET THRUST SPECIFIC FUEL CONSUMPTION

MACH No. = 0.75 HP = 30,000 FT

STANDARD DAY

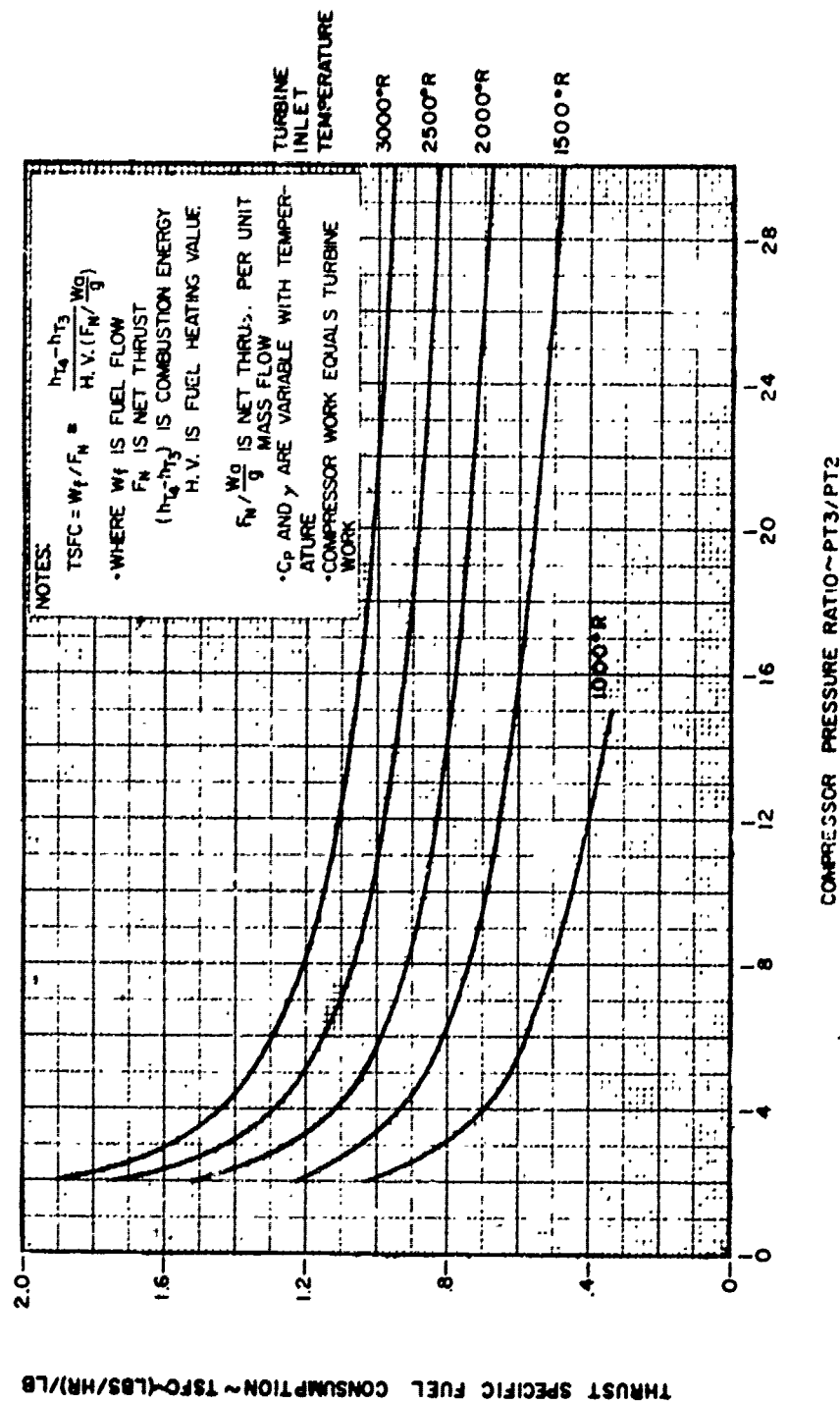


FIGURE 1.5c

1.2 COMPONENT EFFICIENCIES

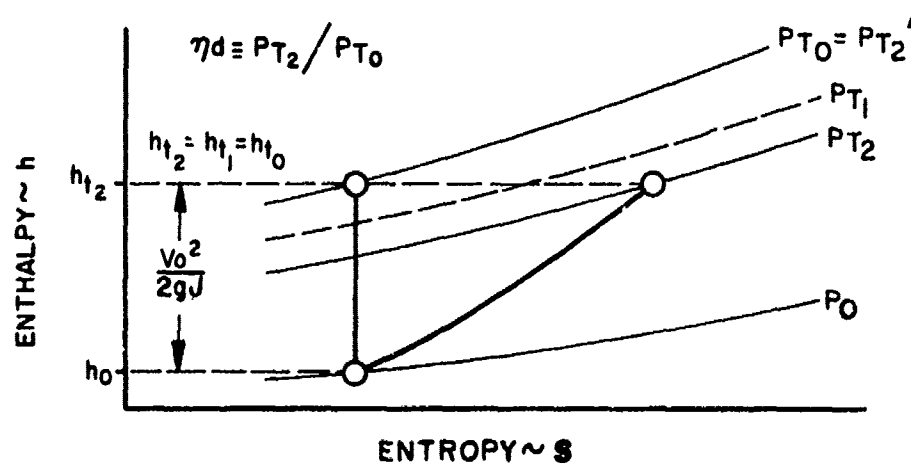
The cycle analysis presented in Section 1.1 was predicated on ideal component performance; that is, no losses. This does not mean the cycle is 100% efficient as shown by the thermal efficiency (Figure 1.3). Rather, given a set of operating conditions, the maximum or best an engine can perform is shown by the figures of the preceding section. The actual jet engine cycle will yield a performance level somewhat worse than the ideal depending on the magnitude of the losses of each component. The purpose of this Section will be to define each of the component efficiencies. The effect on the engine cycle will then be presented.

INLET EFFICIENCY

The process from free stream to the face of the compressor is ideally isentropic. If there exists friction or a shock(s), there will be a decrease in total pressure. The total temperature, which represents the total energy of the flow, will remain constant; data from actual tests show that T_{T2} equals T_{T0} . The inlet efficiency, therefore, is a means of measuring the loss in total pressure. The definition is:

$$\eta_d \equiv \frac{P_{T2}}{P_{T1}} = \frac{P_{T2}}{P_{T0}} \quad (1.15)$$

The ratio P_{T2}/P_{T0} is termed recovery; that is, the total pressure recovered from freestream. Figure 1.6 shows the process schematically. For subsonic inlets, there is no shock system and P_{T1} equals P_{T0} .



INLET EFFICIENCY
FIGURE 1.6

INLET PERFORMANCE H-S DIAGRAM

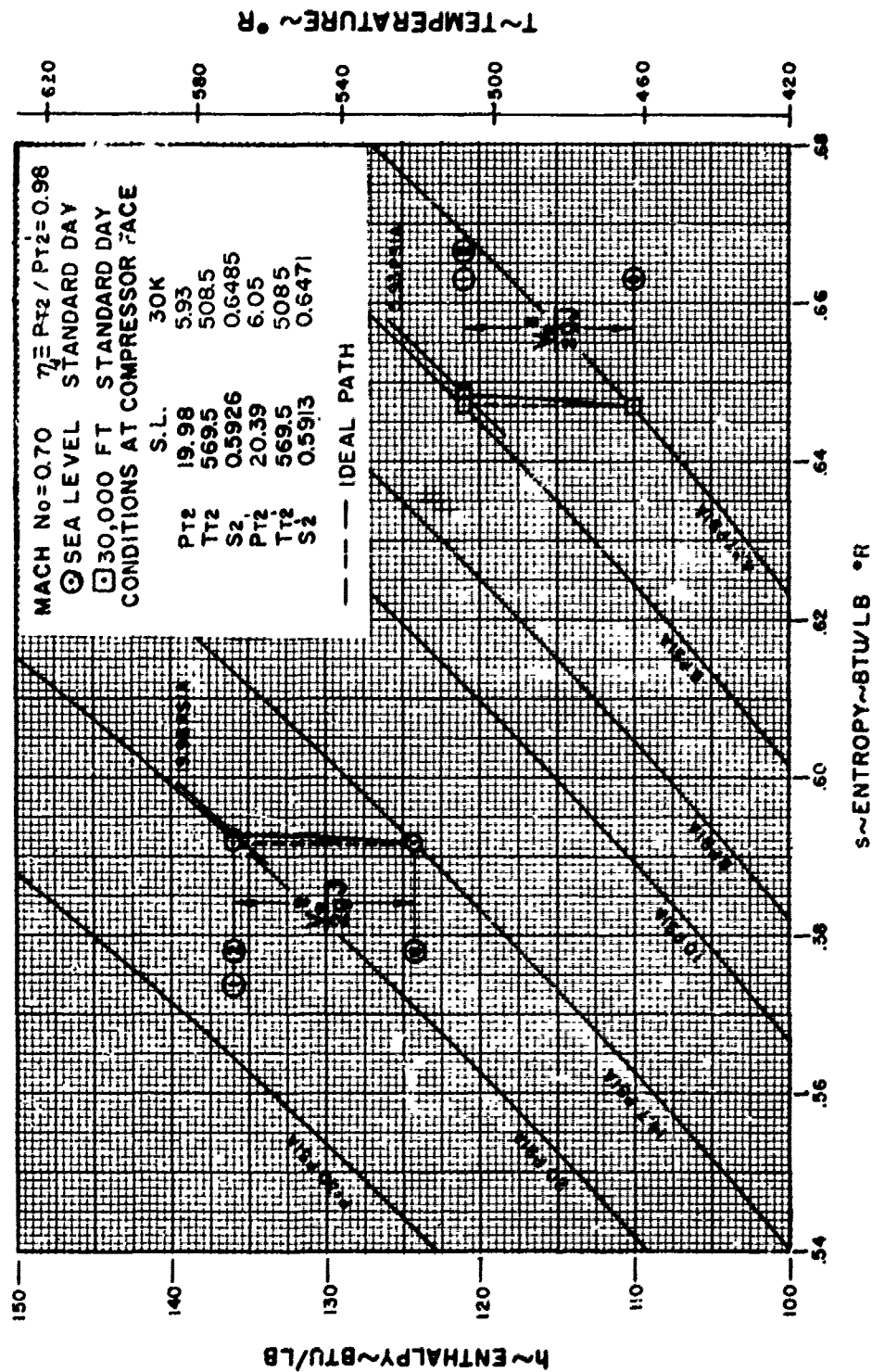


FIGURE 1.7

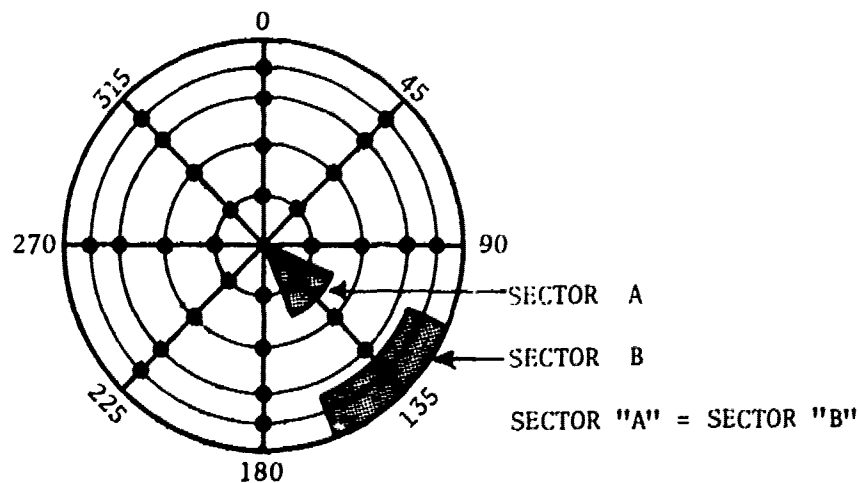
The isentropic total pressure, P_{T_0} , is given by:

$$P_{T_0} = P_0 \left(1 + \frac{\gamma-1}{2} M_0^2 \right)^{\frac{\gamma}{\gamma-1}} \quad (A1-4)$$

Using the definition of inlet recovery (1.15)

$$P_{T_2} = \eta_d P_0 \left(1 + \frac{\gamma-1}{2} M_0^2 \right)^{\frac{\gamma}{\gamma-1}}$$

Figure 1.7 shows the effect on an h-s diagram of an inlet recovery of 0.98 and a free stream Mach number of 0.8 at two altitudes. It is readily seen (refer to Figure 1.2) that any loss in inlet efficiency will be reflected in a loss in net thrust. It is, therefore, mandatory to flight test an aircraft to evaluate the magnitude of this loss in total pressure. These tests are not simply conducted by installing a single pressure probe at the compressor face; rather, a rake is installed to determine the gradient across the face. A typical installation would look like that shown on Figure 1.8. The total probes are usually installed on several radial arms which are evenly spaced around the compressor face. The spacing of the probes on the arms is such that they are area weighted; this means that the individual probes are located in the center of equal area sectors (see Figure 1.8).



COMPRESSOR FACE PRESSURE INSTRUMENTATION

FIGURE 1.8

Suitable instrumentation is installed to measure all probes for any flight/power condition.

For each flight/power condition, the arithmetic average of the readings of all probes is the average total pressure at the face of the compressor. This value, ratioed to free stream total pressure, is the recovery.

Steady state data are obtained covering all normally expected flight/power combinations throughout the aircraft envelope. The effect of sideslip and angle of attack is also determined by flying steady state conditions at various sideslip angles and angles of attack. The latter can be obtained by performing wind up turns at constant Mach number.

Presentation of the data is generally in the form shown on Figure 1.9a & b. Figure 1.9a is generally the working curve. In Section 3.1, the corrected airflow will be shown to be a function of corrected engine speed $N/\sqrt{\theta T_2}$, an easily measured parameter. Knowing $N/\sqrt{\theta T_2}$ and free stream Mach number, the recovery can be determined from a curve similar to Figure 1.9a.

The physical feeling for recovery variation is more easily seen from Figure 1.9b. The mass flow ratio (MFR) is defined as the mass flow entering the inlet divided by the mass flow that could go into the inlet at free stream Mach number. Thus:

$$MFR = \frac{W_a/g}{\rho_0 A_1 V_0} = \frac{\rho_0 A_0 V_0}{\rho_0 A_1 V_0} = \frac{A_0}{A_1}$$

It is seen that the MFR definition simplifies to the ratio A_0/A_1 . The physical interpretation is that the area A_0 (not mechanically bounded) is that free stream area required to pass the airflow entering the inlet at a Mach number M_0 , and A_1 is the inlet area which passes the same airflow at a Mach number M_1 . The mass flow ratio is easily calculated from Figure 1.9a by the following procedure:

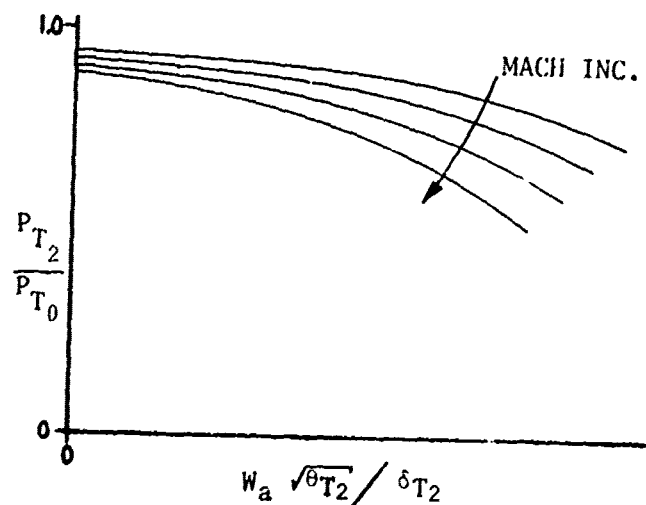
1. Select M_0 .

2. For each $\frac{W_a \sqrt{\theta T_2}}{\delta_{T_2}}$ read P_{T_2}/P_{T_0} .

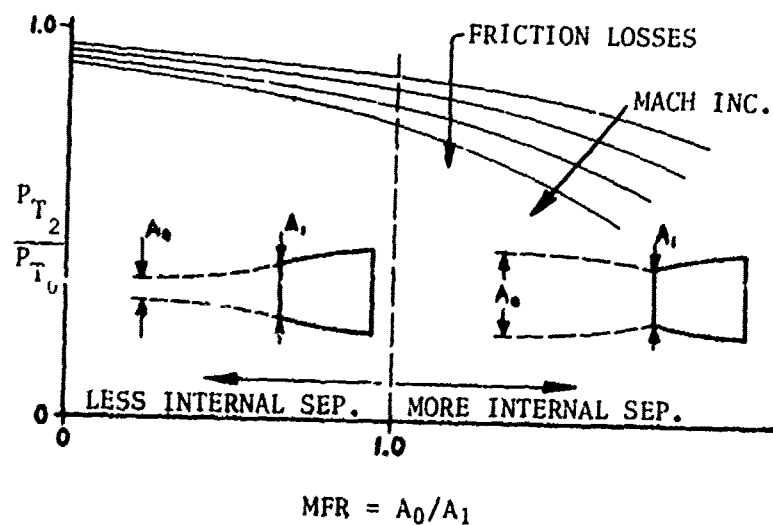
3. Calculate $\frac{W_a \sqrt{\theta T_0}}{\delta_{T_0}} = \frac{W_a \sqrt{\theta T_2}}{\delta_{T_2}} \times \frac{P_{T_2}}{P_{T_0}} \quad (T_{T_2} = T_{T_0})$

4. $A_0 = f(M_0 \text{ and } W_a \sqrt{\theta T_0} / \delta T_0)$

5. $MFR = A_0/A_1$ (A_1 is constant by geometry)



(a) RECOVERY vs. CORRECTED AIRFLOW



(b) RECOVERY vs. MASS FLOW RATIO

INLET RECOVERY GENERALIZATION

FIGURE 1.9

The inlet is operating on design when $A_0/A_1 = 1.0$ (see Figure 1.9b). If the power ($N/\sqrt{\theta T_2}$) were increased at constant M_0 or M_0 decreased at constant corrected airflow, A_0/A_1 would be greater than 1.0 and the inlet would be prone to flow separation within the inlet due to high local angle of attack as shown by the insertion on Figure 1.9b. Conversely, if A_0/A_1 is less than 1.0 (low power or high Mach number), less separation would exist within the inlet. Thus the decrease in recovery with increasing MFR at a given Mach number is primarily due to separation. If MFR is constant, the change in recovery is due primarily to the change in frictional losses. Thus, Figure 1.9b is a descriptive presentation, in that it shows the inlet recovery as effected by flow pattern and friction.

In addition to establishing an average inlet recovery, the total pressure distortion (gradients) can be determined from the same test data. If the measurements, taken at a constant radius, were plotted and distortion existed, the plot would look something like that shown on Figure 1.10.

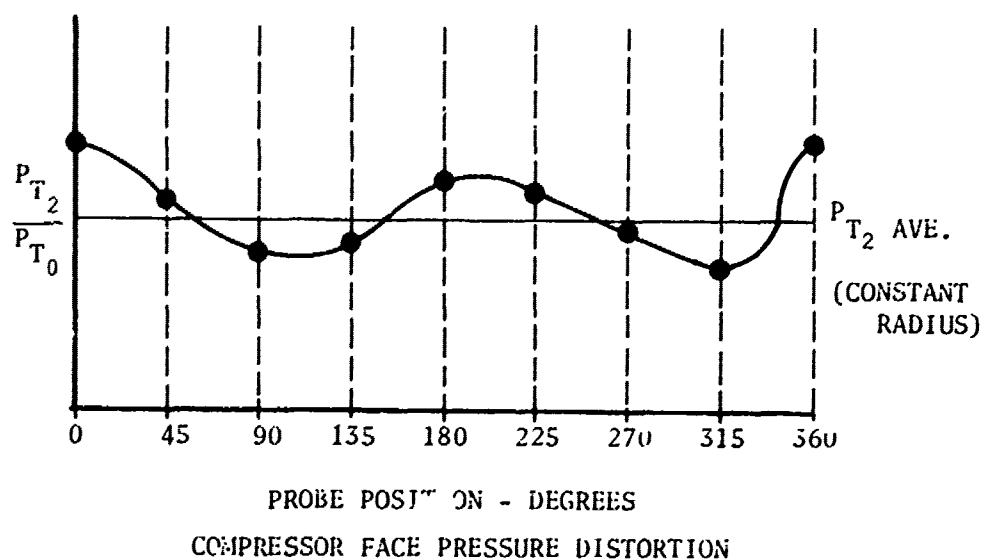
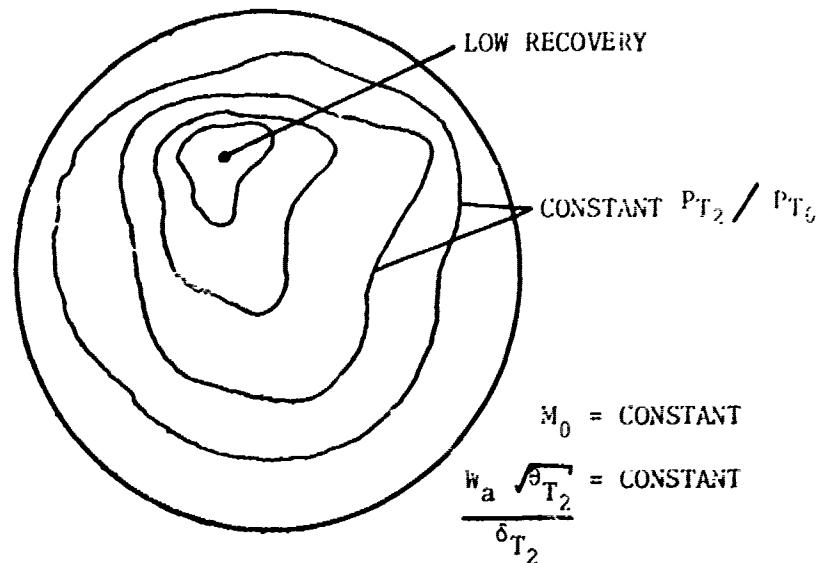


FIGURE 1.10

If each radius were plotted, isobaric contours (constant recovery) could be drawn as shown on Figure 1.11. Localized, low recovery areas can readily be seen from this map. This presentation is made should distortion be a problem. From these data, a distortion index is computed. This index is stipulated by the engine manufacturer and determined from numerous tests he conducted on a given engine design. The distortion index is calculated from test data and an empirical equation which may vary widely between manufacturers. A maximum distortion index value will be attached to each engine design. If, when the engine is installed in an aircraft, the flight tests show that the inlet does not produce a distortion index above the maximum, there should be no distortion problems.

with engine operation. On the other hand, there would exist a potential problem if the tests show that the maximum distortion index is exceeded. It must be emphasized that the index is empirical and the method for determining it will probably differ from manufacturer to manufacturer. The prime purpose is to pinpoint, if possible, the direction that modification work should take if an engine problem associated with an inlet emerges from development tests.



COMPRESSOR FACE ISOBARICS

FIGURE 1.11

COMPRESSOR EFFICIENCY

The compressor efficiency is defined as the amount of work required to compress the air isentropically to a given pressure divided by that required with losses. Therefore:

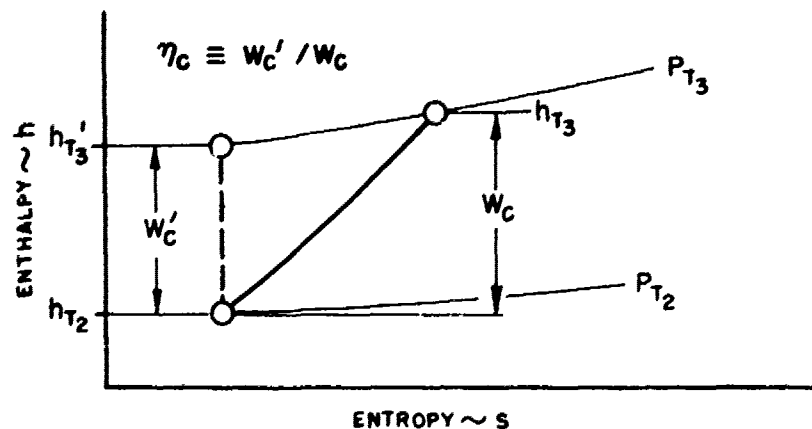
$$\eta_c \equiv \frac{w_c'}{w_c} \quad (\text{same } P_{T3} / P_{T2}) \quad (1.16)$$

The compressor efficiency is shown graphically on Figure 1.12. From this Figure and the equations in Table 1.1:

$$w_c' = h_{T_3'} - h_{T_2}$$

If C_p is constant:

$$w_c' = C_p (T_{T_3'} - T_{T_2})$$



COMPRESSOR EFFICIENCY

FIGURE 1.12

Factoring out T_{T_2} yields:

$$w'_c = C_p T_{T_2} \left[\left(T_{T_3}' / T_{T_2} \right) - 1 \right]$$

Since the process from T_{T_2} to T_{T_3}' is isentropic

$$w'_c = C_p T_{T_2} \left[\left(\frac{P_{T_3}}{P_{T_2}} \right)^{\frac{\gamma-1}{\gamma}} - 1 \right]$$

or substituting into (1.16) and rearranging:

$$w_c = \frac{C_p T_{T_2}}{\eta_c} \left[\left(\frac{P_{T_3}}{P_{T_2}} \right)^{\frac{\gamma-1}{\gamma}} - 1 \right] \quad (1.17)$$

$$\text{or} \quad w_c = C_p (T_{T_3}' - T_{T_2}) \quad (1.18)$$

Either (1.17) or (1.18) may be used to compute the work of compression.

Section 2.2 discusses various compressor designs and presents the variation of compressor efficiency with pressure ratio and airflow.

Figure 1.13 shows the h-s diagram for a compressor with a typical efficiency of 0.85, operating at a pressure ratio of 10.0 at 30,000 feet and a Mach number of 0.7. This Figure utilizes the inlet discharge conditions of Figure 1.7.

COMPRESSOR PERFORMANCE H-S DIAGRAM

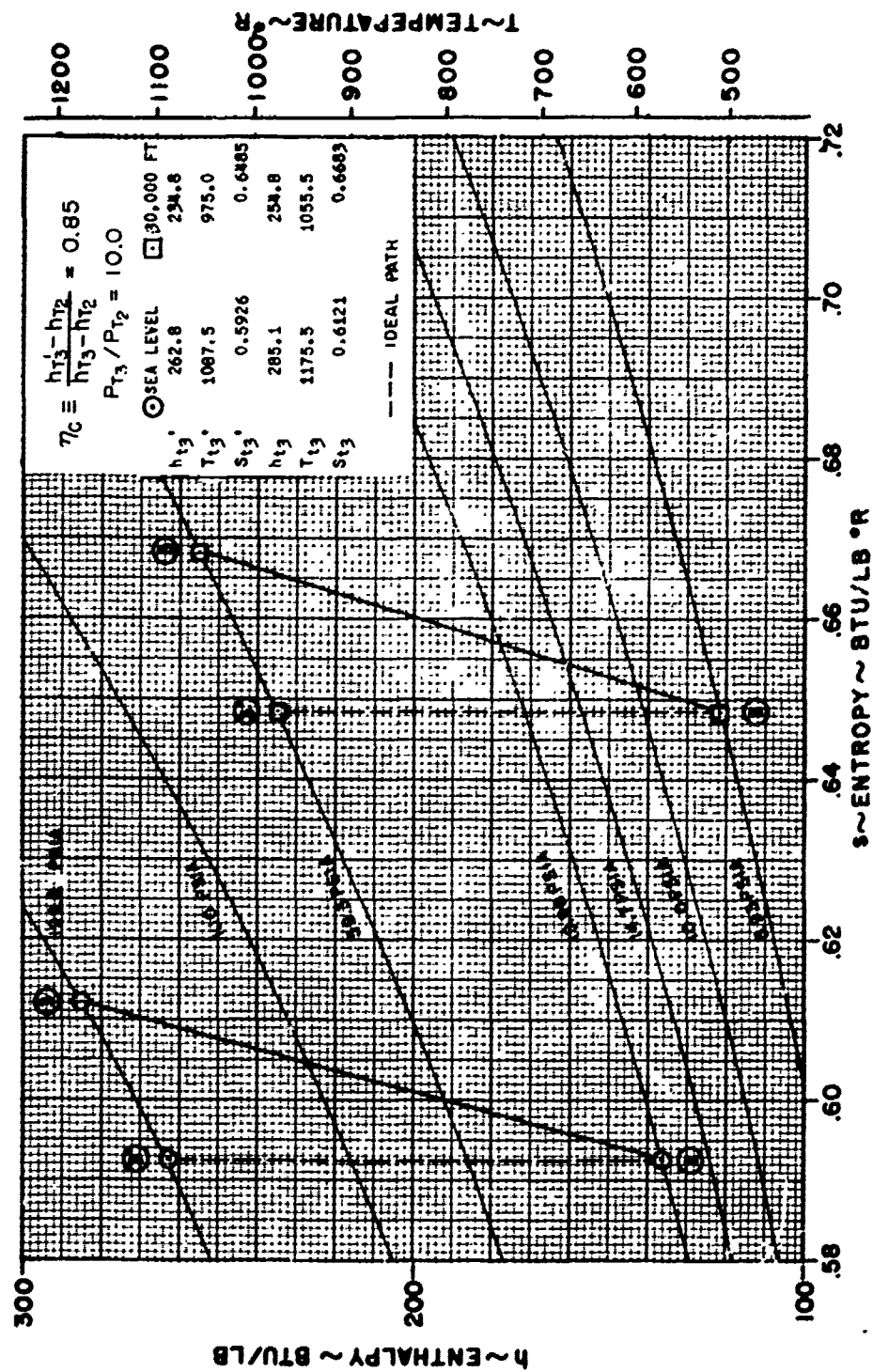


FIGURE 1.13

COMBUSTORS

There are two efficiencies associated with losses encountered in the combustion process. Losses in pressure and incomplete combustion lead to less than ideal operation.

Total Pressure Loss. Ideally, the combustion process should occur at a constant total pressure. However, due to friction and the combustion process itself, there is a total pressure loss. The loss is measured as a percent of the total pressure available. Thus:

$$\eta_b^* = \frac{P_{T_3} - P_{T_4}}{P_{T_3}} \times 100 \quad (1.19)$$

In the strictest sense η_b^* is not an efficiency but a percent loss.

Incomplete Combustion. In order to raise the compressed air from a given total temperature to an arbitrary value, a certain amount of fuel will be required. If complete combustion were possible, the fuel flow required would be:

$$W_f' = \frac{W_a C_p (T_{T_4} - T_{T_3})}{H.V.} \quad (1.20)$$

This equation was obtained from (1.12). The combustion efficiency is defined as the ratio of the ideal fuel flow required to raise the temperature of the air a certain amount, to that fuel flow required with incomplete combustion. Using this definition, the actual fuel flow is:

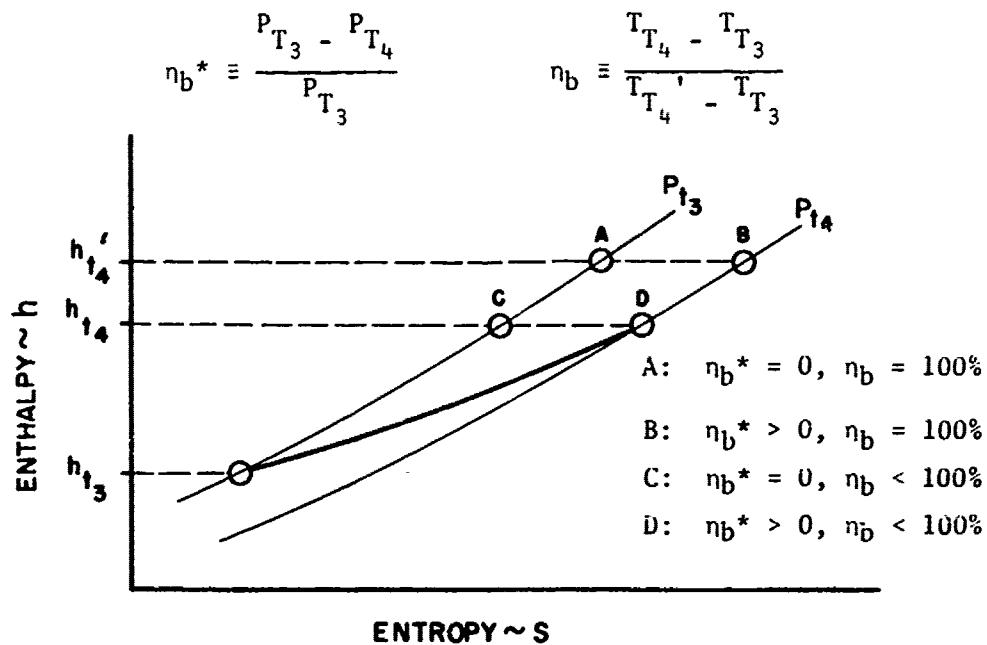
$$W_f = \frac{W_a C_p (T_{T_4} - T_{T_3})}{H.V. \eta_b} \quad (1.21)$$

In order to graphically depict this, consider the result of varying the efficiency keeping fuel flow constant. If, for constant fuel flow, η_b were increased to 100% (complete combustion), the sole effect would be a higher turbine inlet temperature. This leads then to an alternate definition of η_b :

$$\eta_b = \frac{T_{T_4} - T_{T_3}}{T_{T_4}' - T_{T_3}} \quad (1.22)$$

where T_{T_4}' is the combustor discharge temperature with complete combustion holding fuel flow and compressor discharge temperature constant.

Figure 1.14 shows the h-s diagram for both combustor efficiencies. End state points are shown for various combinations of efficiencies.



COMBUSTOR EFFICIENCY

FIGURE 1.14

It is important to note that there is no mathematical relationship between η_b and η_b^* ; generally, however, if η_b^* decreases, so does η_b . Section 2.3 discusses several combustor designs.

Figure 1.15 continues Figure 1.13 for combustor performance. On this Figure $\eta_b^* = 5\%$ and $\eta_b = 0.90$.

COMBUSTOR PERFORMANCE H-S DIAGRAM

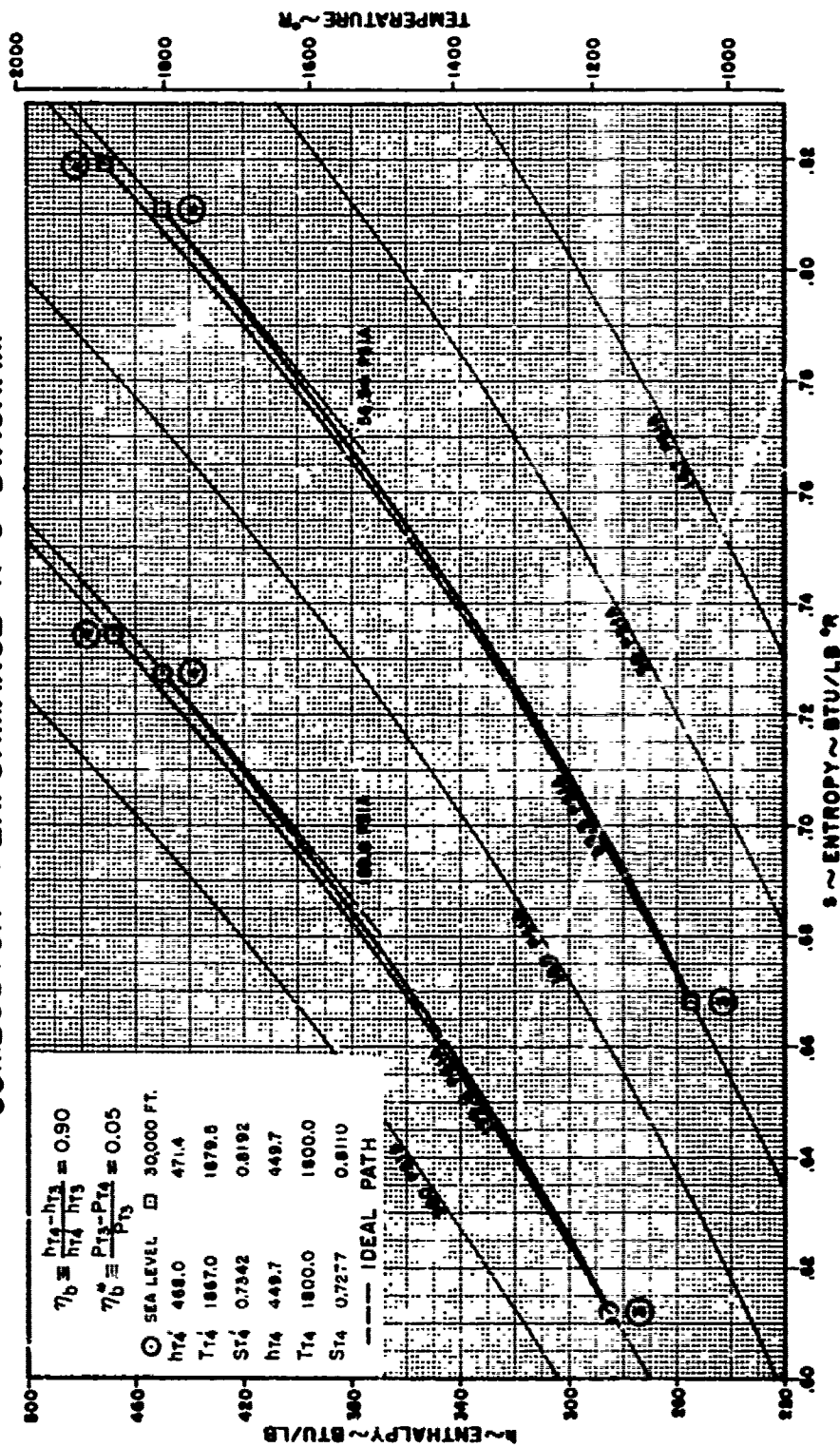


FIGURE 1.15

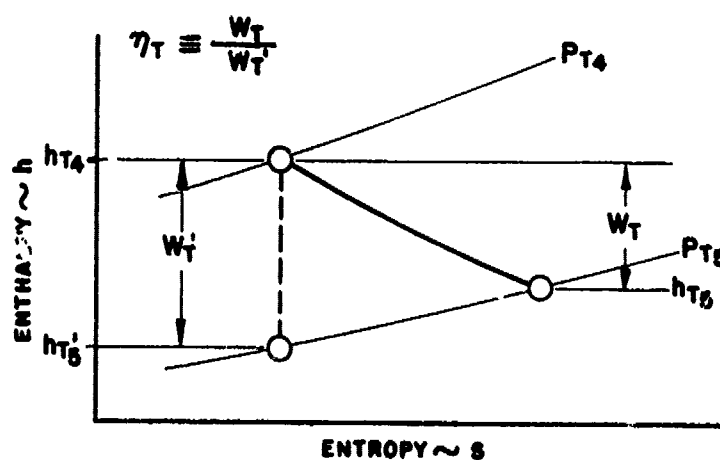
TURBINE EFFICIENCY

The turbine efficiency is defined in a manner similar to the compressor efficiency. Given a total pressure ratio, the turbine efficiency is the ratio of the work actually produced to the isentropic work. In equation form:

$$\eta_T \equiv \frac{W_T}{W_T'} \quad (1.23)$$

From Table 1.1, or Figure 1.16

$$W_T' = h_{T_4} - h_{T_5'}$$



TURBINE EFFICIENCY

FIGURE 1.16

For constant C_p ,

$$W_T' = C_p (T_{T_4} - T_{T_5'}) = C_p T_{T_4} \left[1 - \left(T_{T_5'} / T_{T_4} \right) \right]$$

The process from T_{T_4} to $T_{T_5'}$ is isentropic, therefore:

$$W_T' = C_p T_{T_4} \left[1 - \left(P_{T_5} / P_{T_4} \right)^{\frac{\gamma-1}{\gamma}} \right]$$

Substituting into (1.23) and rearranging yields:

$$W_T = \eta_T C_p T_{T_h} \left[1 - \left(P_{T_5} / P_{T_h} \right)^{\frac{\gamma-1}{\gamma}} \right] \quad (1.24)$$

$$\text{or} \quad W_T = C_p (T_{T_h} - T_{T_5}) \quad (1.25)$$

Either (1.24) or (1.25) can be utilized to compute turbine work.

Combining (1.25) and (1.18) for no accessory loads yields:

$$C_p (T_{T_3} - T_{T_2}) = W_c = W_T = C_p (T_{T_h} - T_{T_5})$$

$$\text{or} \quad T_{T_h} = T_{T_5} + (T_{T_3} - T_{T_2}) \quad (1.26)$$

Now T_{T_2} , T_{T_3} and T_{T_5} are easily measured. Thus, the turbine inlet temperature can be computed. Engines which display turbine inlet temperature in the cockpit usually have a computer which calculates T_{T_h} using an equation similar to (1.26). The actual equation, however, would utilize a variable C_p . Any loads driven by the turbine would obviously have to be accounted for in the computer. Typical loads on a jet engine are about 1% the compressor load. It should be recalled that one of the most important assumptions on which equation (1.26) is based is steady flow.

Figure 1.17 shows, on an h-s diagram, a turbine efficiency of 0.90 at sea level and 30,000 feet and a Mach number 0.7 based on the turbine inlet conditions from Figure 1.15.

TURBINE PERFORMANCE H-S DIAGRAM

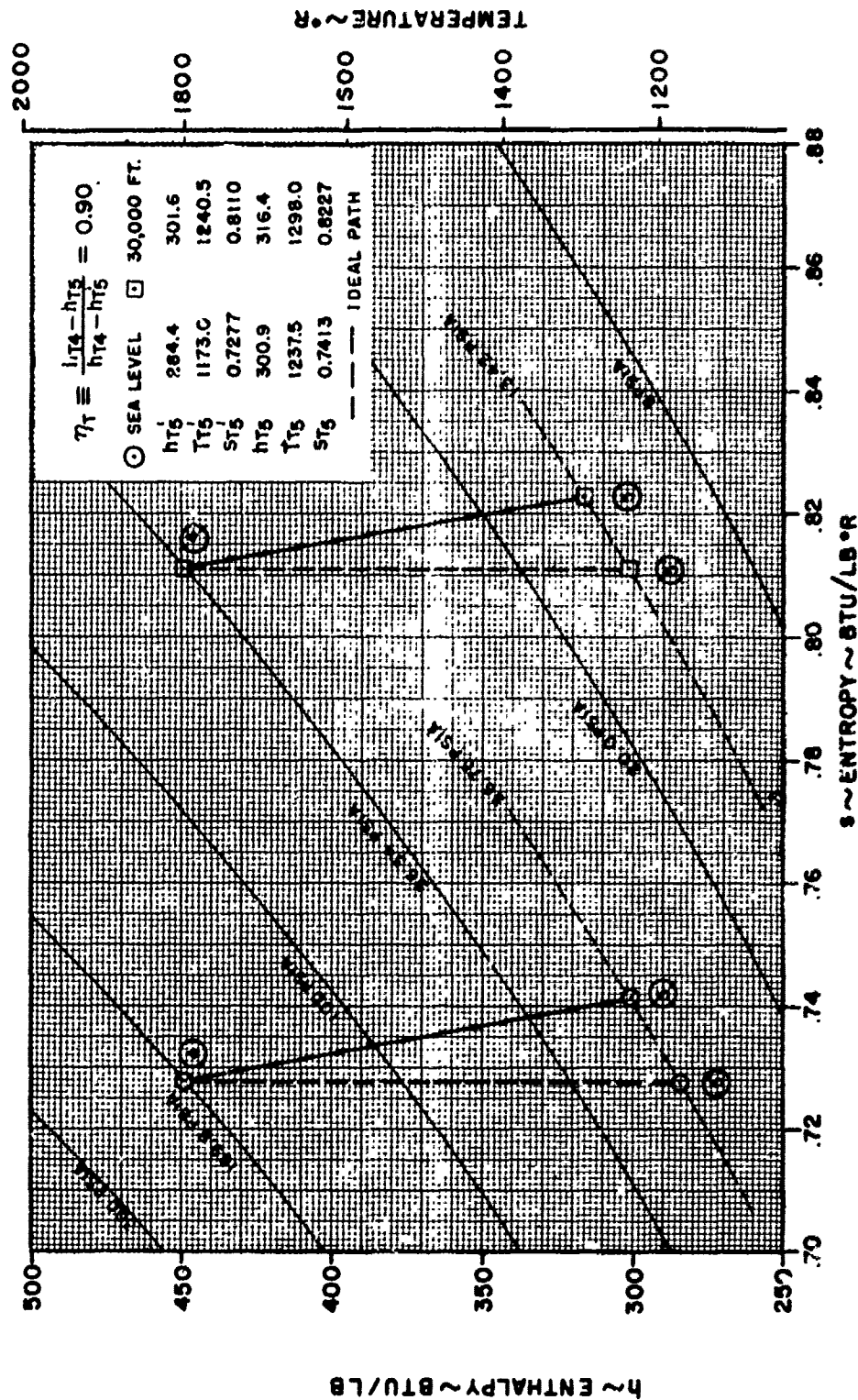


FIGURE 1.37

NOZZLE EFFICIENCY

The performance of the nozzle is defined such that it is a measure of how efficiently the nozzle accelerates (expands) the gases prior to discharge. By definition, the nozzle efficiency is:

$$\eta_n \equiv \frac{V_{10}^2 / 2gJ}{(V_{10}')^2 / 2gJ} \quad (1.27)$$

V_{10}' is the isentropic velocity (see Figure 1.18) and is the maximum velocity that can be produced by the nozzle.

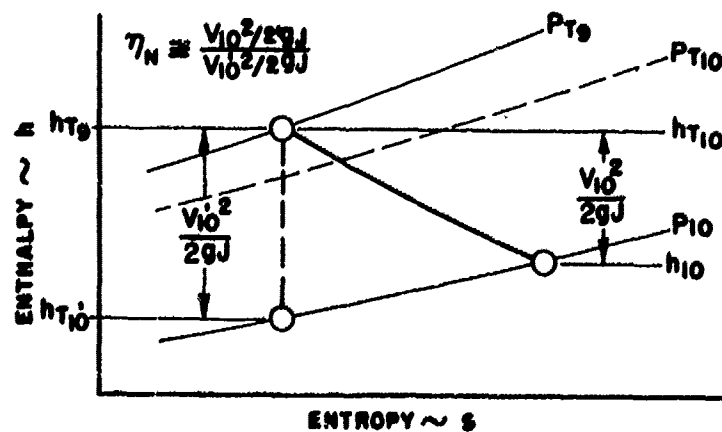
Simplifying (1.27):

$$\eta_n = \left(\frac{V_{10}}{V_{10}'} \right)^2$$

or $V_{10} = \sqrt{\eta_n} (V_{10}')^2$

If $\sqrt{\eta_n} \equiv (CV)$ (the velocity coefficient), then

$$V_{10} = (CV) V_{10}' \quad (1.28)$$



NOZZLE EFFICIENCY

FIGURE 1.18

From Figure 1.18, it can be seen that the efficiency is an indication of the loss in total pressure from the entrance of the nozzle to the discharge. If a nozzle is properly designed, the exit static pressure will be the same as free stream static. It will be shown in Section

2.5 that for most "off design" operations P_{10} does not equal P_0 . The nozzle efficiency, however, is still defined as in (1.27). If the gasses are not completely expanded by a given nozzle, the efficiency is the measure of how that nozzle expands the flow to the actual P_{10} even though a better nozzle design could accelerate it further.

If it is assumed that the exhaust gasses are completely expanded in the nozzle, the momentum thrust per unit mass flow is given by (1.6):

$$F_N / (W_a / g) = V_{10} - V_0 \quad (1.6)$$

The isentropic velocity is

$$V_{10}' = \sqrt{2gJ (h_{T_9} - h_{10}')}$$

If C_p is constant and T_{T_9} is factored out:

$$V_{10}' = \sqrt{2gJ C_p T_{T_9} \left[1 - (T_{10}' / T_{T_9}) \right]}$$

Since the process from T_{T_9} to T_{10}' is isentropic

$$V_{10}' = \sqrt{2gJ C_p T_{T_9} \left[1 - \left(P_{10} / P_{T_9} \right)^{\frac{\gamma-1}{\gamma}} \right]}$$

With complete expansion, P_{10} equals P_0 . Substituting this in the above and combining with (1.28) and (1.6) yields:

$$F_N / (W_a / g) = (CV) \sqrt{2gJ C_p T_{T_9} \left[1 - \left(P_{10} / P_{T_9} \right)^{\frac{\gamma-1}{\gamma}} \right]} - V_0 \quad (1.29)$$

This is the equation for net thrust per unit mass flow for a completely expanded nozzle. Equation (1.29) will be discussed and further expanded in Section 2.5 in order to apply it practically.

Figure 1.19 shows a non-isentropic complete expansion of a nozzle with an efficiency of 0.98 for two altitudes. The nozzle inlet conditions are given by Figure 1.17.

1.40

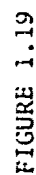


FIGURE 1.19

1.3 ACTUAL JET ENGINE THERMODYNAMIC CYCLE

Section 1.2 has defined the efficiencies of all the components comprising the jet engine. The ideal non-afterburning cycle, as discussed in Section 1.1, is typified graphically by Figure 1.2a. If each component has a performance loss, the cycle will change somewhat in character. Combining Figures 1.7, 1.13, 1.14, 1.17, and 1.19, produces the h-s diagram of a typical actual jet engine cycle. This is shown on Figure 1.20.

Similar to the analysis presented in Section 1.1, all of the design variables (Mach number, altitude, compressor pressure ratio and turbine inlet temperature) can be varied to produce curves not unlike those of Figures 1.3, 1.4, and 1.5. To demonstrate the effects of component performance losses, the thermal efficiency, net thrust per unit mass flow, and specific fuel consumption were computed, for an altitude of 30,000 feet, a Mach number of 0.75 and typical component efficiencies, using a digital computer program. The significant effects are noted below.

THERMAL EFFICIENCY

Compare Figure 1.21 with Figure 1.3c. It is recalled from the discussion on the ideal cycle, that the variation of thermal efficiency with turbine inlet temperature is due to the effect of variable C_p ; as T_{t_4} increased, η_{TH} decreased (slightly). The actual cycle efficiency, for the same T_{t_4} , is seen to be less than that of the ideal cycle. For low values of T_{t_4} , the difference is greater than at higher values, resulting in an increase in efficiency with increasing T_{t_4} . This effect is attributed to the fact that as T_{t_4} increases, the magnitude of the inputs used to compute η_{TH} increases with the effects of the component performance losses getting proportionately smaller.

NET THRUST PER UNIT MASS FLOW

The only significant effects of component losses on net thrust is that the magnitude has decreased for the same turbine inlet temperature, and that the pressure ratio for optimum thrust has also decreased. These results can be seen by comparing Figure 1.22 with Figure 1.4c.

THRUST SPECIFIC FUEL CONSUMPTION

Due to the close correlation of specific fuel consumption with thermal efficiency as discussed in Section 1.1, a rather marked increase in TSFC (as a result of component efficiencies) results at low turbine inlet temperatures, as shown on Figure 1.23, in contrast to the higher temperatures. This Figure should be compared to Figure 1.5c for the ideal cycle.

The basic effects of component performance losses on the jet engine thermodynamic cycle have been presented. Further understanding and appreciation required detailed analysis of the cycle. This study is beyond the scope of this text.

1.42

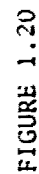


FIGURE 1.20

ACTUAL TURBO JET THERMAL EFFICIENCY

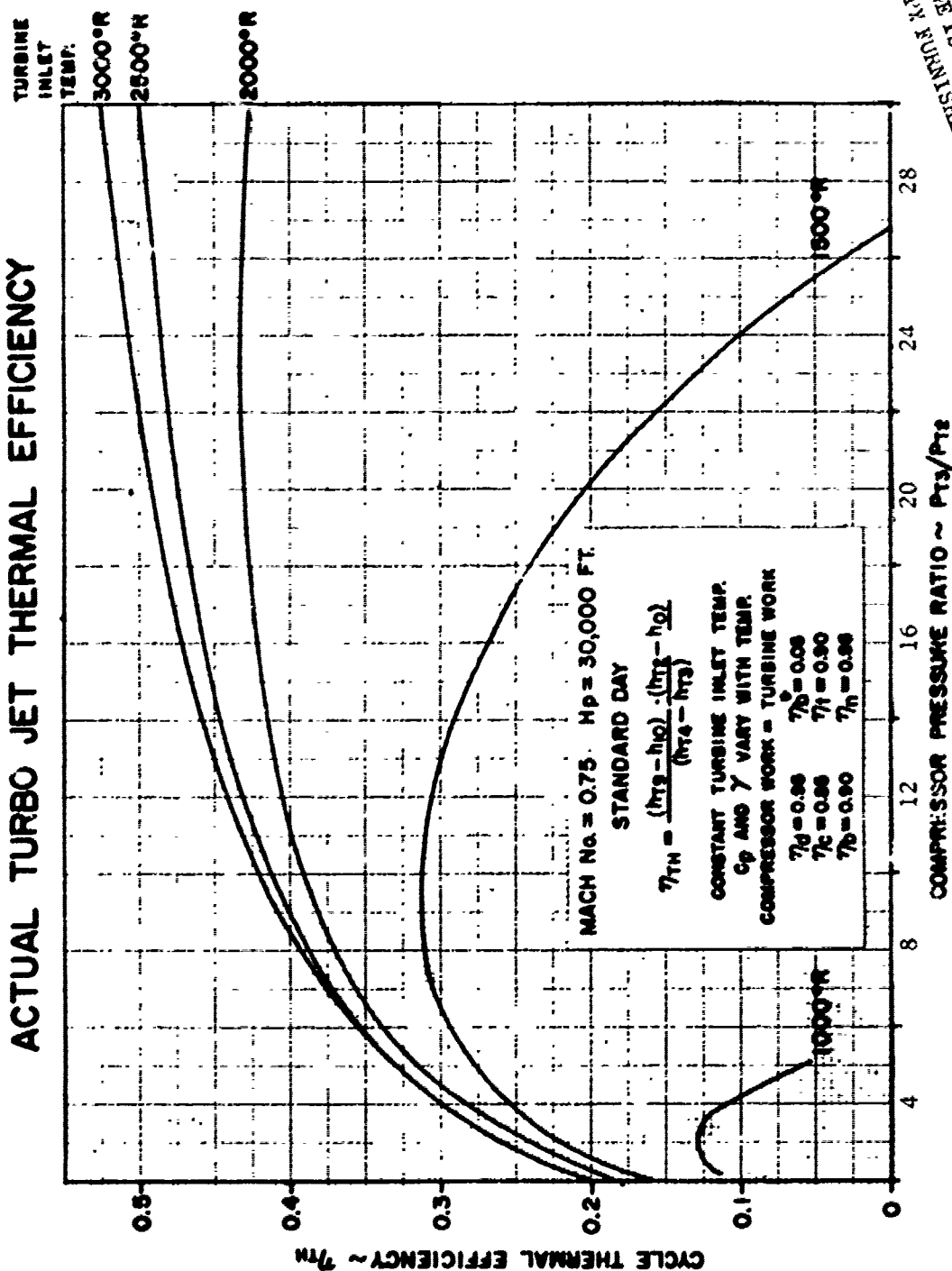


FIGURE 1.21

THIS PAGE IS BEST QUALITY PRACTICABLE
FROM COPY FURNISHED TO DDC

ACTUAL TURBO JET THRUST

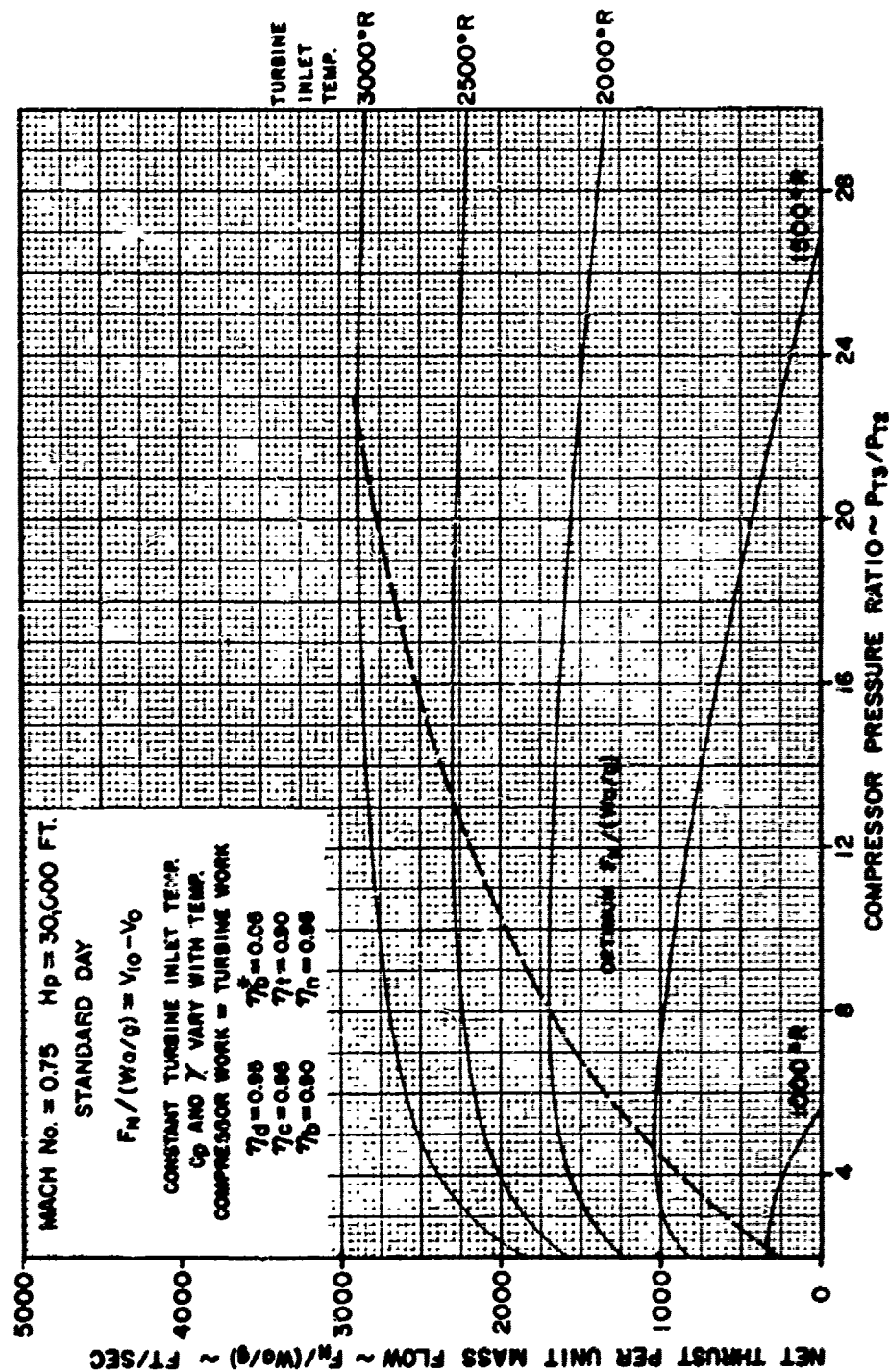


FIGURE 1.22

ACTUAL TURBO JET SPECIFIC FUEL CONSUMPTION

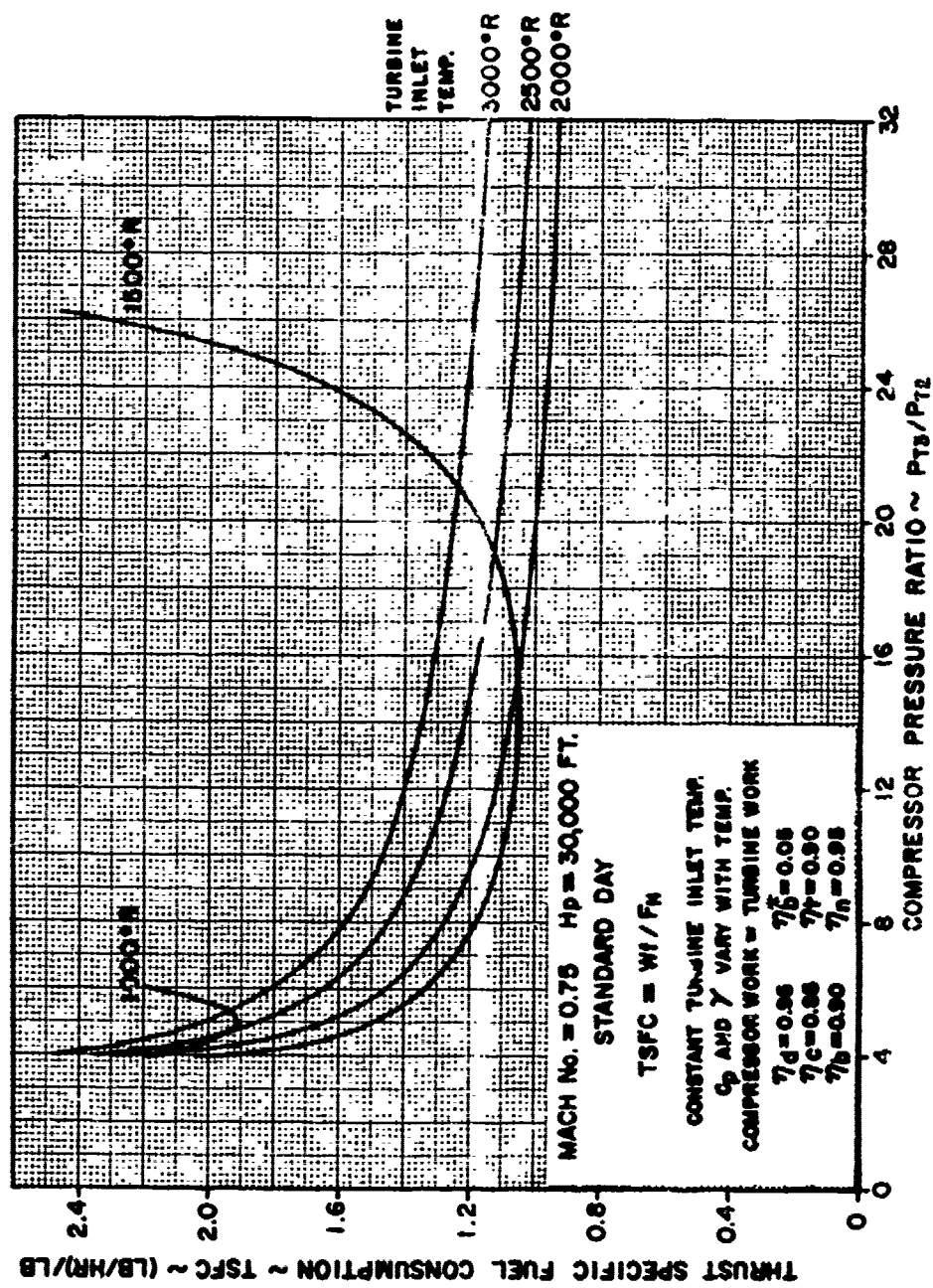


FIGURE 1.23

THIS PAGE INTENTIONALLY LEFT BLANK

1.4 AFTERBURNER CYCLE

Little change is made to the basic jet engine cycle when the afterburner is added. The afterburner process is identical to that of the combustor process in the engine. Figure 1.2b shows a typical ideal afterburning jet engine cycle. A comparison with Figure 1.2a reveals the only difference to be an increase in total temperature entering the nozzle.

Results similar to the basic jet engine cycle would be obtained by comparing the ideal to the actual afterburning cycle; thus, the brief discussion presented here will be limited to the changes in thermal efficiency, thrust, and fuel consumption as a result of adding an afterburner.

The calculation procedure, accounting for the variation in C_p with temperature and component performance losses, is detailed in Appendix A-2. Using this method, the aforementioned parameters were calculated, and are presented on Figures 1.24 through 1.26, for an altitude of 30,000 feet, Mach number of 0.75, a constant turbine inlet temperature of 2000°R and two arbitrarily chosen nozzle inlet temperatures. For comparison, the non-afterburning condition is also shown; this is the same as the 2000°R turbine inlet temperature curve on Figures 1.21, 1.22, and 1.23, respectively.

As expected, the thermal efficiency and specific fuel consumption deteriorated, while thrust increased with increasing afterburner power. It must be emphasized that all other variables are held constant for comparison.

ACTUAL TURBO JET AFTERBURNER THERMAL EFFICIENCY

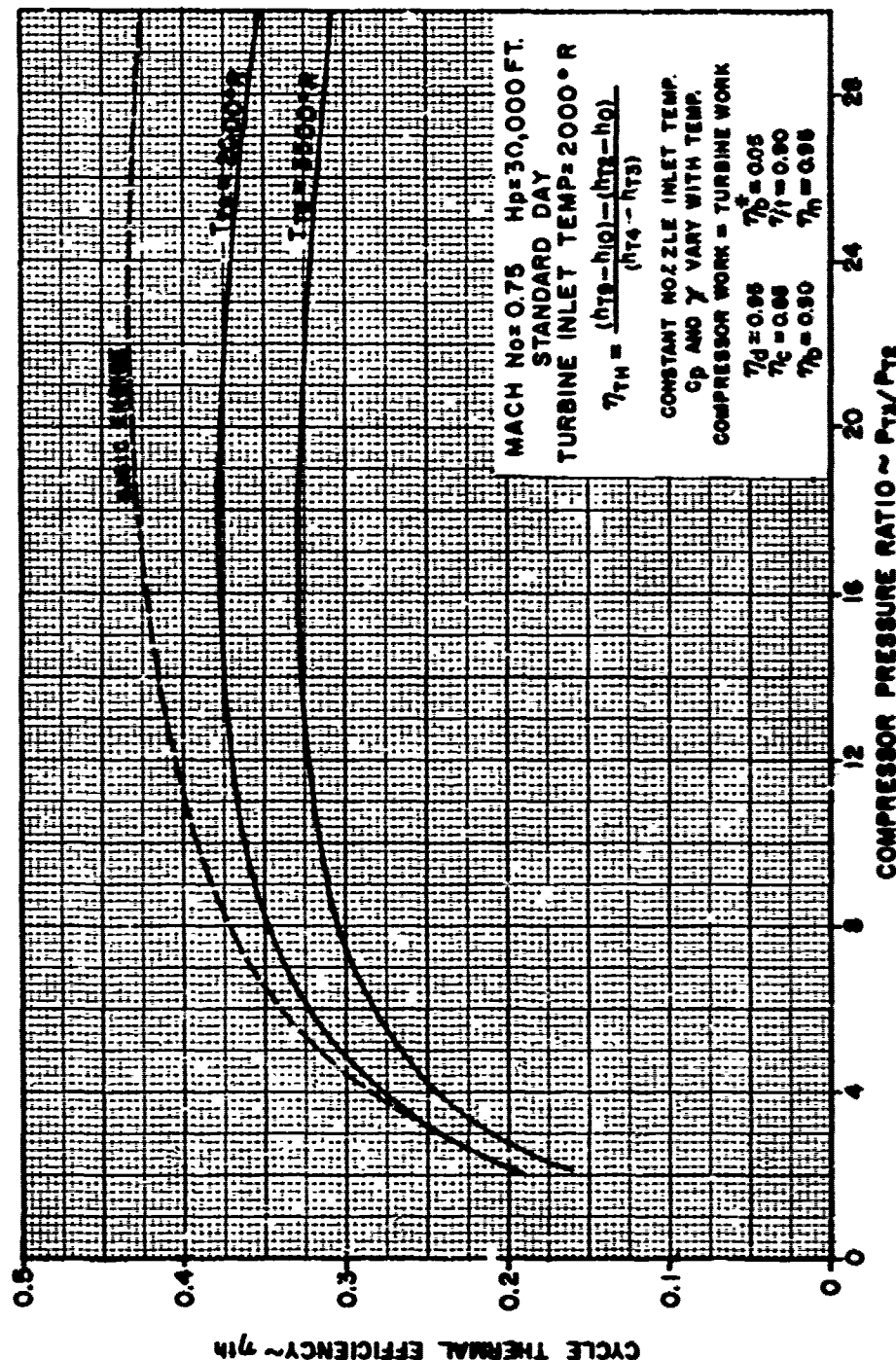


FIGURE 1.24

ACTUAL TURBO JET AFTERBURNER NET THRUST

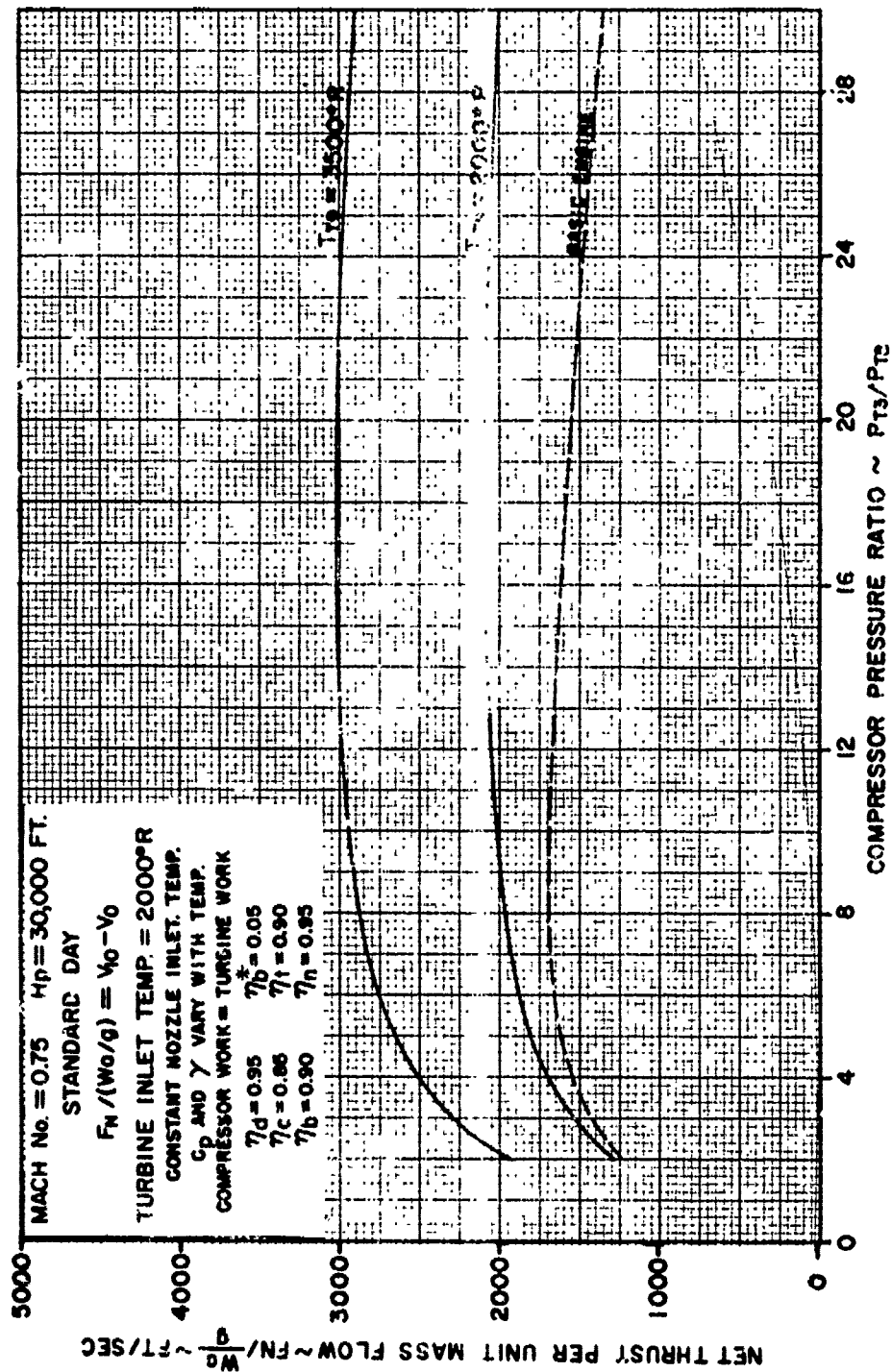


FIGURE 1.25

ACTUAL TURBO JET AFTERBURNER SPECIFIC FUEL CONSUMPTION

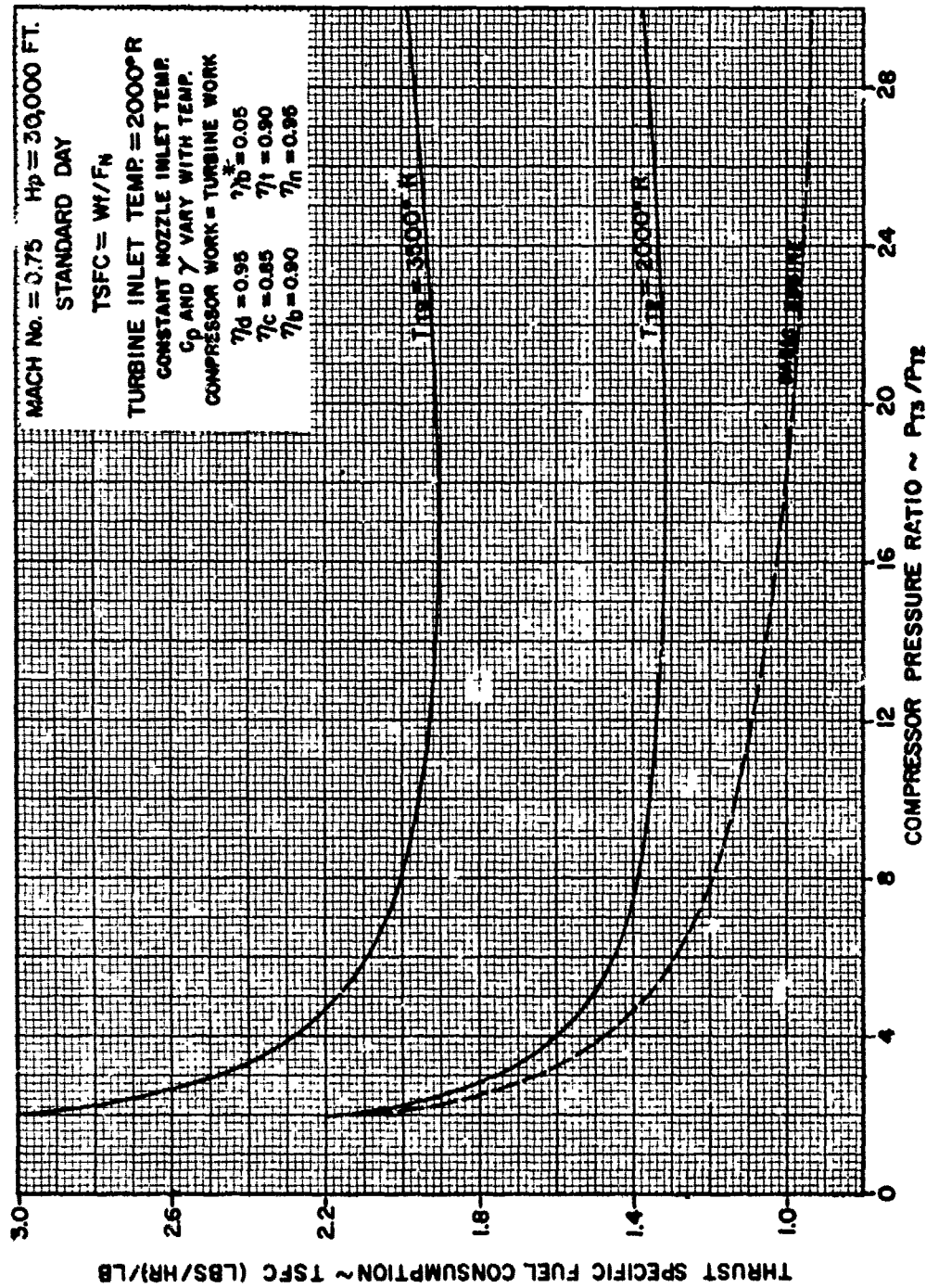


FIGURE 1.26

SECTION 2

COMPONENT PERFORMANCE

2.1 INLETS

The purpose of the inlet is to deliver the required amount of air to the engine with a minimum loss in total pressure (minimum entropy increase), minimum pressure distortion, and minimum pressure oscillations. Section 1.2 briefly described some of the test techniques and data presentation that are utilized to analyze inlet losses. This section will serve to show, basically, how an inlet is designed to provide the correct airflow with minimum total pressure loss.

The design criteria for an inlet are primarily predicated on free stream Mach number and engine airflow. An inlet can be designed rather easily to operate for a unique set of conditions. Simultaneously satisfying combinations of Mach number and airflow for other than design conditions can result in low recovery, separation, added drag, or various combinations of these. Detailed discussion will be given concerning these off design conditions. The basic equation to be utilized for inlet analysis is given below.

$$\frac{dA}{A} = \frac{M^2 - 1}{\left(1 + \frac{\gamma-1}{\gamma} M^2\right)} \frac{dM}{M} \quad (2.0)$$

or in integrated form:

$$\frac{A_x}{A_y} = \frac{M_y}{M_x} \sqrt{\left(\frac{1 + \frac{\gamma-1}{2} M_x^2}{1 + \frac{\gamma-1}{2} M_y^2} \right)^{\frac{\gamma+1}{\gamma-1}}} \quad (2.1)$$

The x and y refer to any two sections in a duct provided that the flow is isentropic.

The inlet is required to supply air to the engine at some Mach number (M_{eng} or M_2) with acceptable levels of efficiency. This air must be decelerated (or accelerated) from the free stream conditions at the free stream Mach number. The inlet can satisfy this ideally by a discharge area (A_2) related to M_0 and M_2 by equation (2.1). The magnitude of M_2 is directly a function of corrected airflow, $W_a \sqrt{\theta T_2}/\delta T_2$ and flow area. It will be shown in Section 3 that the engine cycle operates on corrected airflow ($W_a \sqrt{\theta T_2}/\delta T_2$) and that this term is uniquely related to corrected engine speed ($N/\sqrt{\theta T_2}$). The design of the inlet will, therefore, be based primarily on power setting ($N/\sqrt{\theta T_2}$), which dictates the engine Mach number for a constant inlet/discharge area, and the free stream Mach number.

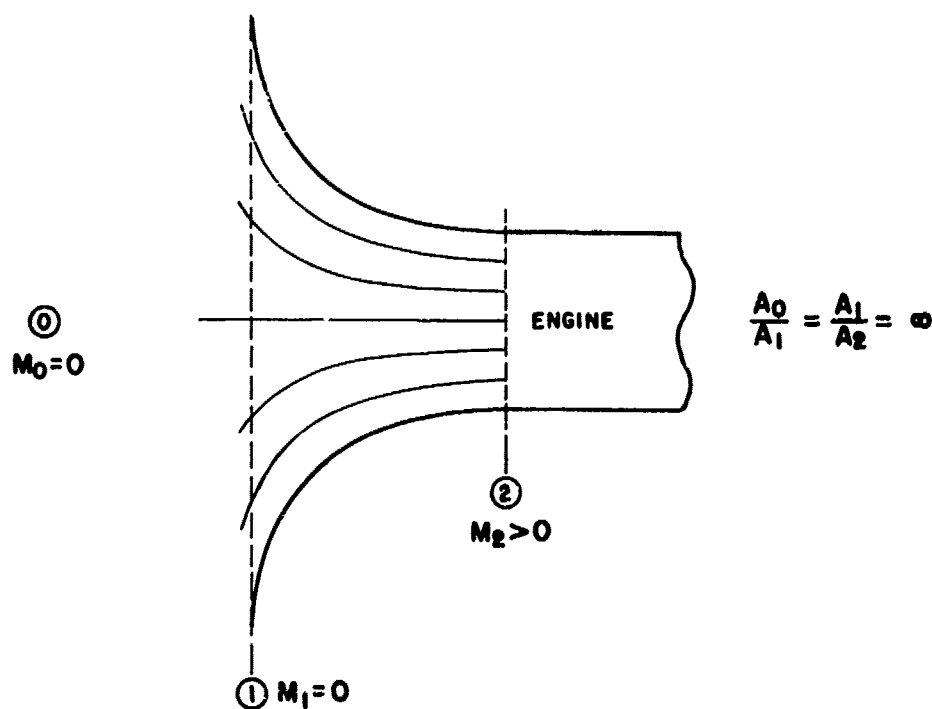
SUBSONIC INLET DESIGNS

Static Operation ($M_0 \equiv 0$)

From equation (2.1) for $M_0 = 0$ and any finite value of M_2 :

$$A_0/A_2 = \infty$$

To avoid separation, a bellmouth inlet is designed such that A_1 is as large as possible, as shown on Figure 2.1. The radius of curvature of the contours is also "large" so as to avoid flow separation. This type of inlet is utilized to provide ideal flow to an engine during calibration tests. Pressure recovery (P_{T2}/P_{T0}) is usually unity with negligible, if any, distortion due to the inlet.



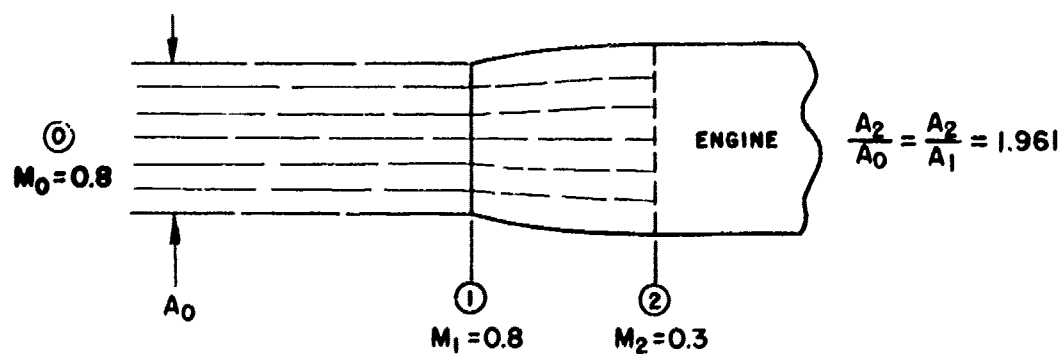
INLET DESIGNED FOR STATIC OPERATION

FIGURE 2.1

Subsonic Operation ($0 < M_0 < 1.0$) - On Design

For subsequent examples, the engine design Mach number M_2 will be arbitrarily selected as 0.3. This is representative of current engine designs.

If an inlet were designed for $M_0 = M_2$, there would be no requirement for A_0 to be different from A_2 and a straight inlet would result. Most of the time, however, a subsonic inlet will be operating with M_0 greater than M_2 . This will require an area A_0 less than A_2 as dictated by equation (2.1). If a design free stream Mach number of 0.8 were selected, the inlet would look like that shown in Figure 2.2.



SUBSONIC INLET OPERATING ON DESIGN

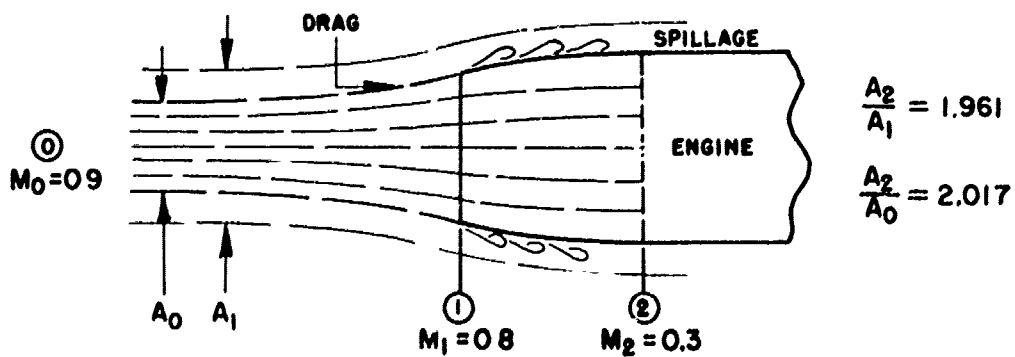
FIGURE 2.2

For the given design conditions, $A_0 = A_1$ and $A_2/A_1 = 1.961$. This value was computed from (2.1) with $\gamma = 1.4$. It is recalled from Section 1.2 that when $A_0 = A_1$ the mass flow ratio is unity.

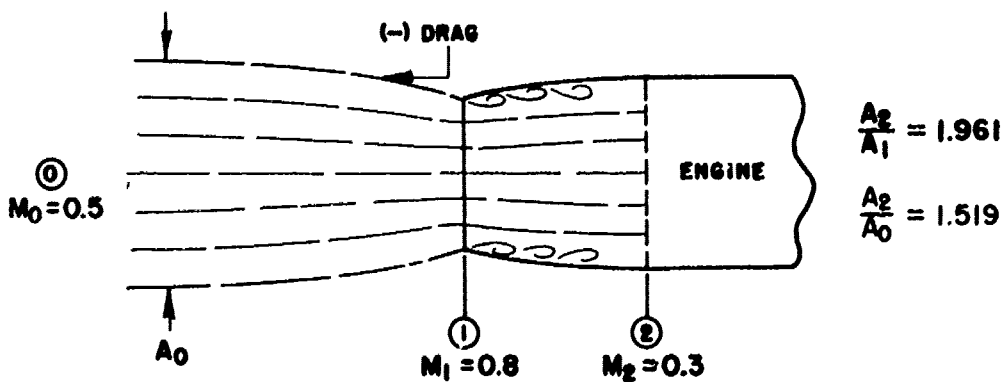
Once the area ratio of a subsonic inlet is determined for a specific condition, the contours are generally fixed and there will exist numerous flight/engine conditions during which the inlet is operating "off design". There will be many flight/engine conditions (e.g., $M_2 = 0.2$, $M_0 = 0.43$) for which the inlet is on design ($A_0/A_1 = 1.0$). It is the "off design" condition ($A_0/A_1 \neq 1.0$) which is of interest now.

Subsonic Operation ($0 < M_0 < 1.0$) - Off Design

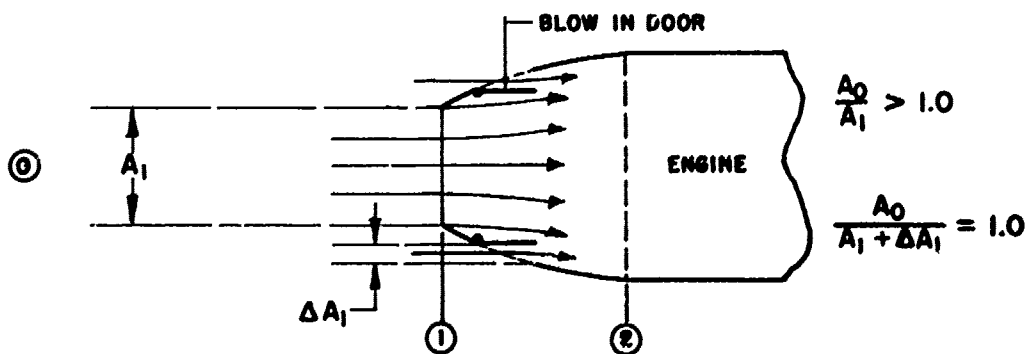
Once the inlet contour is fixed, as in Figure 2.2, the engine Mach number dictates the Mach number that will exist at the entrance to the inlet as long as M_0 is subsonic. If M_2 is held constant at the design Mach number of 0.3, the flow pattern for $M_0 \neq M_{0DES} = 0.8$ will be as shown in Figure 2.3. An added incremental force will result due to the curved stream lines ahead of the inlet face. This force is a drag term (additive drag) if A_1 is greater than A_0 and a "thrust" if A_1 is less than A_0 . When $A_1 > A_0$, the airflow that could have been captured by A_1 at the free stream Mach number is greater than that which is actually captured and the difference is "spilled" over.



(a) Off design Operation ($M_0 > M_0$ design)



(b) Off design Operation ($M_0 < M_0$ design)



(c) Blow In Door Operation ($M_0 < M_0$ design)

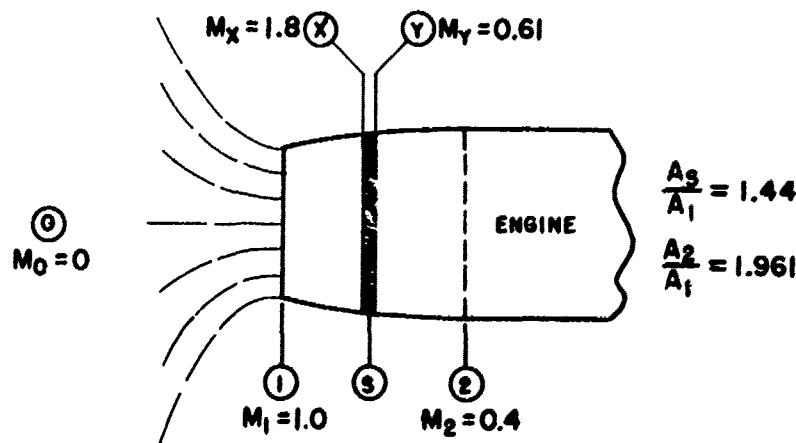
SUBSONIC INLET OPERATING OFF DESIGN

FIGURE 2.3

In addition to the incremental force present when $A_0 \neq A_1$, flow separation is likely to occur either externally when $A_1 \gg A_0$ or internally when $A_0 \gg A_1$. The external separation merely adds an additional drag force. Internal separation, however, can result in distortion on the compressor face as well as low recovery due to the high velocity of the flow entering the inlet. Distortion, if severe enough, can cause compressor stall (see Section 2.2). If the inlet design is such that stall might occur or recovery is unacceptable, auxiliary inlet doors are installed near the inlet entrance to effectively increase A_1 (see Figure 2.3c). These doors may be mechanically actuated, or opened automatically by the static pressure imbalance present if $M_1 > M_0$ ($A_0/A_1 > 1.0$).

Although the preceeding discussion assumed a constant engine Mach number, similar flow patterns will result if M_0 is held on design and M_2 is permitted to vary. For example, if $M_0 = M_{0DES}$ and $M_2 < M_{2DES}$, the flow pattern of Figure 2.3a would result. Conversely the pattern of Figure 2.3b would follow if $M_2 > M_{2DES}$. It is to be noted that the discussion of additive drag also applies here.

One interesting development can occur when the engine Mach number is increased for a constant A_2/A_1 . If M_2 were increased from 0.3 (see Figure 2.2), M_1 would increase. When M_2 reaches 0.315, M_1 approaches unity (critical operation). Further increase in M_2 will not change M_1 but will result in a normal shock wave located within the inlet (supercritical operation). Even if $M_0 = 0$ there would be a shock. Figure 2.4 shows a case with $M_2 = 0.4$ and $M_0 = 0$. Under this mode of operation, the pressure recovery is low due to the large loss in total pressure across the shock. Additionally, flow distortion may result from the interaction of the shock with the boundary layer (shock induced separation). This phenomenon is being explored, however, as a possible means for noise abatement. It would not be necessary to go very much above unity in the inlet to induce separation and the recovery would not be significantly reduced.



SUBSONIC INLET OPERATING SUPERCRITICALLY

FIGURE 2.4

For all subsonic inlets, it is evident that a compromise must be made when selecting the proper A_2/A_1 so that the inlet can operate throughout the aircraft envelope without serious problems.

Although the figures depict sharp inlet lips, all subsonic inlets have rather blunt, smooth lips. This feature reduces the problem of flow separation.

SUPERSONIC INLET DESIGNS

Low Supersonic Applications ($M_0 < 1.2$ to 1.3)

Aircraft designed to fly at maximum Mach numbers of 1.2 to 1.3 may utilize an inlet design much like the subsonic inlet. If an inlet similar to that shown in Figure 2.2 is flown supersonically the following will result: With $M_2 = 0.3$ and $M_0 > 1.0$, a normal shock will form ahead of the inlet as shown in Figure 2.5. The shock will be positioned so as to permit diffusion after the normal shock to the Mach number existing at the inlet lips. If M_2 is held constant, and M_0 is increased, the shock will move closer to the inlet until it attaches.

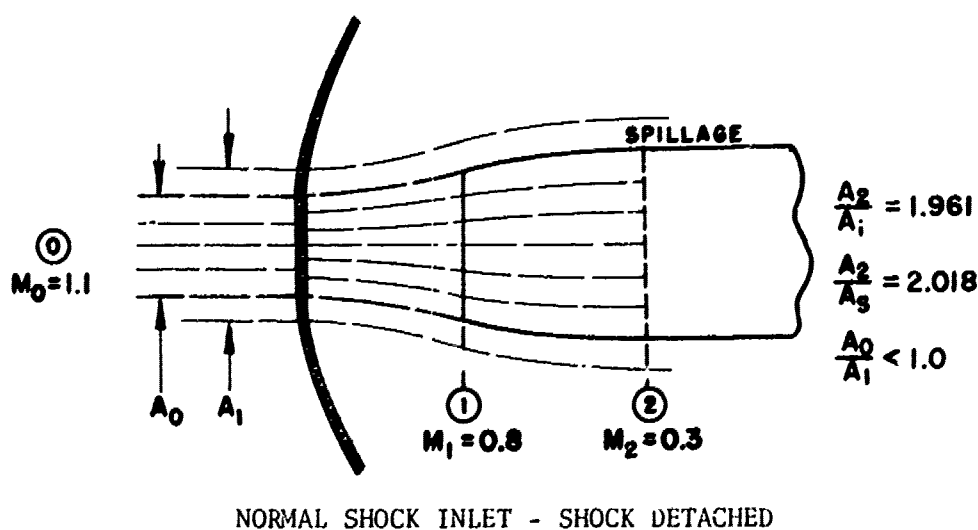


FIGURE 2.5

The free stream Mach number at which attachment occurs will be that supersonic Mach number which will shock down to a subsonic Mach number of 0.8. For the given design ($A_2/A_1 = 1.961$), this value of M_0 is 1.275 (see Figure 2.6). When the shock is attached, the inlet is said to be operating on design and $A_0/A_1 = 1.0$. At this free stream Mach number, there is no spillage as contrasted to the detached shock case. A further increase in M_0 or an increase in M_2 will cause the shock to be swallowed,

its location being a function of M_0 and M_2 . Note that M_1 will be the same as free stream Mach as long as the shock is attached or swallowed.

The inlet just described is classified as a normal shock or all external compression inlet.

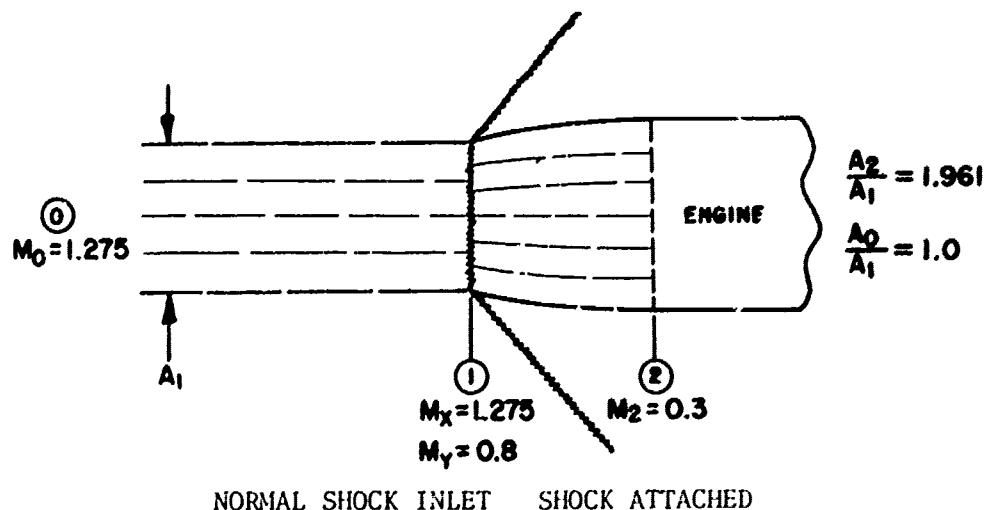
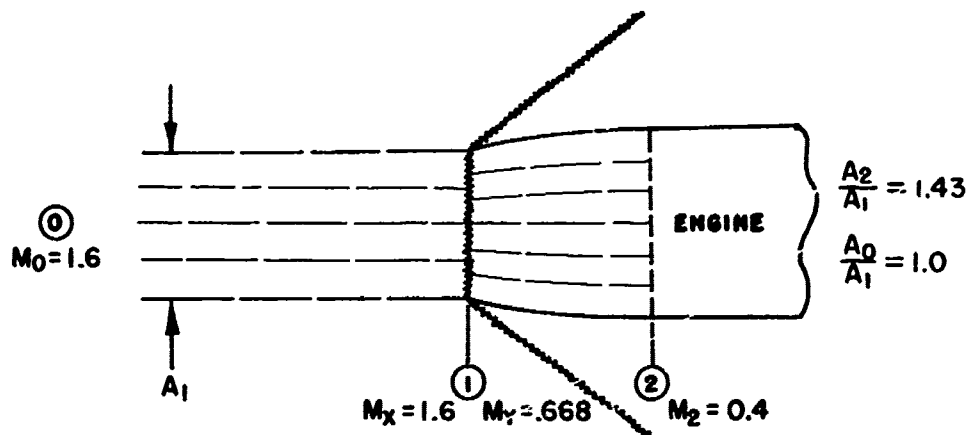


FIGURE 2.6

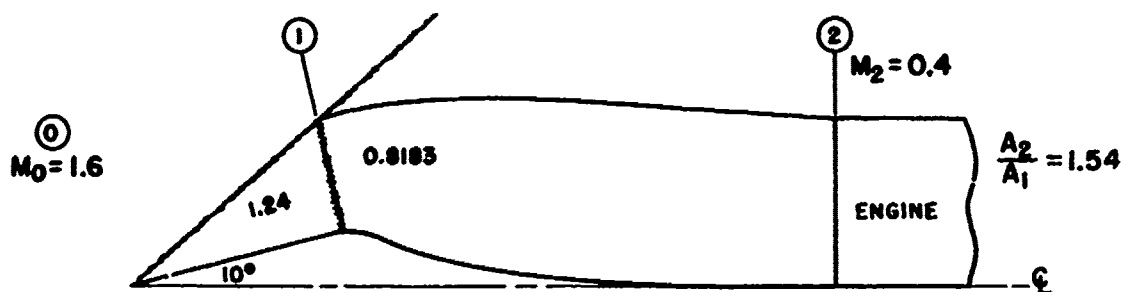
High Supersonic Applications ($M_0 > 1.3$)

It can be seen from Reference (1) that the inlet recovery for a free stream Mach number of 1.3, exclusive of friction and flow separation losses, is 0.979. This loss results from the unavoidable loss in total pressure (entropy increase) across a normal shock. As the free stream Mach number increased, the recovery rapidly decreases with an attendant thrust loss. For aircraft designed to operate above Mach numbers of approximately 1.3, further design features must be utilized to minimize this loss.

If a normal shock inlet were designed to operate at a free stream Mach number of 1.6 and an engine Mach number of 0.4, the ideal recovery would be 0.8952 (Figure 2.7a). If the flow is decelerated first through an oblique shock, then a normal shock, as shown in Figure 2.7b, the ideal recovery will be higher (0.975). The recovery is dependent on the number of oblique shocks and the ramp angle. The recovery is obviously improved with this design termed a single oblique, external compression inlet. The duct diverges aft of the inlet lip to continue an ideally isentropic deceleration to the engine Mach number. On design operation, as shown in the figure, is characterized by intersection of both normal and oblique shocks at the inlet lip. Derivatives of this inlet may utilize multiple oblique shocks which further increase recovery.



(a) Normal Shock Inlet - On Design $M_0 = 1.6$

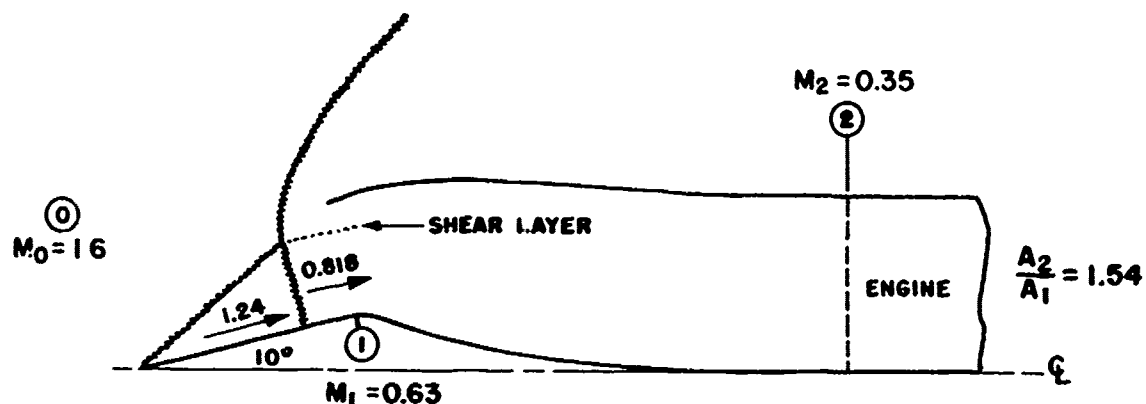


(b) Multiple Shock Inlet - On Design $M_0 = 1.6$

EXTERNAL COMPRESSION INLETS - ON DESIGN

FIGURE 2.7

Operating the inlet shown in Figure 2.7b at "off-design" conditions results in problems not unlike those encountered with the normal shock inlet operating supersonically. If M_2 were decreased ($M_0 = M_0$ design), M_1 (Mach number at inlet lip) must also decrease. The normal shock, however, will no longer be attached since the Mach number after the normal shock will be above M_1 , necessitating diffusion to the lower Mach number. Figure 2.8 shows this situation. It is to be noted that the flow after the oblique shock is similar in character to that shown on Figure 2.5.



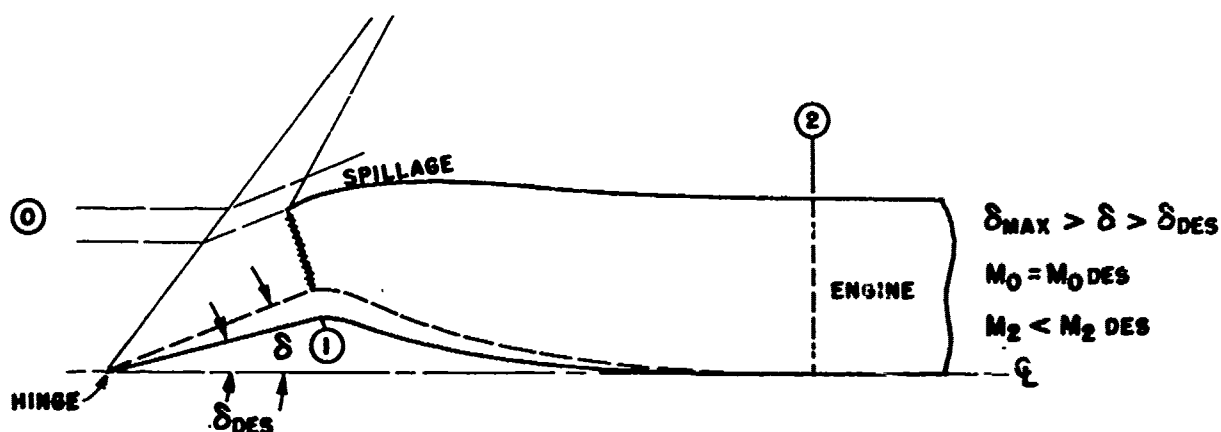
MULTIPLE SHOCK INLET - OFF DESIGN

FIGURE 2.8

The problem with the inlet operating under these conditions is the attendant spillage and the possibility of distortion and inlet flow unsteadiness (buzz). This results because a portion of the air entering the engine has gone through a normal shock from 1.24 and a portion through a normal shock from 1.6. This produces a shear layer (distortion) as shown on Figure 2.8. If the problem is considered severe enough, the normal shock can be adjusted to the inlet lip by one or a combination of several means. If bleed doors are opened downstream of the inlet entrance but prior to the engine, the total airflow through A_1 will increase until M_1 corresponds to the subsonic Mach number downstream of the normal shock. The doors would of course have to be scheduled as a function of both free stream and engine Mach numbers to maintain ideal conditions. Data show that bleeding air in this manner can more than offset the effects of a detached normal shock. A second means used to attach the normal shock is to increase M_1 by decreasing A_1 , in order to match it to the subsonic Mach number after the normal shock. This could be performed by increasing the ramp angle, decreasing A_1 as shown by the dashed line on Figure 2.9. Caution must be exercised when increasing the ramp angle, for if the angle exceeds the maximum permitted by the free stream Mach number (see Reference 1), the oblique shock will detach. If this situation results, a second ramp angle may be added to decrease A_1 . For $M_0 = M_0$ design and $M_2 < M_2$ design, increasing the ramp angle causes the supersonic Mach number after the oblique shock to decrease. The Mach number at the inlet lip (M_1) increases at a faster rate as a result of the decrease in area (A_1). There is one condition where the subsonic Mach number after the normal shock will equal that dictated by the engine Mach number. When this condition results, the normal shock will attach. As shown on Figure 2.9, the oblique shock no longer intersects at the lip, resulting in supersonic spillage and some drag. The drag increase as a result of spillage is generally less than the increase in thrust realized from the variable ramp angle.

The inlet area could also be decreased by deflecting the external lip inboard. This would again prevent the intersection of the oblique shock on the lip.

Similar geometry changes, in the opposite direction, would be required if M_2 were increased above the design value. This condition, like that of the subsonic inlet would cause the normal shock to locate itself inside the inlet. The further the shock moves down the inlet, the stronger the wave will be and the larger the attendant losses.



ADJUSTING INLET AREA WITH A VARIABLE RAMP

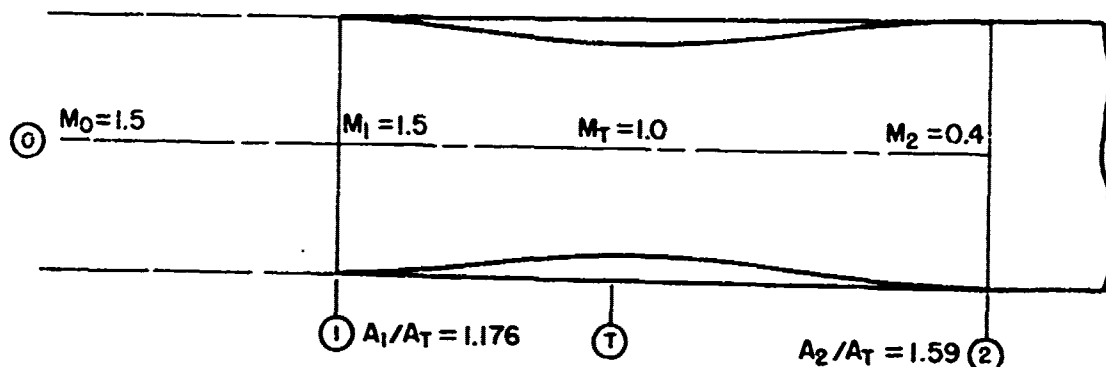
FIGURE 2.9

Thus far, the only off design operation discussed was that resulting from $M_2 \neq M_2$ design. A free stream Mach number (M_0) different from M_0 design will result in an oblique shock which will not intersect the lip. If $M_0 > M_0$ design, the oblique shock will tend to intersect inside the inlet lip. Further, the Mach number after the shock will be greater, causing the normal shock to move downstream and into the inlet. A rather complicated shock pattern will result upstream of the normal shock. With $M_0 < M_0$ design, both shocks will be outside the inlet and a portion of the flow will be spilled over the inlet lips. It is most desirable to relieve this condition by one of the means previously discussed.

It should be clear that any off design operation produces problems. The ultimate goal would be to have a fully variable inlet so that all flight/engine conditions are on design. The variable geometry inlets described above attempt to achieve this goal but caused other problems. The process of selecting the optimum variable geometry inlet is rather detailed to say the least. Obviously each configuration must be weighed, comparing the gains (increased thrust, reduced drag) to the penalties (cost, weight, reliability).

There is another type of supersonic inlet worthy of discussion; this type is the all internal compression inlet. The basic theory is

that if supersonic flow is decelerated isentropically to a Mach number of unity by a converging duct, it can then be further decelerated in a diverging duct to the proper engine Mach number. It will be assumed, for illustration, that this inlet will be designed to operate at a free stream Mach number of 1.5 and an engine Mach number of 0.4. Such a design, as shown in Figure 2.10, will have no shocks and the recovery will be limited only by viscous effects.



INTERNAL COMPRESSION INLET - ON DESIGN

FIGURE 2.10

Assuming fixed contours, the problem with this design is getting the inlet started. The magnitude of this problem will be demonstrated by starting with static conditions ($M_0 = 0$) and progressively increasing the free stream Mach number to the design Mach of 1.5.

Static Operation - $M_0 = 0$

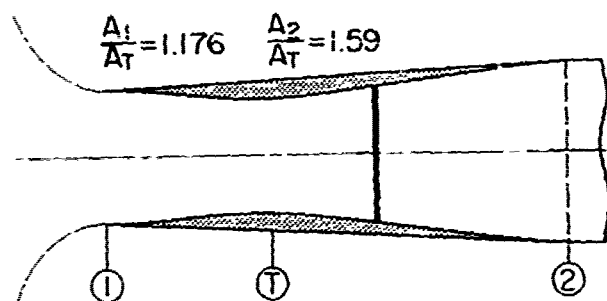
For operation with $M_0 = 0$ and with $M_2 \leq 0.4$, the inlet will have an M_1 range from 0 to 0.6 and a corresponding M_T range of 0 to 1.0. There will be no shock wave present.

With $M_0 = 0$, if $M_2 \geq 0.4$, M_1 will remain constant at 0.6 while the throat Mach number holds at 1.0. In this case, a normal shock will be located at or downstream from the throat. See Figure 2.11a.

Subsonic and Sonic Operation - $M_0 \leq 1.0$

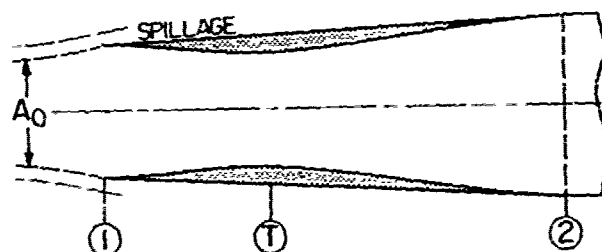
As long as $M_2 \geq 0.4$, the flow pattern outside the inlet will be solely dependent on M_0 since M_T will be unity fixing M_1 at 0.6. Under these conditions, with $M_0 < 0.6$, $A_0 > A_1$ resulting in possible internal flow separation. When $M_0 > 0.6$, $A_0 < A_1$ and there will be flow spillage. In any case, the normal shock wave will still stand downstream from the throat.

If $M_2 < 0.4$, all internal flow will be subsonic and external flow patterns will be a function of both M_2 and M_0 . Figure 2.11b summarizes subsonic and sonic operation.



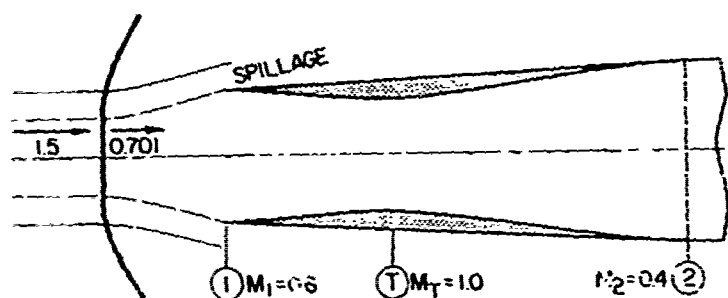
M_0	M_1	M_T	M_2	NOTES
0	0	0	0	NO FLOW
0	.43	.66	.3	ALL SUBSONIC
0	.6	1.0	.4	NO SHOCK
0	.6	1.0	.5	SHOCK

(a) Static Operation

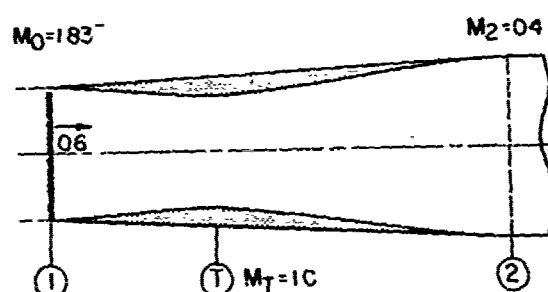


M_0	M_1	M_T	M_2	NOTES
<1.0	<0.6	<1.0	<0.4	ALL SUBSONIC
<1.0	0.6	1.0	≥0.4	$M_2 > 0.4$ SHOCK
1.0	0.6	1.0	≥0.4	$A_0 = A_T$

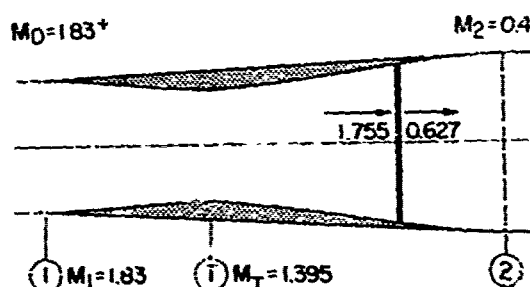
(b) Subsonic-Sonic Operation



(c) Design Conditions (Approached from $M_0 = 1.5$)



(d) Shock Attached



(e) Shock Swallowed

INTERNAL COMPRESSION INLET - STARTING PROCESS

FIGURE 2.11

Supersonic Operation - $1.0 < M_0 < 1.5$

When the engine is operating below a M_2 of 0.4 in a supersonic free stream, a normal shock will be formed ahead of the inlet such that the subsonic Mach number behind the shock will diffuse to the Mach number at the inlet lips. All internal flow will again be subsonic.

If $M_2 \geq 0.4$, the inlet entrance Mach number is 0.6 and two shocks will be present, one ahead of the inlet and the other between the throat and the engine. Figure 2.11c shows the inlet operating at the design condition ($M_0 = 1.5$, $M_2 = 0.4$). Though the design parameters are satisfied, the flow is not the same as that shown in Figure 2.10. The inlet is termed "unstarted".

Several techniques available to start the inlet will be discussed here. The first technique is called overspeeding. If M_0 is increased, the subsonic Mach number behind the external shock will decrease. When this Mach number reaches 0.6 (assuming $M_2 \geq 0.4$), the shock will attach. This attachment will occur, for the given design, at $M_0 = 1.83$, as shown in Figure 2.11d. As soon as the shock attaches, any further increase in M_0 will cause the shock to be swallowed and to stand in the diverging portion of the duct as shown in Figure 2.11e. Once the inlet is started, M_0 may be reduced to 1.5 and the flow will be like that shown in Figure 2.10. Any disturbance which will make M_0 less than 1.5 or M_2 less than 0.4 will cause the shock to be expelled. Because of this possibility, the normal shock is ordinarily located just downstream from the throat, providing a range of free stream Mach numbers at which to operate. A slight decrease in recovery will result, but operation will be stable down to some minimum M_0 . Although this starting technique is quite adequate for a wind tunnel, it is not used in aircraft for obvious reasons.

An alternate scheme, useable in aircraft applications, for starting the inlet utilizes variable geometry. Referring to Figure 2.11c, the inlet will start if M_1 is 0.701. To make $M_1 = 0.701$, A_1/A_T must be decreased from 1.176 to 1.09 since $M_T = 1.0$. This may be accomplished by either decreasing A_1 or increasing A_T . Decreasing A_1 would be the simpler course from an aerodynamic point of view, but mechanization may be difficult. Alternatively, A_T may be increased, whereupon both M_T and M_1 will decrease with M_2 constant. In order to increase M_1 , as was desired, M_2 must also be increased so as to keep $M_T = 1.0$ while the throat area increases. While M_2 could be increased by increasing power, a simpler solution would be the incorporation of bleed doors just upstream from the compressor to effectively increase M_2 without necessitating power changes. The flow through the engine will be the same since the additional flow admitted is bypassed. When the shock is swallowed, the bleed doors are closed and A_T decreased to locate the shock in a stable position, usually just downstream from the throat. In practice, as soon as the aircraft goes supersonic, the shock is swallowed by means of the geometry changes described above.

This, basically, is the operation of a converging-diverging inlet or internal compression inlet. It has the advantage of having the best recovery at high supersonic speeds. The main disadvantage is that the restarting process is comparatively long if the normal shock is expelled. In addition, these inlets prove to be long and heavy.

There are many other inlet designs which are in use. All supersonic inlets use one or combinations of the designs discussed here. The basic design philosophy for all inlets has been presented above.

INLET CONTROLS

It is difficult to present a treatise on inlet controls without getting into a discussion of a particular inlet. Basically, the inlet will work if it is contoured to M_0 and M_2 with the variable geometry parts governed by these two basic parameters. In theory, measuring both M_0 and M_2 is simple; problems arise in that M_2 , being a function of P_{T2}/P_2 , cannot be sensed by a single probe if there is distortion. One probe will not permit proper inlet operation unless discretely located to represent the average M_2 . Measurement of M_0 may appear much less complex. In aircraft where the inlet is away from the fuselage, the free-stream Mach number is the same Mach number presented to the inlet. With fuselage mounted engines, the inlet Mach number is different from M_0 due to shock waves or expansion due to the aircraft. Thus, a total-static probe must be located at the engine or corrected for these conditions. In addition to the problem of finding a good average (P_T/P_S) location, the flow conditions may change as a function of angle of attack or sideslip. If this is so, the inlet control system must adequately measure the effect and respond fast enough to alter the geometry.

2.2 COMPRESSORS

The function of the compressor in a turbojet is to increase the total pressure of the air. This section will describe how a particular form of energy (work) is mechanically converted into a total pressure rise. It would be of no advantage to include compressor efficiency for this discussion, thus, an ideal compressor will be assumed. In addition, all basic concepts will be developed for a single stage compressor (stage to be defined later). Most turbojet engines utilize multi-stage compressors, the consequences of which will be discussed in turn. Finally, a perfect gas will be assumed in which γ and C_p are constant. Variable γ and C_p would only confuse the derivation to the point where the basic purpose of the discussion (to show how a compressor works) would be obviated.

The energy equation for a compressor with steady flow and no heat addition is, from Table 1.1:

$$W_c = h_{T_3} - h_{T_2} \quad (2.2)$$

Equation 2.2 can be expanded into static conditions with associated velocities as:

$$W_c = (h_3 - h_2) + (C_3^2 - C_2^2) / 2gJ$$

Where: C is the absolute velocity of the air relative to the engine (not the rotor).

Since C_p is assumed constant:

$$W_c = C_p (T_3 - T_2) + (C_3^2 - C_2^2) / 2gJ$$

or

$$W_c = C_p T_2 [(T_3/T_2) - 1] + (C_3^2 - C_2^2) / 2gJ$$

The assumption of 100% compressor efficiency permits the use of the isentropic relations, thus:

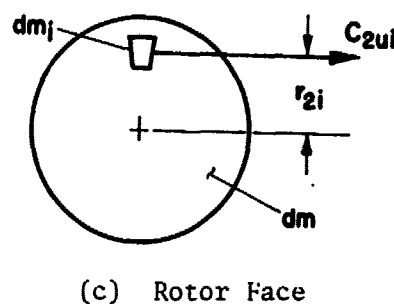
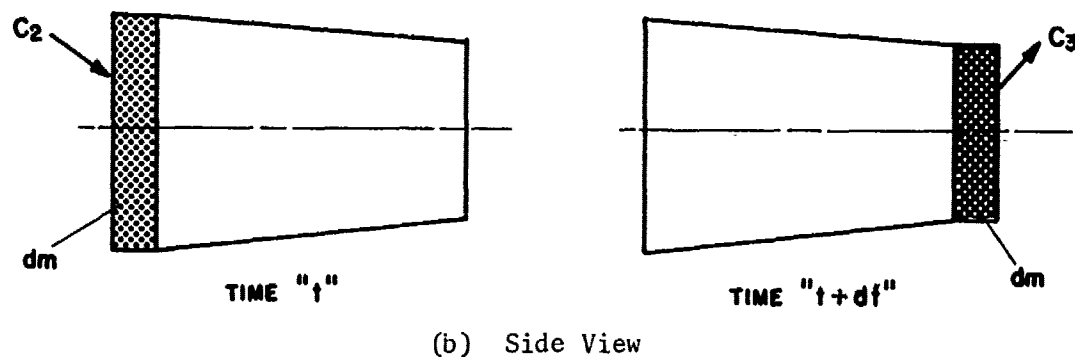
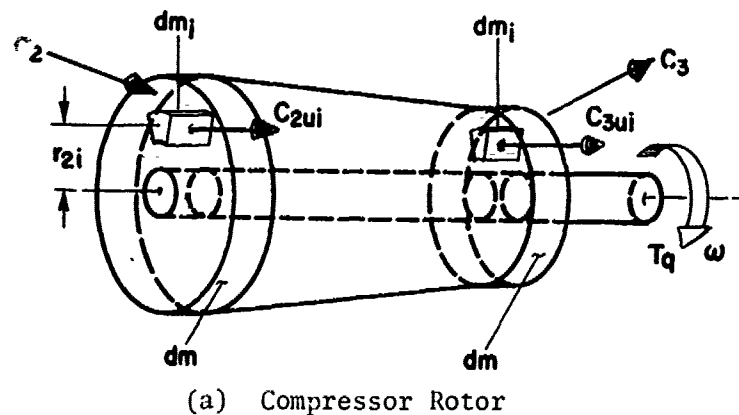
$$\frac{T_3}{T_2} = \left(\frac{P_3}{P_2} \right)^{\frac{\gamma-1}{\gamma}}$$

Substituting:

$$W_c = C_p T_2 \left[\left(\frac{P_3}{P_2} \right)^{\frac{\gamma-1}{\gamma}} - 1 \right] + (C_3^2 - C_2^2) / 2gJ \quad \text{BTU/lb} \quad (2.3a)$$

$$W_c = C_p T_{T_2} \left[\left(\frac{P_{T_3}}{P_{T_2}} \right)^{\frac{\gamma-1}{\gamma}} - 1 \right] \text{ BTU/lb} \quad (2.3b)$$

Thus, the work that is put into the flow "in some way" increases the static pressure (P_3/P_2) and the kinetic energy ($C_3^2 - C_2^2$) combining to increase the total pressure (P_{T_3}/P_{T_2}). The problem now is to determine how the work gets into the flow. It will be assumed that the work is available in the form of a torque acting on a rotating disk as shown in Figure 2.12a.



COMPRESSOR ROTOR DISK

FIGURE 2.12

The torque, supplied through a shaft rotating with an angular velocity, produces the power. When the power is divided by the airflow, the work per pound of air is determined. With the proper design, the rotor will impart a change in angular momentum to the entering gas. The time rate of change in angular momentum is the torque. To relate this to a total pressure increase, the following derivation is presented.

It is assumed that at time "t" a slug of gas with mass dm enters the rotor disk at a uniform absolute velocity C_2 as shown in Figure 2.12. A small particle of that mass, dm_i , will have an angular momentum of:

$$\text{Angular Momentum} = dm_i r_{2i} C_{2ui}$$

where r_{2i} is the radius to dm_i and C_{2ui} is the tangential component of the absolute velocity C_2 . The total momentum will, therefore, be the sum of the momentums of all small particles dm_i .

$$dm C_{2u} r_2 = \sum_{i=0}^{\infty} dm_i r_{2i} C_{2ui} \quad (2.4)$$

The radius r_2 may be visualized as the radius of a ring with mass dm, having the same angular momentum as the total disk.

A similar argument can be formulated for the angular momentum of the same slug of gas when it reaches the exit section of the rotor at time $t + dt$. Thus, the angular momentum of the mass dm leaving the rotor is:

$$dm C_{3u} r_3 = \sum_{i=0}^{\infty} dm_i r_{3i} C_{3ui} \quad (2.5)$$

In the time interval dt , the only change in angular momentum, for steady flow, is the difference between (2.5) and (2.4). The torque, therefore, is:

$$Tq = \frac{dm C_{3u} r_3 - dm C_{2u} r_2}{dt}$$

or

$$Tq = (dm/dt) (C_{3u} r_3 - C_{2u} r_2) \quad (2.6)$$

But the mass flow rate (dm/dt) , has been assumed constant and expressed as W/g .

$$Tq = (W/g) (C_{3u} r_3 - C_{2u} r_2) \quad (2.7)$$

Now the power is the product of the torque and the angular velocity.

$$P = (W a / g) (C_{3u} r_3 - C_{2u} r_2) \omega$$

Noting that the rotor tangential velocity at a radius r is:

$$u = r \omega$$

and substituting:

$$P = (W a / g) (C_{3u} u_3 - C_{2u} u_2)$$

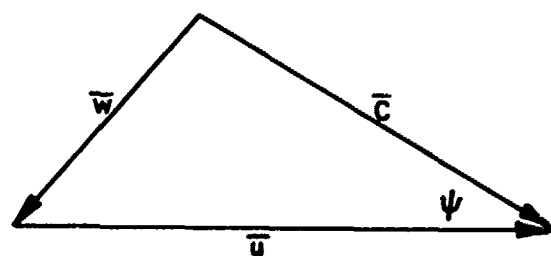
The compressor work per pound of air is simply P/Wa , thus:

$$W_c = \frac{C_{3u} u_3 - C_{2u} u_2}{gJ} \text{ BTU/lb} \quad (2.8)$$

The numerator of this expression is termed the "change in whirl".

The form of (2.8) does not lend itself directly to understanding how a pressure rise is obtained, since C_u is not an easy velocity to work with.

Figure 2.13 shows the vector relationship of C and u . It should be recalled that we are considering the angular momentum change of a ring with u_2 and u_3 the velocity at the radius of the ring.



\vec{C} = ABSOLUTE VELOCITY VECTOR OF AIR

\vec{u} = ABSOLUTE VELOCITY VECTOR OF ROTOR

\vec{w} = VELOCITY OF AIR RELATIVE TO THE ROTOR

$$\vec{C} = \vec{w} + \vec{u}$$

COMPRESSOR VELOCITY VECTORS

FIGURE 2.13

Applying the law of cosines to the vector diagram of Figure 2.13,

$$|\vec{w}|^2 = |\vec{C}|^2 + |\vec{u}|^2 - 2 |\vec{u}| |\vec{C}| \cos \psi$$

where \bar{w} is the magnitude of \vec{w} and is equal to w . This also holds for $|\vec{u}|$ and $|\vec{C}|$, then:

$$w^2 = C^2 + u^2 - 2 u C \cos \psi \quad (2.9)$$

Noting that $C \cos \psi$ is C_u , the tangential component of the absolute velocity vector, we have:

$$w_2^2 = C_2^2 + u_2^2 - 2 C_{2u} u_2$$

for the inlet to the rotor and, for the exit:

$$w_3^2 = C_3^2 + u_3^2 - 2 C_{3u} u_3$$

Combining these two equations:

$$C_{3u} u_3 - C_{2u} u_2 = \frac{1}{2} [(w_2^2 - w_3^2) + (C_3^2 - C_2^2) + (u_3^2 - u_2^2)]$$

Substituting this expression into (2.8) yields:

$$W_c = \frac{1}{2gJ} [(w_2^2 - w_3^2) + (C_3^2 - C_2^2) + (u_3^2 - u_2^2)] \quad (2.10)$$

Comparing (2.10) with (2.3a) and (2.3b), shows how the pressure increase is accomplished in a compressor.

Referring to (2.10), the terms $(w_2^2 - w_3^2)$ and $(u_3^2 - u_2^2)$ are referred to as the "internal" effect, while $(C_3^2 - C_2^2)$ is termed the "external" effect. (The term $(u_3^2 - u_2^2)$ is also called the "centrifugal" effect.)

The total pressure will increase across a stage if:

1. The absolute velocity increases $(C_3^2 - C_2^2) > 0$, and/or
2. The air is discharged at a radius greater than that at which it was admitted $(u_3^2 - u_2^2) > 0$, and/or
3. The relative velocity decreases through the rotor $(w_2^2 - w_3^2) > 0$.

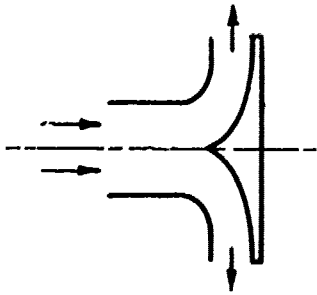
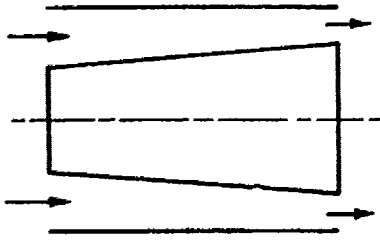
It is seen, by comparing (2.10) with (2.3a), that any static pressure rise occurring, results from the terms comprising the internal effect.

So far, there has been no mention regarding the physical construction of the rotor which produces the vector diagram shown in Figure 2.13. Air compressors for turbojet engines are divided into two categories; the first is termed a centrifugal compressor so named because it utilizes the centrifugal effect $(u_3^2 - u_2^2 > 0)$. Air is admitted to the rotor in an axial direction (parallel to the axis of rotation of the compressor) and discharged from the rotor radially (perpendicular to the axis of rotation). In contrast, the axial flow compressor both admits and discharges the air from the rotor in an axial direction. This type of compressor does not utilize the centrifugal effect to achieve a pressure rise.

A comparison is made in Table 2.1 between the centrifugal and axial flow compressors.

TABLE 2.1

COMPARISON OF CENTRIFUGAL AND AXIAL FLOW COMPRESSORS

	Centrifugal	Axial
Sketch		
Stage Pressure Ratio	3.0 to 4.0	1.05 to 1.15
Efficiency	70 to 80%	80 to 85%
Multistaging	Complex Ducting	Simple Ducting
Airflow	Low - Compared to Frontal Area	High - Compared to Frontal Area
Applications	Turboprops Auxiliary Power Units "Low" Thrust Engines	Turbojets - "High" Thrust Turbfans

for most contemporary turbojet powered aircraft applications, the axial flow compressor is utilized. The remainder of the discussion will, therefore, be devoted to the axial flow compressor.

The equation to be applied for the analysis of the axial flow compressor is:

$$\begin{aligned}
 W_c &= \frac{1}{2gJ} [(C_3^2 - C_2^2) + (\bar{w}_2^2 - \bar{w}_3^2)] = C_p T_{T_2} \left[\left(\frac{P_{T_3}}{P_{T_2}} \right)^{\frac{\gamma-1}{\gamma}} - 1 \right] \\
 &= C_p T_2 \left\{ \left[\left(\frac{P_3}{P_2} \right)^{\frac{\gamma-1}{\gamma}} - 1 \right] + \frac{(C_3^2 - C_2^2)}{2gJ} \right\} \quad (2.11)
 \end{aligned}$$

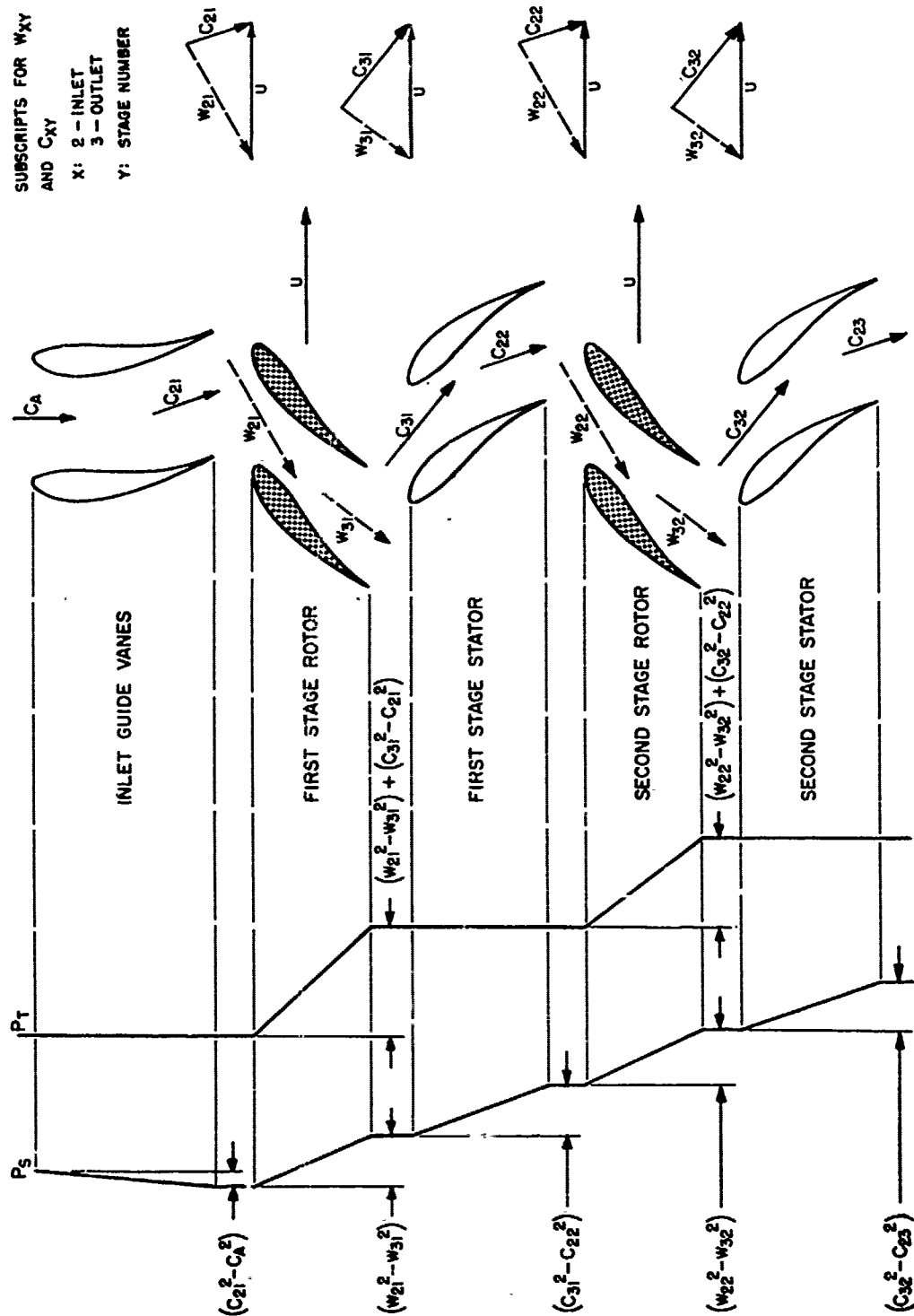
Notice that the term $(u_3^2 - u_2^2)$ is missing, since, for the axial flow compressor, $u_3 \approx u_2$.

From Figure 2.13, it is seen that one of the prime variables, controlling the pressure rise, is the angle ψ between vectors \vec{C} and \vec{u} . This angle is controlled by fixed inlet guide vanes (IGV). The function of the IGV is to direct the absolute velocity vector to the rotor. Some engine manufacturers choose to slightly accelerate the air through the IGV; this technique tends to reduce the effects of separation from the inlet walls. After the IGV, is a row of rotor blades followed by another set of fixed blades termed stators.

In most axial flow compressors, there are additional rotors installed on the same shaft. The rotor's prime functions are to increase the kinetic energy of the air ($C_3^2 - C_2^2$) and increase the static pressure ($w_2^2 - w_3^2$). The stators serve to direct the flow in the proper direction to the next rotor stage and increase the static pressure by slowing down the absolute velocity. A stage in an axial flow compressor is a rotor-stator combination. A two stage compressor would, for example, be composed of: IGV, rotor, stator, rotor, stator.

Figure 2.14 shows the pressure variation through a two stage axial flow compressor. The following should be considered to better understand the figure:

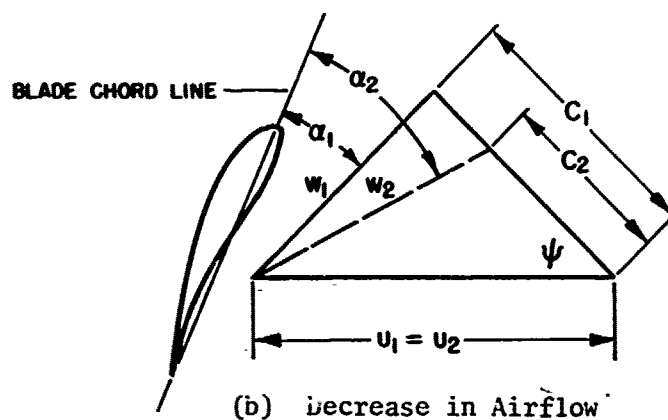
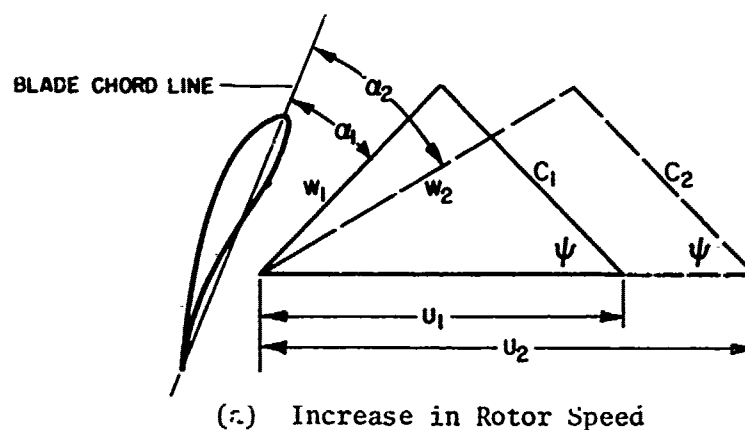
1. The schematic represents a cut at a constant radius. Another flow pattern would result at other radii due to the variation in u with radius.
2. Equation (2.11) is applied at each rotor.
3. There is no change in energy in the stators, merely an exchange of kinetic energy for static pressure rise.



COMPRESSOR ENERGY TRANSFER

FIGURE 2.14

It has been shown that the total pressure rise in an axial flow compressor is the result, in part, of increasing the absolute velocity across the rotor. The increase is the result of a momentum change, which requires a force in the direction of the change. The force is transmitted to the gas by the blades of the rotor. It is clear that the magnitude of the force, and therefore the pressure rise, is going to be a function of the velocity at which the blade is approached (relative velocity), the angle of attack that the blade makes with this velocity, and the characteristics of the blade. The sources of angle of attack variation are shown in Figure 2.15.

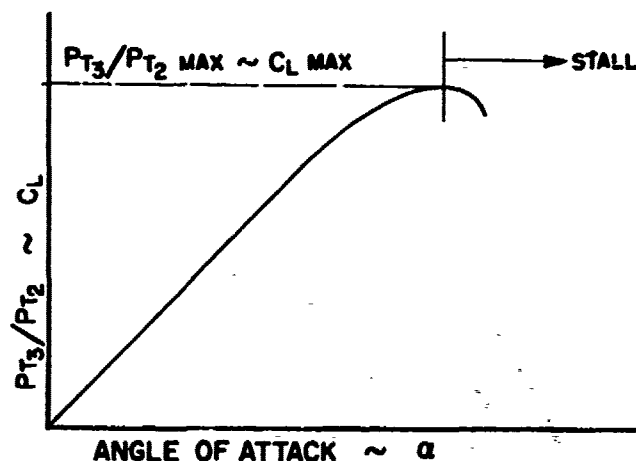


COMPRESSOR BLADE ANGLE OF ATTACK

FIGURE 2.15

The energy transfer to the air through a rotor blade is similar to what occurs with an aircraft wing. The lift on a wing is analogous to the force producing a momentum change and pressure rise through the rotor blade. The lift is a function of angle of attack, which when increased will cause the lift to reach a maximum value and then decrease with further increases in angle of attack. It would be expected, therefore, that in a compressor, a maximum pressure ratio would be reached depending

on the angle of attack of the rotor blades. This is indeed the case, and a plot of pressure ratio as a function of angle of attack is similar to that of wing lift coefficient as a function of angle of attack, as shown in Figure 2.16.



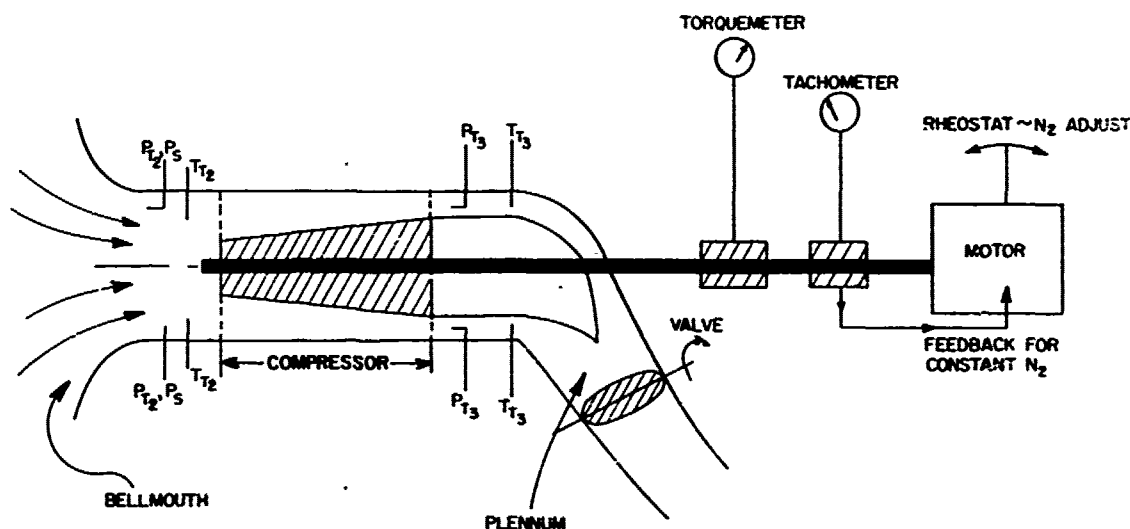
PRESSURE RATIO - WING LIFT ANALOGY

FIGURE 2.16

At angles of attack greater than that for maximum lift coefficient, a wing is said to be stalled. If a compressor is operated in a similar region, it too is termed stalled.

To continue the analogy, the plot of C_L vs α for a wing section exhibits a decrease in maximum lift with increasing altitude or decreasing Reynolds number. The maximum pressure ratio available for a given angle of attack will also be less in a compressor at high altitudes.

The purpose of the analogy of a compressor with a wing is to make the compressor performance map become a logical consequence. When a compressor is designed and built, the performance is determined experimentally. The pressure ratio will be determined as a function of rotor speed and airflow. Rotor speed and airflow are directly proportional to the tangential rotor speed and the absolute velocity vector, respectively. By referring to Figure 2.15, it is clear that for a constant ψ (a fixed quantity for fixed geometry engines), the angle of attack on the blade is going to increase with increasing engine speed or decreasing airflow. The test procedure is to set a rotor speed and vary the airflow by adjusting an air valve (see Figure 2.17). Usually the air valve is wide open initially and as the valve is closed down, pressure ratio is tabulated as the airflow decreases. When pressure ratio starts to decrease with decreasing airflow, the compressor is stalled. The stall point on a multistage compressor is defined whenever any one stage



COMPRESSOR PERFORMANCE TEST RIG

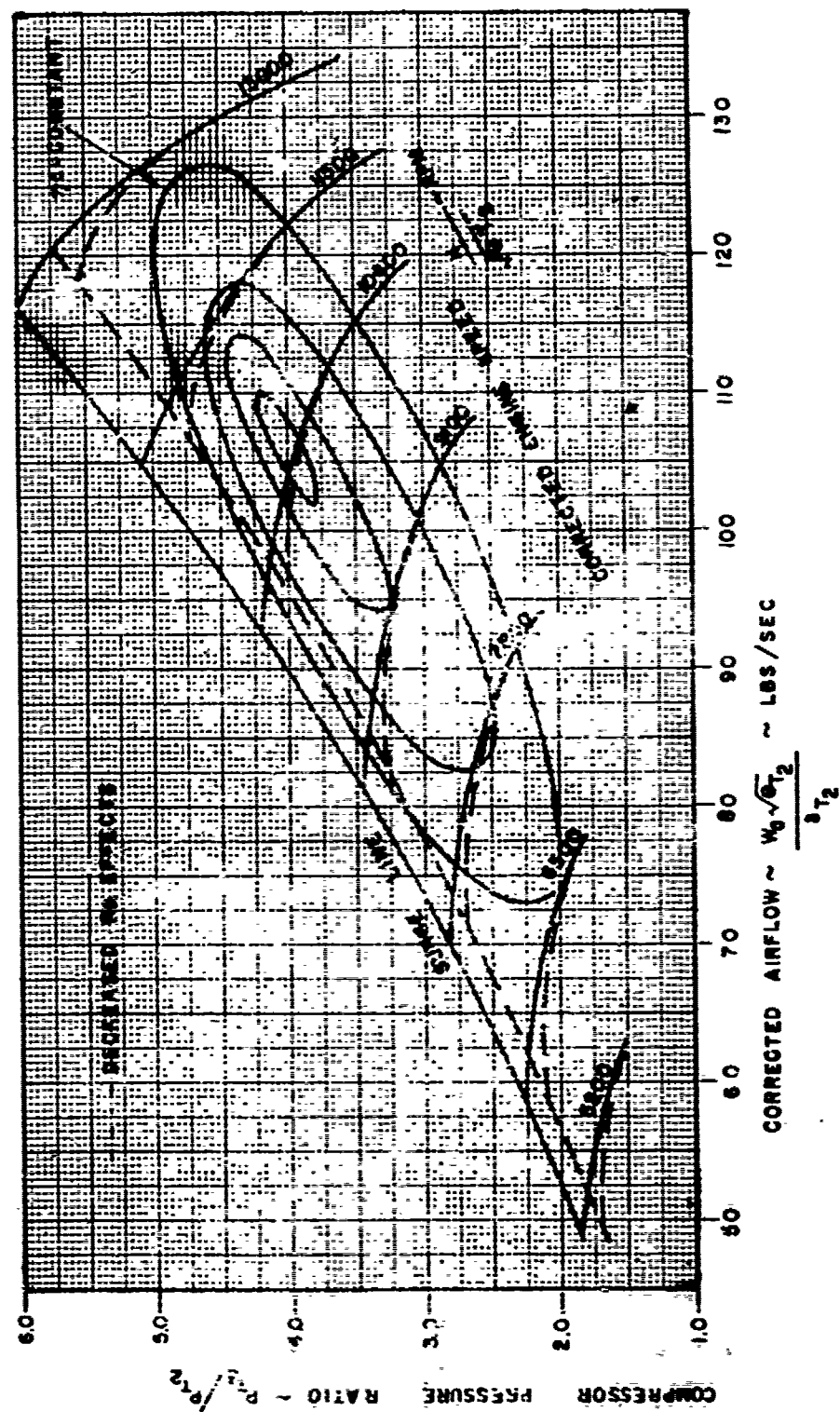
FIGURE 2.17

is stalled even though other stages may not be stalled. The procedure is continued for other rotor speeds and when all the data are obtained, a performance map is plotted. A typical map is shown on Figure 2.18. It is seen that the pressure ratio is presented as a function of corrected airflow and corrected rotor speed. It can be shown from (2.3a) and (2.10) that this form generalizes the data. The effects of decreased Reynold's number (increased altitude) are shown as the dashed lines. Notice that at high altitude for a given corrected airflow and rotor speed, the stall margin (the increment in rotor speed to the stall line at constant airflow, or the increment in airflow to the stall line at constant rotor speed) is reduced.

During the test to define the performance map, sufficient test data can be obtained to determine the compressor efficiency. With P_{T3}/P_{T2} and T_{T2} (all are measured quantities), the ideal work can be computed from equation (2.2). The actual work per pound of air is computed from the torque, rotor speed, and airflow, which are also measured. Contours of constant efficiency can then be established. Figure 2.18 also shows these curves. It is seen that there is one point on the compressor map that produces the highest efficiency. Operation here, at the design point, is most desirable since it contributes to high overall engine efficiency. This leads to the discussion of "off-design" operation.

When an inlet was designed, there were many more flight/engine conditions producing off-design operation than those resulting in on design operation. Since an acceptable inlet design depends, in part, on satisfactory off-design operation, modification by an inlet control system for off-design conditions may have been required. The compressor is not unlike the inlet in this respect. Some operating conditions must be

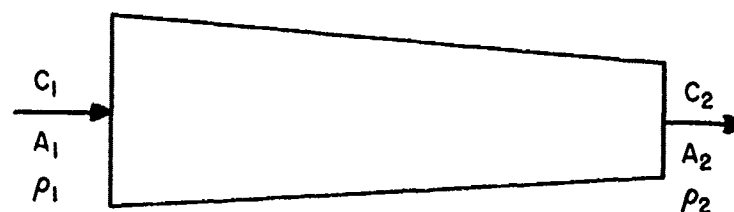
COMPRESSOR PERFORMANCE MAP



selected to which the compressor is designed. When this is done, the consequences of off-design operation must be considered, and geometry changes programed if deemed necessary.

For a single compressor blade, there will be a unique angle of attack that will prove most efficient when producing a pressure rise. Compare this to a wing producing lift; for all angles of attack below stall, the lift will increase with increasing angle of attack. There will be an angle of attack that is most efficient. That angle is at maximum lift to drag ratio, more lift can be generated by increasing angle of attack, but the drag will increase rapidly. Conversely less lift can be generated but the drag won't go down as fast. It can be seen, that for optimum operation at the design point, it is necessary to have the angle of attack on all blades the same. Since most axial flow compressors have multiple stages, the absolute velocity of the air entering a rear stage should, therefore, be the same as that entering a forward stage. To clarify, the change in tangential rotor speed from forward stages to rear stages is negligible, and the angle that the chord line makes with the plane of rotation of the blade is approximately constant. These two requirements restrict the absolute velocity to be constant front to rear.

Since the absolute velocity is very close to being uniform, the variation in tangential rotor speed from hub to tip is compensated for by twisting the blade to hold angle of attack constant along the blade. By restricting the absolute velocity to be constant at the design point, the flow area must decrease from front to rear as shown below (refer to Figure 2.19).



AREA VARIATION IN A MULTISTAGE COMPRESSOR

FIGURE 2.19

The airflow through the compressor is given by:

$$W_a = \rho_3 A_3 C_3 = \rho_2 A_2 C_2$$

or

$$\frac{A_3}{A_2} = \frac{\rho_2 C_2}{\rho_3 C_3} = \frac{\rho_2}{\rho_3} = \frac{v_3}{v_2}$$

(2.12)

since $C_3 = C_2$ at design. v is the specific volume.

For an isentropic process,

$$\left(\frac{v_3}{v_2}\right)^{-\gamma} = \frac{P_3}{P_2} \quad \text{or} \quad \frac{v_3}{v_2} = \left(\frac{P_3}{P_2}\right)^{-\frac{1}{\gamma}}$$

$$\frac{A_3}{A_2} = \left(\frac{P_3}{P_2}\right)^{\frac{1}{\gamma}}_{\text{DES}} = 1 / \left(\frac{P_3}{P_2}\right)^{\frac{1}{\gamma}} < 1.0 \quad (2.13)$$

From (2.13), the area ratio A_3/A_2 will be fixed by a pressure ratio (P_3/P_2) corresponding to the design compressor pressure ratio $(P_{T3}/P_{T2})_{\text{DES}}$. Ideally, a variable area ratio would permit tailoring the engine to off design operation, however, this is not possible.

The consequences of fixing the area ratio will be considered. From a mechanical point of view, the engine diameter can be reduced, permitting installation of the various accessories which would otherwise make the engine larger in diameter. Also, by shortening the radius on the rear blades in addition to shortening the blades themselves, the centrifugal forces are decreased. This is of prime importance considering that the temperature on the rear blades is higher than that on the front blades. Thus, it is seen, from a mechanical point of view, that an area ratio A_3/A_2 less than unity is no major problem; in fact, it may be an asset.

From a thermodynamic viewpoint, operation at an off design condition is a different situation.

OPERATION WITH P_{T3}/P_{T2} GREATER THAN DESIGN PRESSURE RATIO

From equations (2.12) and (2.13),

$$\frac{A_3}{A_2} = \frac{C_2}{C_3} \left(\frac{P_3}{P_2}\right)^{-\frac{1}{\gamma}} = 1 / \left(\frac{P_3}{P_2}\right)^{\frac{1}{\gamma}}_{\text{DES}}$$

Thus,

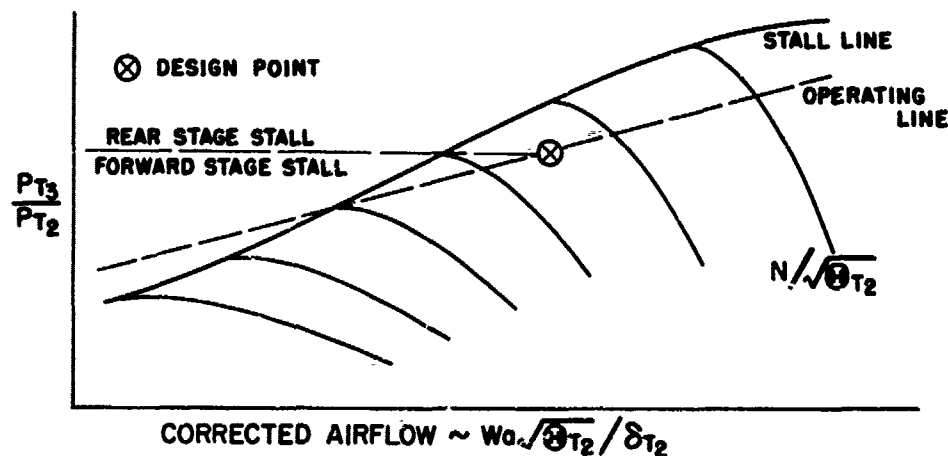
$$\frac{C_2}{C_3} = \left[\frac{(P_3/P_2)}{(P_3/P_2)_{\text{DES}}} \right]^{\frac{1}{\gamma}} \quad (2.14)$$

If $(P_3/P_2) > (P_3/P_2)_{\text{DES}}$, then $C_2/C_3 > 1$ and the angle of attack on the rear stages will be greater than that on the forward stages. Since the performance map represents the net or sum of the performance of all stages, the stall line above $(P_{T3}/P_{T2})_{\text{DES}}$ will be the result of the rear stages stalling since $\alpha_3 > \alpha_2$ ($C_2 > C_3$).

The design of the compressor is such that the engine will not operate so far above the design pressure ratio so as to cause the engine to stall. It should be remembered that, if an engine does stall at high power settings, it is the result of rear stage stall.

OPERATION WITH P_{T3}/P_{T2} LESS THAN DESIGN PRESSURE RATIO

Operation at pressure ratios less than design pressure ratio will produce a condition in which the angle of attack on the front stages is greater than that on the rear. In fact, tests show that the rear stages approach such a low angle of attack that the flow chokes. This condition will then cause the front stages to stall. If the engine is to be operated in this regime scheduled geometry changes will be required. It will be shown in Section 3, that a turbojet engine, when matched with all the components, will have a unique operating line which could look like that shown on Figure 2.20. As long as the engine is operated with corrected airflow above the intersection of the operating line and the stall line there would be no serious problem. Many times operation below this intersection is required and, in order to maintain engine operation, the stall line must be adjusted up or the operating line adjusted down. Adjusting the operating line will be discussed in Section 3 when the engine is matched. The following will deal with altering the stall line, which will require some means of geometry change.



OFF-DESIGN COMPRESSOR OPERATION

FIGURE 2.20

Bleed Valves

The problem to be alleviated is the high angle of attack on the forward stages. One of the ways to decrease the angle is to increase

the airflow. This can be accomplished by bleeding some of the air at a point downstream from the stages at high angles of attack. This will relieve the choked condition on the rear stages since, if an airflow passage is choked, the only way the airflow can be varied is to change the area. Opening bleed valves effectively increases the area. These valves are placed circumferentially around the compressor case, aft of the stalled blades but before the choked blades, in such a way to bleed air uniformly and avoid airflow distortion with resulting unequal blade loading. The air that is bled off is dumped overboard or utilized for cooling the nacelle. Bleed valves can be scheduled as a function of corrected rotor speed $N/\sqrt{\theta T_2}$ such that for decreasing rotor speed, the valves will program open on a schedule such that they will be fully open at some lower rotor speed. Another much simpler technique is to have the valves open below a specified pressure ratio and close above. Either method usually utilizes the fuel control to schedule by $N/\sqrt{\theta T_2}$ or P_{T3}/P_{T2} .

One of the main disadvantages is that there is a performance loss since work has been performed on the air that is spilled overboard.

Variable Stators

The bleed valves solve the high angle of attack problem by relieving the situation that causes it in the first place, i.e., choked flow in the rear stages. By utilizing variable stators, the angle of attack on the rotor blades can be controlled directly to keep the angle below the stall. Referring to Figure 2.13, the angle ψ is altered by directing the C vector, thus changing the vector w. The schedule for the variable stators is based on corrected rotor speed. Some of the main disadvantages are the mechanical complexity involved in linking all the rows of stators together and the increased air leakage resulting in lower compressor efficiency.

Twin Compressors

If a single compressor were divided into two separate compressors with the rear half designed to operate at a higher angle of attack, by rotating at a higher speed, the stalled condition on the forward stages would be relieved. The higher angle of attack on the rear stages increases the passage area, permitting an increase in airflow and lowering the angle of attack on the forward stages. This solution is considered the most efficient means of solving the problem since it does not involve bleeding (lost energy) or complex variable stators with associated air leakage. The prime disadvantage is the greatly increased weight due to the multiple shafts.

The geometry changes which must be incorporated to have a compressor operate over a wide range have, as expected, advantages and disadvantages. Selection of a given solution must consider all advantages and disadvantages.

Other problems associated with compressor operation will be discussed when this component is matched with the turbine and nozzle.

2.3 COMBUSTORS

The usual process by which energy gets into the engine to be converted into kinetic energy for thrust is by combustion. Part of this energy, in a turbojet, is utilized to drive the turbine. For the purpose of understanding the design of a combustor, it will be assumed that the combustion process will be required to attain a given turbine inlet temperature and that the combustion process takes place with a minimum of total pressure loss. In actual operation, a specific turbine inlet temperature will not necessarily be stipulated; the fuel control will supply the necessary amount of fuel to maintain a given rotor speed. This will be discussed in more detail in Section 3. In order to obtain a given turbine inlet temperature, there are generally four items which must be considered.

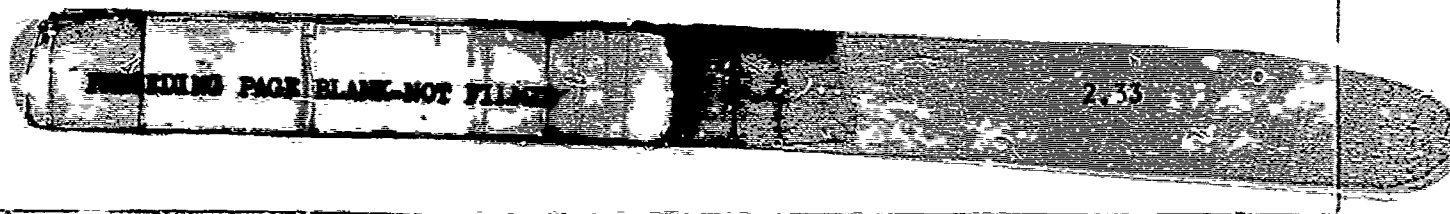
PROPER FUEL AIR PROPORTIONS

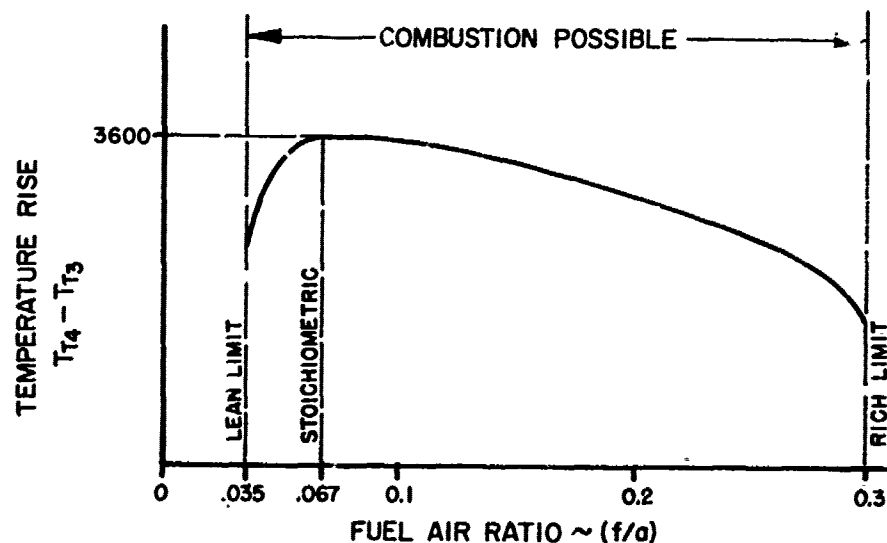
For all of the fuel to be burned, there will exist a unique fuel air ratio (f/a) such that all of the fuel combines with all of the air releasing all of the latent energy in the fuel. For the turbine fuels utilized at present (JP-4 and JP-5), if 100% combustion is realized, 18,500 BTU of heat will be released for each pound of fuel burned. The proper mixture, called stoichiometric $(f/a)_{st}$, for 100% combustion is approximately 0.067 or 15 parts air to 1 part fuel. It is obviously desirable to have the maximum heat released.

If a container had a mixture which was richer than stoichiometric, i.e. $(f/a) > (f/a)_{st}$, and this mixture were ignited, the temperature rise would be less than if the mixture were stoichiometric. This is so because there is insufficient air to burn all of the fuel, and the unburned fuel must be heated, thus reducing the potential temperature rise of the mixture. If $(f/a) \gg (f/a)_{st}$, a limit will be reached for which combustion cannot take place. This limit, called the rich limit, is approximately 0.30 or 3 parts air to 1 part fuel.

If the container had a lean mixture, i.e. $(f/a) < (f/a)_{st}$, and this mixture were ignited, the temperature rise would also be less than if the mixture were stoichiometric because the air which is not burned must be heated, reducing the maximum temperature rise. If $(f/a) \ll (f/a)_{st}$, the lean limit, below which combustion cannot take place, will be reached. This value is approximately 0.035 or 30 parts of air to 1 part fuel. It is seen that the increment $[(f/a)_{st} - (f/a)_{lean}]$ is much smaller than $[(f/a)_{st} - (f/a)_{rich}]$.

Figure 2.21 shows a sketch of the temperature rise as a function of fuel/air ratio. The maximum temperature rise shown is 3600°R. Theoretically a rise of 4000°R could be obtained, but gas disassociation reduces this value to approximately 3600°R.





COMBUSTION TEMPERATURE RISE

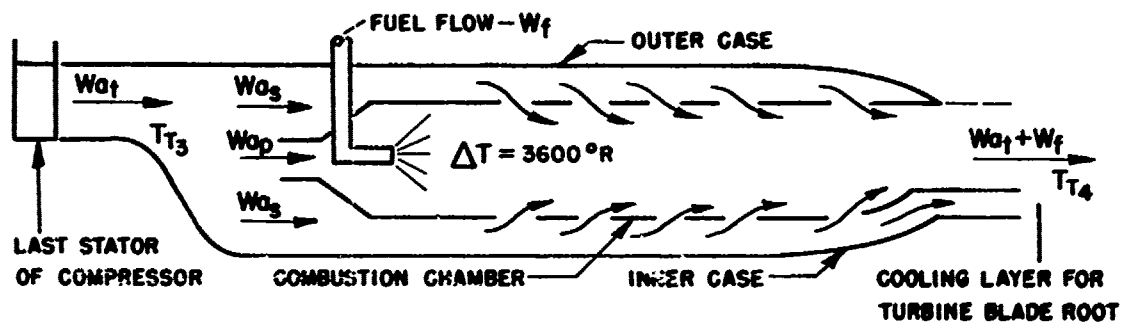
FIGURE 2.21

In Section 1, the equation (1.20) for the ideal fuel flow was derived; this equation is repeated below, slightly modified.

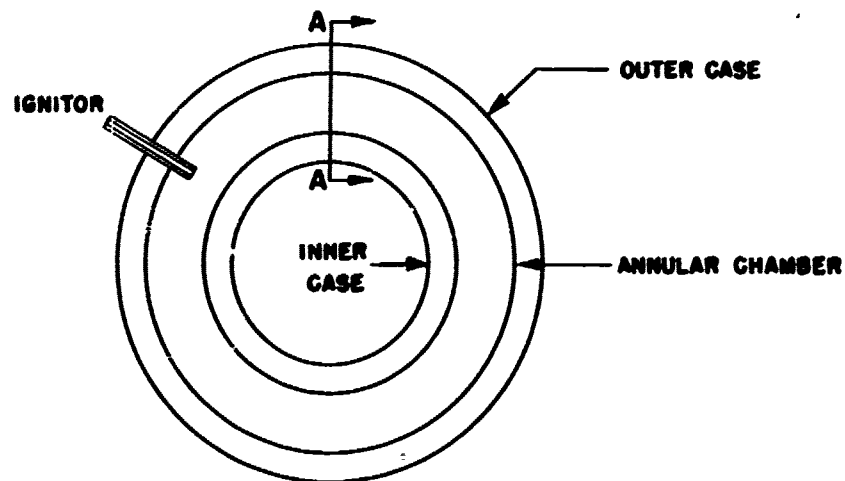
$$(f/a) = C_p \frac{T_{T_4} - T_{T_3}}{H.V.} \quad (2.15)$$

As mentioned in that section, the above equation is a simplified form of a more complex relationship which accounts for C_p variations with temperature and fuel/air ratio.

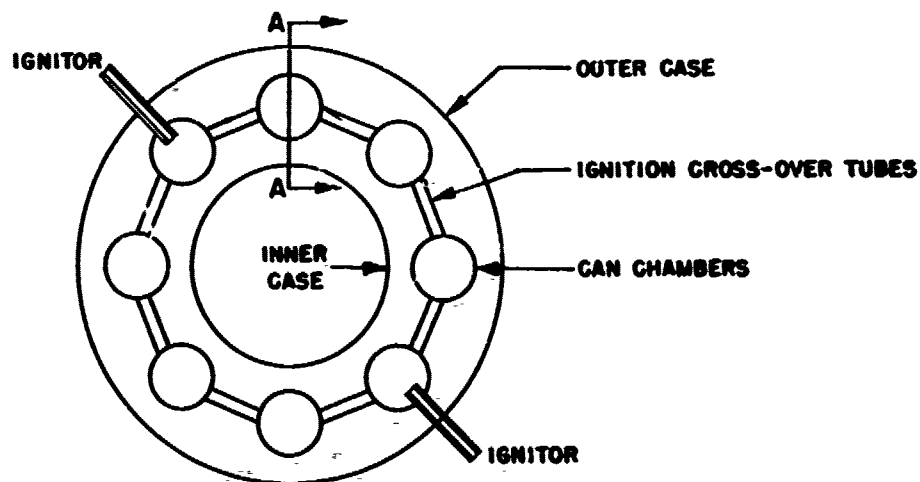
Most turbojet engines currently in production are operating at maximum power with a temperature rise not exceeding 2000°R . This is the result of limitations placed on turbine blades. It is seen from (2.15) that the fuel/air ratio for $T_{T_4} - T_{T_3} = 2000^\circ\text{R}$ is roughly 0.02 ($C_p = 0.24$, $H.V. = 18,500$). The maximum fuel/air ratio that the engine requires is, therefore, less than the fuel/air ratio that can support combustion. In addition, for power settings below maximum, the required fuel/air ratio is even less. This problem requires a device which would be able to support combustion, yet still limit the combustor discharge temperature. The solution is a combustion chamber in which a portion of the air is mixed with fuel, preferably in stoichiometric proportions, to get complete combustion, and then gradually combined with the balance of the air to reduce the temperature. A schematic of a combustion chamber cross section for the annular and can-annular type combustors is shown in Figure 2.22. The performance of both are essentially the same.



(a) Side View Cross Section



(b) Front View Annular Chamber



(c) Can-Annular Chamber

COMBUSTION CHAMBER CROSS SECTION

FIGURE 2.22

All of the airflow (W_a_t) is ducted from the compressor into the combustor. Fuel will be introduced at such a rate to correspond to the desired temperature rise. If the rise is 2000°R , for example, the ratio W_f/W_a_t is approximately 0.02. Prior to introducing the fuel, the airflow is split into two parts: Primary air (W_a_p) and secondary air (W_a_s). The proportions are such that $W_f/W_a_p = 0.067$. Thus:

$$\frac{W_f}{W_a_p} = 0.067, \quad \frac{W_f}{W_a_t} = 0.02, \quad \text{and} \quad W_a_t = W_a_p + W_a_s$$

But,

$$\frac{W_a_s}{W_a_p} = \frac{W_a_t}{W_a_p} - 1 = \left[\frac{\frac{W_f}{0.02}}{\frac{W_f}{0.067}} \right] - 1$$

which yields:

$$\frac{W_a_s}{W_a_p} = \left(\frac{0.067}{0.02} - 1 \right) = 3.35 - 1 = 2.25$$

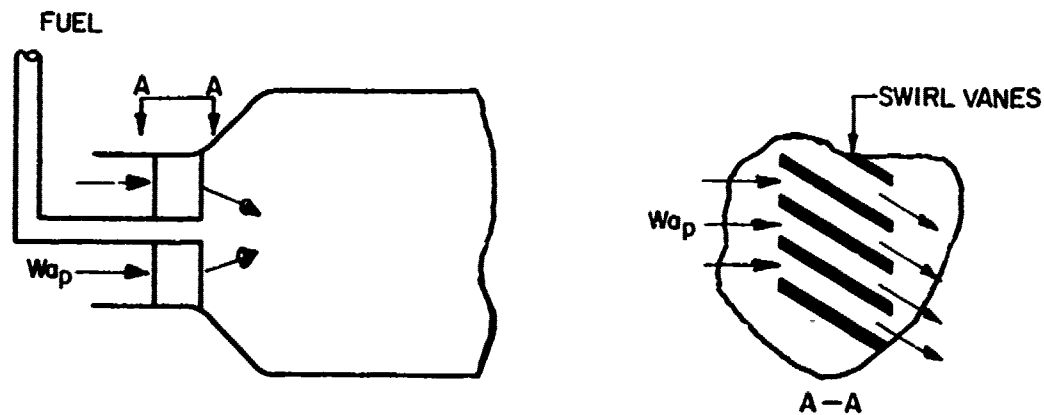
Thus for a combustion chamber designed for a 2000°R temperature rise, the bypass ratio would be approximately 2.25:1.

When the primary fuel/air mixture is burned, the mixture temperature rise will be about 3600°R . As the gas is burning, the secondary airflow is introduced. This flow is admitted to the primary flow in such a way that a film of relatively cool air insulates the chamber lining to keep it from melting. By the time the primary flow gets to the discharge of the combustor, it is combined with all but a small portion of the secondary flow. The desired turbine inlet temperature is therefore obtained. That part of the secondary flow not mixed with the primary air, is directed at the root of the turbine blades for cooling; this is the location of the highest blade stresses.

TURBULENCE - MIXING

The combustion chamber has provided a means for obtaining the correct fuel/air ratio. Combustion will not be possible unless the proportion of fuel and air is completely mixed. Laminar flow is not conducive to good mixing and any means that can be devised to produce turbulence will aid in mixing the primary air with the fuel. Several ways of achieving this are given below.

Swirl Vanes. Primary air is generally flowing in an axial direction prior to entering the combustion chamber. The entrance to the chamber may be fitted with vanes to produce vortices in the flow. This technique is shown on Figure 2.23.



SWIRL VANES

FIGURE 2.23

Baffle Plates. A second means of producing turbulence is through the use of baffle plates. The primary air is admitted to the combustion chamber and then forced through a plate with a series of openings. The openings cause separation, reverse flow, and significant turbulence. Figure 2.24 shows schematically the baffle plate design.

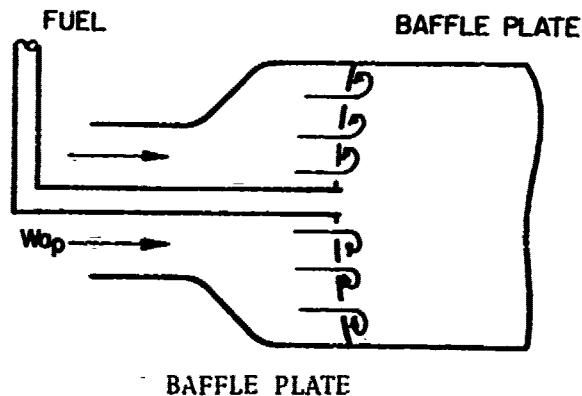
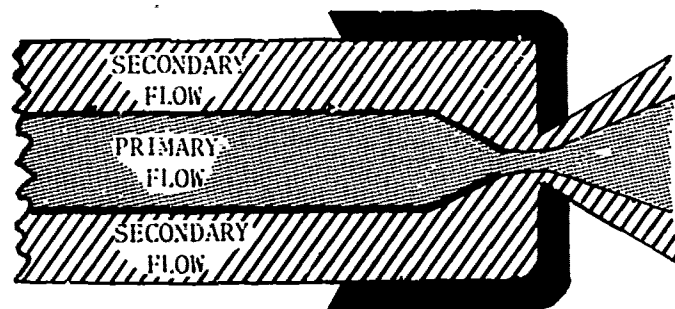


FIGURE 2.24

Spray Pattern. The means by which the fuel is injected into the flow effects the mixing of the fuel and air to a significant degree. Most fuel injectors utilize a spray nozzle to provide a swirling cone-shaped spray pattern. The purpose is to produce small particles of fuel spread over a large area to obtain maximum contact area with the air. By introducing the fuel in a swirl pattern, usually opposite that of the air, thorough mixing is assured. Most nozzle spray heads feature dual concentric orifices (duplex nozzle). The optimum spray pattern (cone-shape) will be obtained, for a given orifice size, at a

given flow. For a fixed discharge area, as the flow decreases, the spray pattern deteriorates. If both orifices are open for high flow and one closed for low flow, the optimum spray pattern will be realized over a larger range of flows. The flow distribution can be governed by the fuel control or internal to the fuel nozzle. A duplex nozzle is shown schematically on Figure 2.25.



DUPLEX NOZZLE

FIGURE 2.25

One other type of fuel injection system is the so-called "candy cane". Basically, fuel is injected in a downstream direction and passes through the "candy cane" along with part of the primary combustor air. This mixture is then returned upstream, mixes with the rest of the primary air and is burned. Advantages of this type system are good fuel vaporization and low fuel pressures required. The main disadvantage is the tendency for the "canes" to crack or break.

IGNITION

In order for combustion to take place, the air and fuel, thoroughly mixed in the proper proportions, must have a temperature above 475°F. During start, the temperature of the air is well below this value. Ignitors, placed in the primary combustion zone, provide the necessary temperature. Usually two ignitors are installed in engines utilizing the can-annular type of combustion chamber (one in each of two cans). When ignition is obtained in these two cans, it is passed onto the remaining cans by cross-over tubes. The process of combustion occurs at temperatures well above 475°F, negating the need for continuous ignition.

TIME FOR COMBUSTION

The flow through the combustion chamber is continuous. Nowhere does it stop, burn, mix with the secondary air, and then start up and enter the turbine. Because the burning mixture is flowing, consideration must be given to the size (length and diameter) of the chamber to insure that the gasses are completely burned and mixed prior to entering the turbine.

Flame propagation speed for laminar flow is approximately 5 FPS and increases to as high as 100 FPS for turbulent flow. The velocity of the air leaving the compressor can be as high as 450 to 600 FPS. It is

obvious that the flow must be slowed down to at least 100 FPS to permit continuous ignition. In addition, the average velocity of the gasses (fuel flow, primary and secondary airflows) must be such that the combustion process is complete before the gasses enter the turbine. This then requires the chamber to be a certain length and diameter.

COMBUSTION CHAMBER OPERATION

The design of the combustion chamber is based on a specific total fuel/air ratio. The bypass ratio W_a_s/W_a_p is defined by selecting the proper primary to secondary area ratio, based on the design W_f/W_a_t , to produce stoichiometric conditions in the primary zone of the combustion chamber. If the W_f/W_a_t changes to a value other than design, stoichiometric conditions will not exist in the chamber. This is demonstrated below:

$$\frac{W_f}{W_a_p} = \frac{W_f}{W_a_t} \times \frac{W_a_t}{W_a_p}$$

But

$$W_a_t = W_a_s + W_a_p$$

thus,

$$\frac{W_f}{W_a_p} = \frac{W_f}{W_a_t} \left(\frac{W_a_s + W_a_p}{W_a_p} \right)$$

Simplifying this:

$$\frac{W_f}{W_a_p} = \frac{W_f}{W_a_t} \left(\frac{W_a_s}{W_a_p} + 1 \right) \quad (2.16)$$

Now at design conditions, $W_f/W_a_p = 0.067$ with $W_f/W_a_t = (W_f/W_a_t)_{DESIGN}$. With these restrictions, (2.16) becomes:

$$\frac{W_a_s}{W_a_p}_{DES} = \frac{0.067}{(W_f/W_a_t)_{DES}} = 1 \quad (2.17)$$

Now $(W_a_s/W_a_p)_{DES}$ is achieved by the ratio of secondary to primary area in the combustor. When selected, the ratio of (W_a_s/W_a_p) becomes essentially constant. Thus, from (2.17)

$$\frac{W_f}{W_a_p} = \left(\frac{W_f}{W_a_t} \right) \cdot k \quad (2.18)$$

Where
$$k = \frac{0.067}{(W_f/W_{a_t})_{DES}}$$

It is seen that only when $(W_f/W_{a_t}) = (W_f/W_{a_t})_{DES}$ does $(W_f/W_{a_p}) = 0.067$. For all other conditions W_f/W_{a_p} will be rich or lean. Care must be taken, obviously, when selecting $(W_f/W_{a_t})_{DES}$ so that the rich or lean limits are not encountered during normal operation. Normal operation includes, not only steady state, but also engine accelerations and decelerations. For the latter, schedules are programed into the fuel control to avoid loss of combustion.

COMBUSTION LOSSES

Section 1.2 defined the two types of losses which will be encountered in the combustion process. It was stated that the ideal combustion process occurs at a constant total pressure. The actual process suffers a loss in total pressure. It can further be seen that the need to install a chamber for combustion and some means to induce turbulence will also cause a drop in total pressure. All losses considered, the pressure drop is roughly 5% for most engines.

The criteria for complete combustion has already been discussed and will not be repeated. Test results show that combustion efficiency generalizes fairly well when plotted against $P_3 T_3 / C_3$ as shown by Figure 2.26.

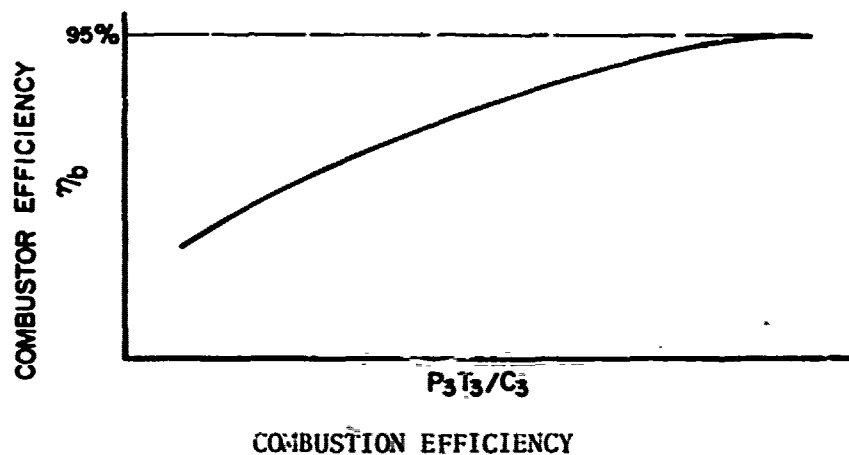


FIGURE 2.26

The rationale for this result is as follows:

Combustion Chamber Pressure. Low combustion chamber pressure indicates low weight flow resulting in low fuel flow with attendant lower pressure

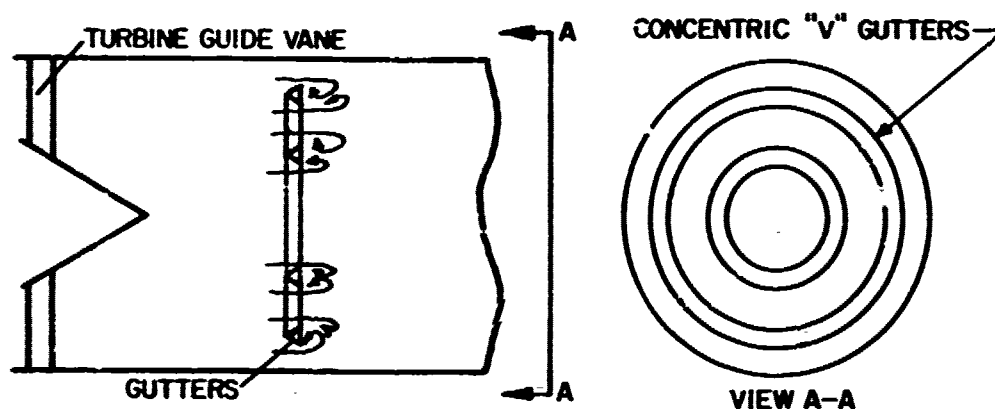
drop across the fuel nozzle. This causes a relatively poor spray pattern compared to the higher flows. As mentioned the duplex nozzle attempts to minimize this.

Combustion Chamber Temperature. Since combustion efficiency depends on good mixing of the fuel and air, the higher the temperature the higher the fuel vaporization rate.

Inlet Velocity. The discussion on time for combustion indicated the relationship of the mixture velocity and combustion chamber length. For any given chamber length, the lower the velocity entering, the more time there will be for complete combustion.

This section has shown how heat is added to a flowing gas in a combustion chamber. The same considerations must be made when an afterburner is designed. Because there is considerable air which did not enter into combustion in the main engine, additional combustion can take place aft of the turbine. Because of this, the maximum temperature entering the nozzle is limited by the amount of air that can be burned. This assumes that there is adequate cooling flow over the afterburner casing. Nozzle area is another factor limiting the maximum nozzle inlet temperature. Section 3 will discuss this limitation.

Thorough mixing of the fuel and air is accomplished through the use of "V" shaped gutters shown schematically on Figure 2.27. These gutters generally are concentric and their purpose is to produce vortices. In addition to serving as a mixing device, the gutters slow the mixed gasses down so that reignition of the mixture can take place. This function led to the term flame holders. Obviously, the complete mixture will not be slowed down. This is the reason for the relatively long afterburner section (often the same length as the basic engine). Even with this length some combustion may take place outside the nozzle.



TYPICAL "V" SHAPED GUTTERS (FLAME HOLDERS)

FIGURE 2.27

Primary ignition may be accomplished by utilizing a pilot burner; a small combustion chamber whose discharge is directed in the vicinity of the flame holders, or through the use of a "hot streak". The latter is merely a burning stream of fuel injected at the discharge of a combustion chamber. Once lit, the A/B is self sustaining. Ignition is initially required because the large quantity of fuel introduced is sufficient to cause rapid cooling when evaporated during mixing.

2.4 TURBINES

The purpose of a turbine in a jet engine is to extract work from the flow to drive the compressor. In addition, the power required for the various accessories is also drawn from the turbine.

Analysis of the energy transfer within the turbine is identical to that performed on the compressor. Reference is made to Section 2.2 for detailed review; only the pertinent concepts will be repeated.

The energy equation for the turbine, assuming 100% efficiency, is:

$$h_{T_4} - h_{T_5} = W_T$$

Expanding this equation yields, for constant C_p :

$$W_T = C_p T_{T_4} \left[1 - \left(\frac{P_{T_5}}{P_{T_4}} \right)^{\frac{\gamma-1}{\gamma}} \right] \quad (2.19)$$

and

$$W_T = C_p T_{T_4} \left[1 - \left(\frac{P_5}{P_4} \right)^{\frac{\gamma-1}{\gamma}} \right] + \frac{C_4^2 - C_5^2}{2gJ} \quad (2.20)$$

The work, per pound of air, produced by the turbine is:

$$W_T = \frac{1}{gJ} \left(C_{4u} u_4 - C_{5u} u_5 \right) \quad (\text{Ref. 2.8}) \quad (2.21)$$

Using (2.9) and Figure 2.13, the turbine work is:

$$W_T = \frac{1}{2gJ} [(C_4^2 - C_5^2) + (u_4^2 - u_5^2) + (w_5^2 - w_4^2)] \quad (2.22)$$

A comparison of this equation with (2.19) and (2.20) shows that the static pressure ratio (P_4/P_5) increases as a function of the increase in the last two terms of (2.22). These terms are called the internal effect (centrifugal and diffusion, respectively). Thus, work is extracted from the flow by:

1. Introducing the flow at a radius greater than that at which it is discharged ($u_4 > u_5$). This will increase $[1 - (P_5/P_4)^{\gamma-1/\gamma}]$ or, since P_4 is constant, decrease P_5 .
2. Expand the flow through the rotor so that $w_5 > w_4$. This is accomplished by decreasing the flow passage. The result is to lower P_5 since P_4 is constant. This term ($w_5^2 - w_4^2$) is often-times called reaction.

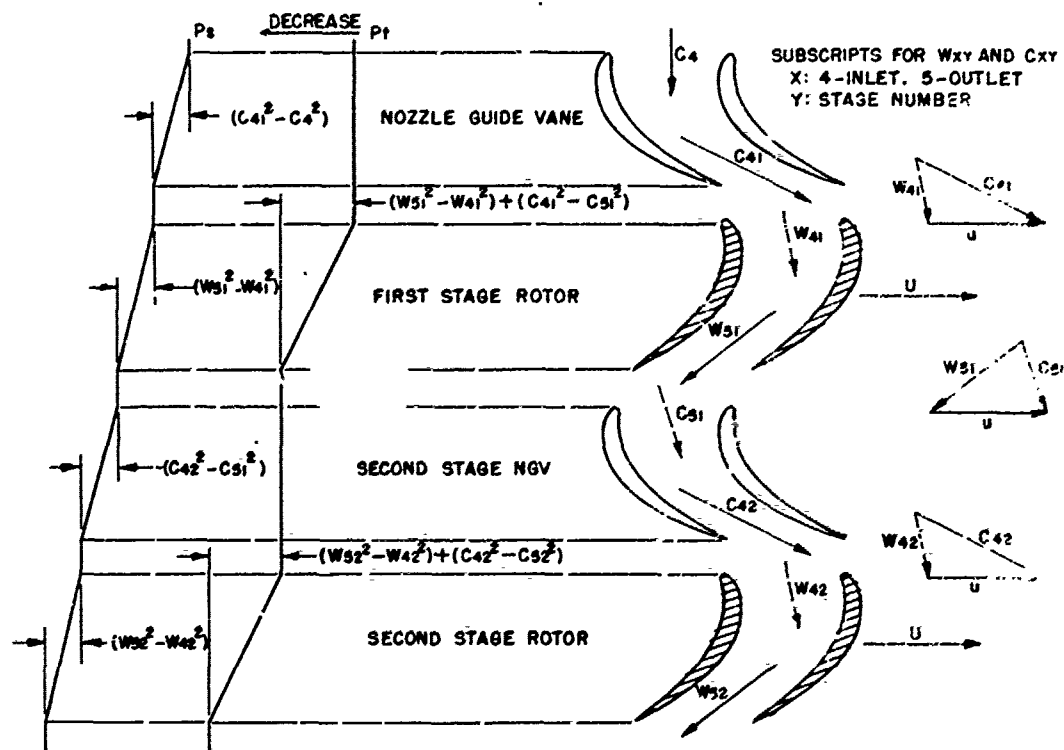
3. Finally, decrease the absolute velocity of the flow ($C_5 < C_4$). This is performed by letting the rotor turn (see Figure 2.13). Since this effect is related to momentum, $(C_4^2 - C_5^2)$ is termed impulse.

Similar to the compressor, there are two general categories of turbines; these are the centrifugal and axial flow turbines. The centrifugal type is not utilized because of size, ducting and problems associated with operating a casting at elevated temperatures and speeds. All turbine powered aircraft utilize the axial flow type. Deletion of the contribution of the centrifugal effect leaves the kinetic and internal diffusion (see equation 2.22). Recall that the axial flow compressor also relied only on these two functions to obtain a pressure rise. It was determined in Section 2.2, that the pressure rise per stage of an axial flow compressor is lower than that of the centrifugal compressor, primarily due to the lack of the centrifugal effect. Theoretically, the remaining terms could make up for this loss, but it was shown that the impulse was derived from a blade which, if at high enough angle of attack, would stall limiting the maximum pressure rise and therefore, the work that could be put into the flow. The stall was triggered by flow separation due to the adverse (increasing in the direction of flow) pressure gradient. In a turbine, there is a negative pressure gradient ($P_5 < P_4$). The cause of the flow separation is removed, permitting a larger energy transfer into a turbine stage. In an axial flow turbine, fewer stages are required to produce the same work that is produced in as much as five times as many compressor stages.

A single stage in a rotor is comprised of a set of fixed vanes called nozzle guide vanes (NGV) followed by a set of rotor blades. The function of the NGV is to increase the kinetic energy of the air (increase C_4). This produces a larger momentum and consequently a larger force to impinge on the blades. The purpose of the rotor is to deflect the velocity of the gas. As the amount of deflection increases, the force on the blade increases. If the blades are then permitted to turn, the absolute velocity of the air leaving the rotor is lower than that entering. Work is therefore performed. In addition to the "impulse" work, the rotor blades are designed to converge such that the relative velocity within the blades increases ($w_5 > w_4$). The greater the increase in relative velocity, the greater will be the work. This portion of the work is called reaction. It is seen then, that the work of the turbine is derived from both reaction and impulse. A pure reaction turbine is one in which the absolute velocity across the turbine is unchanged and ($w_5 > w_4$). Conversely, a pure impulse turbine merely deflects the flow with no increase in relative gas flow ($C_4 > C_5$, $w_4 = w_5$). The percent reaction is defined as:

$$\%R = \frac{(w_5^2 - w_4^2)}{(w_5^2 - w_4^2) + (C_4^2 - C_5^2)} \times 100$$

and is merely an indication of the amount of static pressure drop due to reaction. Tests show that a 50% reaction turbine has higher efficiency than one with more or less reaction for the same work output. Most turbines are therefore designed to operate with 50% reaction. Figure 2.28 shows the variation in total and static pressure through a two stage axial flow turbine.



TURBINE ENERGY TRANSFER

FIGURE 2.28

TURBINE PERFORMANCE MAP

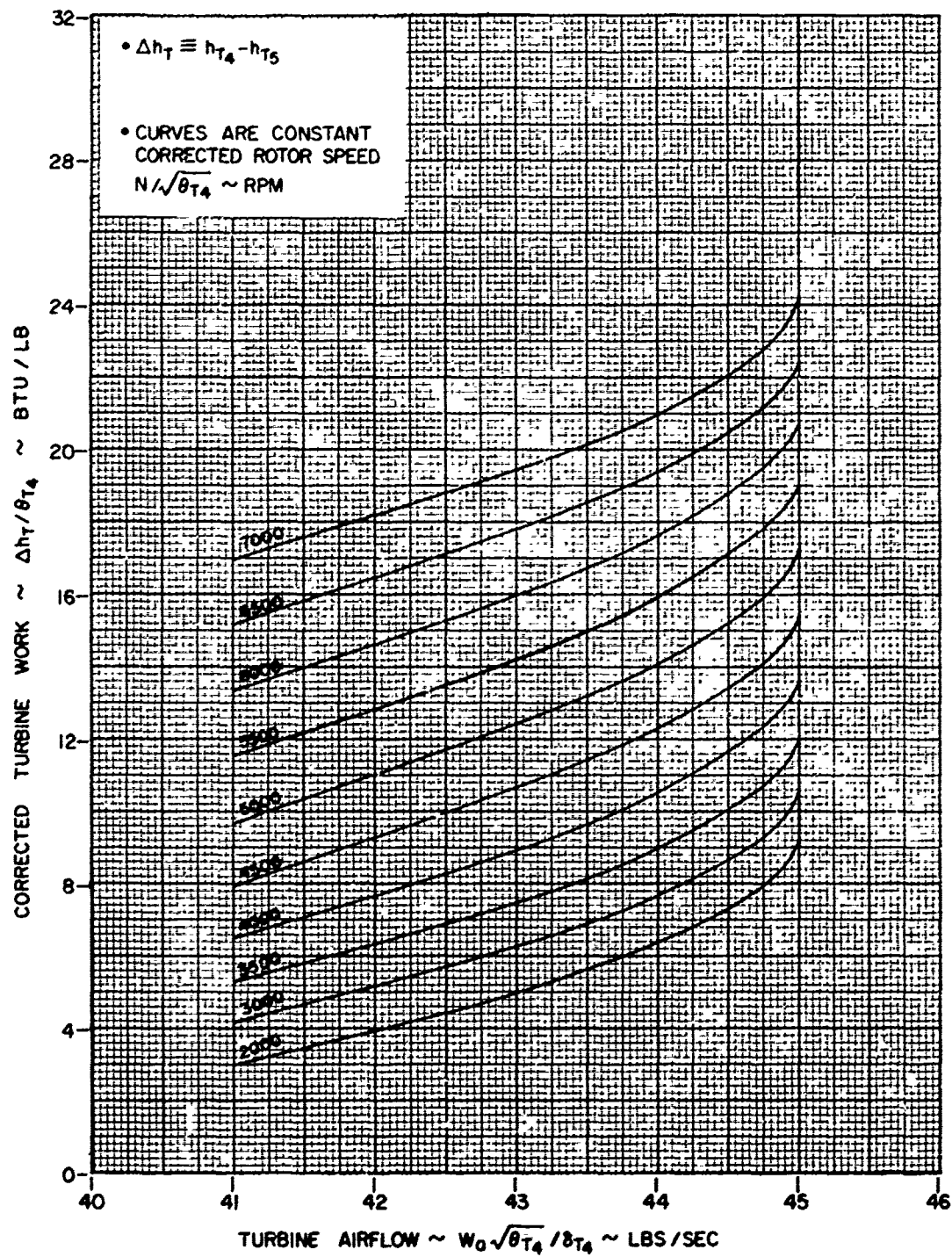


FIGURE 2.29

The performance of a turbine is determined in much the same way as the compressor performance. Work, airflow, total pressure and total temperatures are measured. A similar derivation can be performed as on the compressor to show that the total pressure ratio across the turbine is a function of corrected rotor speed and corrected airflow. Convention has replaced the pressure ratio with $\Delta h / \theta T_4$ where Δh equals $h_{T_4} - h_{T_5}$. This term, called corrected turbine work, can be shown, by rearranging (1.22), to be proportional to P_{T_4} / P_{T_5} . Figure 2.29 shows a typical, experimentally determined, turbine performance curve.

2.5 NOZZLES

The thrust of a jet engine is produced by increasing the momentum of the air. The equation used to calculate the net thrust due to the momentum change is:

$$F_n = (W_a/g) (V_{10} - V_0) \quad (\text{reference 1.6}) \quad (2.23)$$

The function of the nozzle is to produce the maximum attainable exit velocity. When the gasses leave the turbine, the velocity is such that the Mach number is subsonic. From (2.1a), a decreasing area is required to accelerate the flow. The maximum velocity that can be attained will exist at the exit of the nozzle. There are two limiting factors on this velocity; the first is ambient pressure and the second Mach number. As the gas is accelerated (expanded), the static pressure decreases. The minimum value obtainable is the ambient pressure outside the nozzle. In addition to the static pressure decreasing, the Mach number in the nozzle is increasing. From (2.1a), the maximum Mach number obtainable with a converging nozzle is unity and the velocity is therefore limited to a value corresponding to this Mach number. If $\gamma = 1.33$, the total-static pressure ratio at the converging nozzle exit plane that will produce this condition is $P_{T10}/P_0 = 1.849$. It is evident then, that for pressure ratios below and equivalent to 1.849, P_{10} will be equal to P_0 and for pressure ratios above, P_{10} will be greater than P_0 . When $P_{T10}/P_0 > 1.849$, the nozzle is said to be choked and $M_{10} = 1.0$.

Even though the velocity has accelerated to a maximum value, there exists a force $(P_{10} - P_0)A_0$ which acts on the gas. This force adds to the net thrust. Thus, the net thrust produced by an engine with a converging nozzle is:

$$F_n = [(W_a/g)V_{10} + (P_{10} - P_0)A_{10}] - (W_a/g)V_0 \quad (2.24)$$

for $P_{T10}/P_0 > 1.849$ (nozzle choked) and,

$$F_n = [(W_a/g)V_{10}] - (W_a/g)V_0 \quad (2.25)$$

for $P_{T10}/P_0 \leq 1.849$ (nozzle unchoked).

The quantity in the brackets in both equations is that portion of the net thrust attributed to the nozzle and is termed the gross thrust. The product $(W_a/g)V_0$ has been termed ram drag.

Although the thrust of a converging nozzle does increase with pressure ratios above 1.849, a greater thrust can be realized at these pressure ratios by further acceleration of the flow. From (2.1a), a diverging portion is required to accelerate the flow above a Mach number of 1.0. It is to be recalled that even though supersonic Mach numbers exist

in the diverging portion of a converging-diverging (C-D) nozzle, the Mach number at the minimum area (throat) is unity and the nozzle is still choked. During this acceleration process, the ambient pressure is decreased. The ideal C-D nozzle will expand the flow to P_0 . The equation, therefore, for the net thrust of an ideal C-D nozzle is:

$$F_n = [(W_a/g)V_{10}] - (W_a/g)V_0 \quad (\text{Ideal C-D nozzle}) \quad (2.26)$$

This is the equation generally utilized to calculate the thrust of a C-D nozzle. As in the converging nozzle, the term in brackets is called the gross thrust.

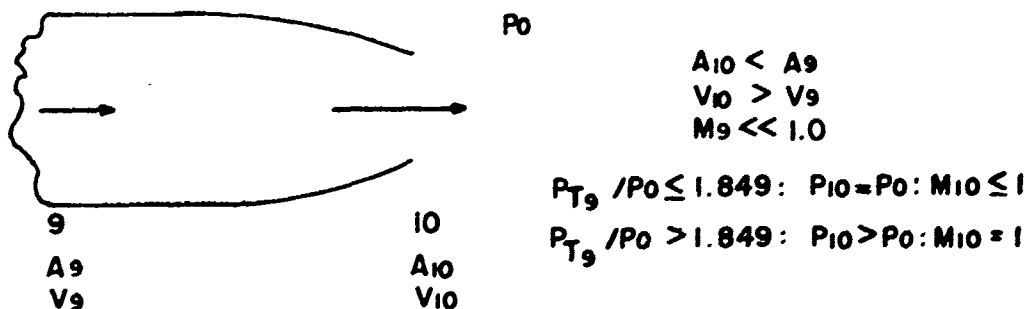
Comparing the gross thrust portions of the net thrust equations (2.24, 2.25, and 2.26) shows that the converging nozzle equations attempt to calculate the actual gross thrust by accounting for incomplete expansion. As will be seen, errors due to friction and the like, will exist preventing a simple calculation. An experimentally determined gross thrust coefficient will be defined to permit calculation of actual gross thrust. The equation (2.26), used to calculate the thrust of a C-D nozzle is conceptually different from the converging equations. It is based on an ideal nozzle; one which expands the gasses completely to ambient pressure. Thus, the calculation of gross thrust for an engine with a C-D nozzle will be somewhat in error due to the assumption of complete expansion. In addition, the same friction errors encountered in the converging nozzle, will be present. Additional terms could be added to (2.26) to account for the assumption of complete expansion, but its complexity would not improve the final result.

Three equations have been presented which can be utilized to calculate net thrust for a simple converging nozzle engine, and for the more complex converging-diverging nozzle engine. This section will further develop the above equations into a form that is readily useable; a form which utilizes easily measureable parameters. Further, the experimentally determined coefficients that make the theoretical calculation agree with the actual will be formulated. Finally the design of some basic convergent-divergent nozzles will be presented along with a discussion of variable geometry nozzles.

CONVERGING NOZZLE - SUB-CRITICAL AND CRITICAL OPERATION

The gross thrust equation to be developed for this mode of operation is:

$$F_g = (W_a/g)V_{10} \quad (P_{10} = P_0) \quad (2.27)$$



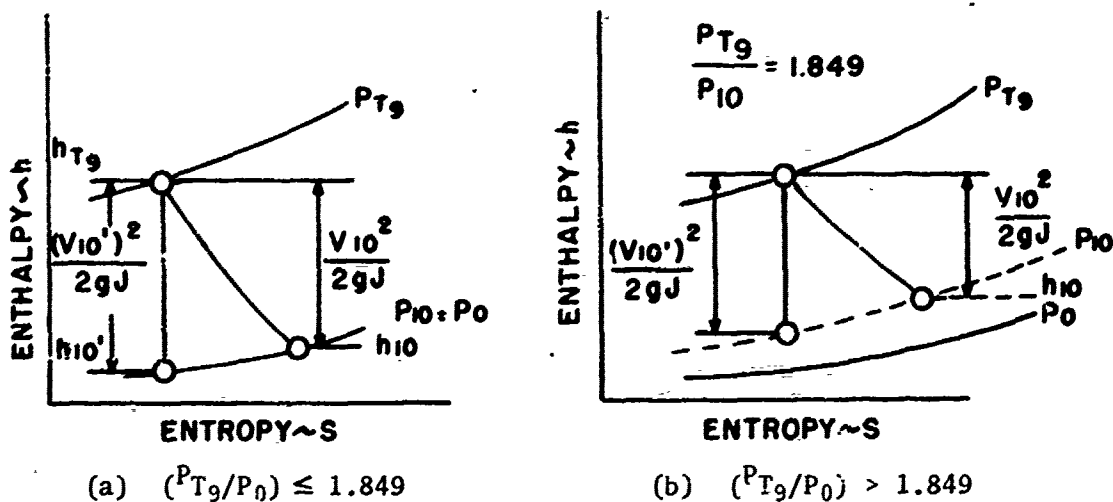
CONVERGING NOZZLE

FIGURE 2.30

Figure 2.30 shows schematically the type of nozzle under discussion. It was shown in Section 1.2 that the nozzle efficiency is defined as:

$$\eta_n = \frac{V_{10}^2 / 2gJ}{(V_{10}')^2 / 2gJ} = \frac{h_{T9} - h_{10}}{h_{T9} - h_{10}'} \quad (\text{ref. 1.27}) \quad (2.28)$$

This efficiency is illustrated in Figure 2.31a below, which may be compared to Figure 1.18.



CONVERGING NOZZLE H-S DIAGRAM

FIGURE 2.31

From Section 1.2, $V_{10} = \sqrt{\eta_n} V_{10}'$ and substituting V_{10}' from (2.28) gives us:

$$V_{10} = \sqrt{\eta_n (h_{T_9} - h_{10}') 2gJ} \quad (2.29)$$

Equation (2.29) is the one to be used for analysis, but from the equation $V_{10} = \sqrt{\eta_n} V_{10}'$, a physical feeling for η_n can be obtained. The square root of the nozzle efficiency is merely the ratio of the actual discharge velocity to the isentropic discharge velocity. Sometimes $\sqrt{\eta_n}$ is termed the "velocity coefficient" (C.V.).

$$C.V. = V_{10}/V_{10}' \quad (2.30)$$

Substituting (2.29) and (2.30) into (2.27), we get:

$$F_g = (W_a/g) (C.V.) \sqrt{(h_{T_9} - h_{10}') 2gJ} \quad (2.31)$$

The airflow in the above equation is the actual airflow which is not easily measured. To compensate for any error between actual and isentropic airflow, we introduce a second coefficient called "discharge coefficient" (C.D.), defined as the ratio of actual airflow to ideal airflow. $C.D. = W_a/W_a'$.

Solving this expression for actual airflow and expanding,

$$W_a = (C.D.) W_a' = (C.D.) \rho_{10}' g A_{10} V_{10}'$$

Now, $\rho_{10}' g = P_{10}' / RT_{10}'$, thus:

$$W_a = (C.D.) (P_{10}' / RT_{10}') A_{10} V_{10}'$$

Further, $V_{10}' = \sqrt{(h_{T_9} - h_{10}') 2gJ}$, therefore:

$$W_a = (C.D.) (P_{10}' / RT_{10}') A_{10} \sqrt{(h_{T_9} - h_{10}') 2gJ} \quad (2.32)$$

This expression, when substituted into (2.31), yields:

$$F_g = (C.V.) (C.D.) (P_{10}' / RT_{10}') A_{10} (h_{T_9} - h_{10}') 2J$$

If C_p is assumed constant,

$$F_g = 2 (C.V.) (C.D.) (J C_p / R) A_{10} (P_{10}' / T_{10}') (T_{T_9} - T_{10}')$$

Factoring out T_{T_9} yields:

$$F_g = 2 (C.V.) (C.D.) (JC_p / R) A_{10} P_{10}' (T_{T_9} / T_{10}') \left[1 - (T_{10}' / T_{T_9}) \right]$$

or, since $(JC_p / R) = (\gamma / \gamma - 1)$,

$$F_g = 2 (C.V.) (C.D.) (\gamma / \gamma - 1) A_{10} P_{10}' \left[(T_{T_9} / T_{10}') - 1 \right]$$

Since T_{T_9} / T_{10}' is isentropic:

$$F_g = (C.V.) (C.D.) (2\gamma / \gamma - 1) A_{10} P_{10}' \left[\left(P_{T_9} / P_{10}' \right)^{\frac{\gamma-1}{\gamma}} - 1 \right] \quad (2.33)$$

Finally, since $P_{10}' = P_0$,

$$\frac{F_g}{\delta_0} = (C.V.) (C.D.) \frac{2\gamma}{\gamma-1} P_{SL} A_{10} \left[\left(\frac{P_{T_9}}{P_0} \right)^{\frac{\gamma-1}{\gamma}} - 1 \right] \quad (2.34)$$

From (2.34), the referred gross thrust, for a converging nozzle with $P_{T_9} / P_0 \leq 1.849$ is determined by measuring the nozzle pressure ratio (P_{T_9} / P_0) and ambient pressure P_0 . The velocity and discharge coefficients cannot be separately determined and are generally combined as a gross thrust coefficient (C_g).

$$C_g = (C.V.) (C.D.)$$

This coefficient is determined by measuring (F_g / δ_0) on a thrust stand and calculating the theoretical gross thrust from the equation:

$$\left(\frac{F_g}{\delta_0} \right)^t = \frac{2\gamma}{\gamma-1} P_{SL} A_{10} \left[\left(\frac{P_{T_9}}{P_0} \right)^{\frac{\gamma-1}{\gamma}} - 1 \right] \quad (2.35)$$

The value of C_g is then determined by dividing the measured thrust by the theoretical. To determine any altitude effect on C_g , P_0 is varied in an altitude chamber while measuring gross thrust.

Reviewing the evolution of the gross thrust coefficient, we find that, as defined, the coefficient adjusts for non-isentropic flow. When determined on a thrust stand as above, C_g further adjusts for errors in:

1. A_{10} - The area used should be the actual "hot A_{10} " acted upon by the force resulting from the difference in pressure between P_{10} and P_0 . Ordinarily the cold area is used.

2. P_{T9} - The total pressure measured is normally not the exact average but some other value.
3. C_p - Specific heat as well as γ varies with temperature. The utilization of $\gamma = 1.33$ compensates, in part, for this variation.

It is theoretically possible to eliminate all errors listed above, but the effort and expense for necessary measurements would likely outweigh the slight improvement in accuracy.

CONVERGING NOZZLE - SUPERCRITICAL OPERATION

When the nozzle pressure ratio reaches 1.849 ($\gamma = 1.33$), the exit Mach number is unity. Any further increase in P_{T9}/P_0 will not accelerate the gasses above this value. An additional thrust term, $[(P_{10} - P_0) A_{10}]$ must be added to arrive at the gross thrust.

$$F_g = (C.V.) (C.D.) \frac{2\gamma}{\gamma-1} A_{10} P_{10}' \left[\left(\frac{P_{T9}}{P_{10}'} \right)^{\frac{\gamma-1}{\gamma}} - 1 \right] + A_{10} (P_{10} - P_0) \quad (2.36)$$

The H-S diagram for this case is shown in Figure 2.31b. Manipulating the last term of the equation, we have:

$$F_g = (C.V.) (C.D.) \frac{2\gamma}{\gamma-1} A_{10} P_{10}' \left[\left(\frac{P_{T9}}{P_{10}'} \right)^{\frac{\gamma-1}{\gamma}} - 1 \right] + A_{10} P_0 \left(\frac{P_{T9}}{P_0} \frac{P_{10}}{P_{T9}} - 1 \right)$$

Dividing through by δ_0 and rearranging pressures in the first term,

$$\frac{F_g}{\delta_0} = (C.V.) (C.D.) \frac{2\gamma}{\gamma-1} A_{10} P_{SL} \frac{P_{10}'}{P_{T9}} \frac{P_{T9}}{P_0} \left[\left(\frac{P_{T9}}{P_{10}'} \right)^{\frac{\gamma-1}{\gamma}} - 1 \right] + A_{10} P_{SL} \left(\frac{P_{T9}}{P_0} \frac{P_{10}}{P_{T9}} - 1 \right) \quad (2.37)$$

Now the factors P_{T9}/P_{10}' and P_{T9}/P_{10} , appearing in the equation, can be expressed as:

$$P_{T9}/P_{10}' = P_{T9}/P_{10} = \left(\frac{\gamma+1}{2}\right)^{\frac{\gamma}{\gamma-1}}$$

Substituting this expression into (2.37) and rearranging:

$$\begin{aligned} \frac{F_g}{\delta_0} = A_{10} P_{SL} \left[(C.V.) (C.D.) \frac{2}{\gamma-1} \left(\frac{2}{\gamma+1}\right)^{\frac{\gamma}{\gamma-1}} \frac{P_{T9}}{P_0} \left(\frac{\gamma+1}{2} - 1\right) \right. \\ \left. + \frac{P_{T9}}{P_0} \left(\frac{2}{\gamma+1}\right)^{\frac{\gamma}{\gamma-1}} - 1 \right] \end{aligned}$$

or,

$$\frac{F_g}{\delta_0} = A_{10} P_{SL} \left\{ \frac{P_{T9}}{P_0} \left(\frac{2}{\gamma+1}\right)^{\frac{\gamma}{\gamma-1}} \left[\gamma (C.V.) (C.D.) + 1 \right] - 1 \right\} \quad (2.38)$$

Although (2.38) is the gross thrust equation for supercritical operation, it will be further simplified for actual use. Note that, unlike the subcritical case, the term (C.V.) (C.D.) cannot be multiplied by the theoretical gross thrust to obtain actual gross thrust. For simplification, the (C.V.) (C.D.) will be replaced by a gross thrust coefficient (C_g) as shown below:

$$\frac{F_g}{\delta_0} = C_g A_{10} P_{SL} \left[(\gamma + 1) \left(\frac{2}{\gamma+1}\right)^{\frac{\gamma}{\gamma-1}} \frac{P_{T9}}{P_0} - 1 \right] \quad (2.39)$$

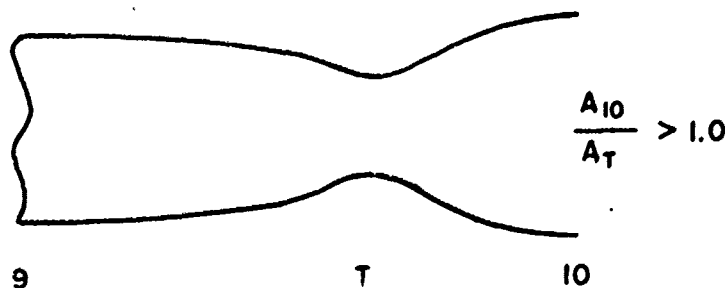
All terms to the right of C_g comprise the theoretical or ideal gross thrust. With this simplification, C_g is determined in precisely the same way as for the subcritical mode of operation.

Some discussion of these equations is warranted. Referring to (2.36) and (2.38), the (C.D.) (C.V.) term is really a constant for $P_{T9}/P_0 > 1.849$. If (C.D.) (C.V.) represents the departure from isentropic expansion within the nozzle, the value of the (C.D.) (C.V.) to be used in (2.38) could be determined by calculating C_g for $P_{T9}/P_0 = 1.849$ using (2.36). Considering the discussion following the gross thrust equation for subcritical operation, the C_g term included errors other than those resulting

directly from nonisentropic flow in the nozzle. Because of this, the ability to pinpoint the correct value of C_g , or even the choked flow point, to be utilized in (2.38) is questionable. It is, therefore, evident why the simplification from (2.38) to (2.39) was made.

CONVERGING-DIVERGING NOZZLE

If a converging nozzle, as in Figure 2.30, is operating at a pressure ratio $P_{T9}/P_0 > 1.849$, it will produce an ideal thrust given by (2.39) with $C_g \equiv 1.0$. By adding a diverging section to the converging nozzle (see Figure 2.32), such that the exit area is adjusted to isentropically expand the gases to P_0 , the thrust will be increased. This is easily shown by an example, but first the thrust equation of a C-D nozzle must be developed.



CONVERGING-DIVERGING NOZZLE

FIGURE 2.32

As previously mentioned, the gross thrust equation will be based on an ideal isentropic expansion of the gases to ambient not accounting for any nonisentropic process (such as shocks due to overexpansion) within the nozzle, or for $(P_{10} - P_0)A_{10}$ resulting from an under expanded flow. (The terms under and over expansion will be amplified.)

The throat of a C-D nozzle will be choked for $P_{T9}/P_0 > 1.849$ ($\gamma = 1.33$). The corrected airflow through the nozzle is:

$$\frac{W a \sqrt{T_{T9}}}{P_{T9}} = A_T \sqrt{\frac{\gamma g}{R}} \left[\frac{1}{\left(1 + \frac{\gamma-1}{2}\right)^{\frac{\gamma+1}{\gamma-1}}} \right]^{\frac{1}{2}} = A_T \left[\frac{\gamma g}{R} \left(\frac{2}{\gamma+1} \right)^{\frac{\gamma+1}{\gamma-1}} \right]^{\frac{1}{2}}$$

Therefore:

$$W_a = \frac{A_T P_{T_9}}{\sqrt{T_{T_9}}} \left[\frac{\gamma g}{R} \left(\frac{2}{\gamma+1} \right)^{\frac{\gamma+1}{\gamma-1}} \right]^{\frac{1}{2}} \quad (2.40)$$

The exhaust velocity for an isentropically expanded nozzle is:

$$V_{10} = \left\{ 2gJ C_p T_{T_9} \left[1 - \left(\frac{P_0}{P_{T_9}} \right)^{\frac{\gamma-1}{\gamma}} \right] \right\}^{\frac{1}{2}} \quad (2.41)$$

Substituting (2.40) and (2.41) into the gross thrust term of (2.26) yields the ideal gross thrust for a converging-diverging nozzle.

$$F_{g \text{ C-D}}' = \frac{A_T P_{T_9}}{g \sqrt{T_{T_9}}} \left\{ \frac{\gamma g}{R} \left(\frac{2}{\gamma+1} \right)^{\frac{\gamma+1}{\gamma-1}} 2gJ C_p T_{T_9} \left[1 - \left(\frac{P_0}{P_{T_9}} \right)^{\frac{\gamma-1}{\gamma}} \right] \right\}^{\frac{1}{2}}$$

Simplifying and dividing by δ_0 gives the ideal referred gross thrust.

$$\left(\frac{F_g}{\delta_0} \right)'_{\text{C-D}} = A_T P_{SL} \gamma \left[\left(\frac{2}{\gamma-1} \right) \left(\frac{2}{\gamma+1} \right)^{\frac{\gamma+1}{\gamma-1}} \right]^{\frac{1}{2}} \frac{P_{T_9}}{P_0} \left[1 - \left(\frac{P_0}{P_{T_9}} \right)^{\frac{\gamma-1}{\gamma}} \right]^{\frac{1}{2}} \quad (2.42)$$

Equation (2.42) is the gross thrust for a completely expanded isentropic C-D nozzle. The actual thrust will be determined by multiplying (2.42) by an experimentally determined gross thrust coefficient C_g . Thus:

$$\left(\frac{F_g}{\delta_0} \right)_{\text{C-D}} = C_g \left(\frac{F_g}{\delta_0} \right)'_{\text{C-D}} \quad (2.43)$$

It will now be shown that the thrust of a C-D nozzle, operating at a $P_{T_9}/P_0 > 1.849$ and isentropically expanded to ambient pressure, produces more thrust than a converging nozzle whose discharge area is the same as the throat area of the C-D nozzle. The comparison should be made

between (2.39) with $C_g = 1.0$ and (2.42). Observation shows that for "large" P_{T9}/P_0 the limit of

$$\frac{(F_g/\delta_0)'_{C-D}}{(F_g/\delta_0)_{Conv}} \text{ Approaches } \frac{\gamma \left[\left(\frac{2}{\gamma-1} \right) \left(\frac{2}{\gamma+1} \right)^{\frac{\gamma+1}{\gamma-1}} \right]^{\frac{1}{2}}}{\left[(\gamma+1) \left(\frac{2}{\gamma-1} \right)^{\frac{\gamma}{\gamma-1}} \right]}$$

For a specific case such as $P_{T9}/P_0 = 8.0$ and $\gamma = 1.33$,

$$\begin{aligned} \left(\frac{F_g}{\delta_0} \right)'_{C-D} &= A_T P_{SL} (1.33) \left[\left(\frac{2}{0.33} \right) \left(\frac{2}{2.33} \right)^{7.061} \right]^{\frac{1}{2}} (8) \left[1 - \left(\frac{1}{8} \right)^{0.248} \right] \\ &= 9.67 A_T P_{SL} \quad (\text{Equation 2.42}) \end{aligned}$$

and

$$\begin{aligned} \left(\frac{F_g}{\delta_0} \right)_{Conv} &= A_{10} P_{SL} 2.33 \left(\frac{2}{2.33} \right)^{4.03} (8 - 1) \\ &= 9.10 A_{10} P_{SL} \quad (\text{Equation 2.39, } C_g = 1.0) \end{aligned}$$

Since A_T of (2.42) equals A_{10} of (2.39), the increase in gross thrust at sea level is:

$$\frac{9.67 - 9.1}{9.1} \times 100 = 6\%$$

There will be a larger percentage increase in net thrust. It appears then that whenever a supercritical pressure ratio exists, a C-D nozzle should be utilized. This is true if the engine will always be working at the design point of the nozzle. The remaining discussion will deal with the losses and off design operation of a fixed geometry C-D nozzle and variable geometry C-D nozzle.

C-D Nozzle $P_{T9}/P_0 < 1.849$ ($\gamma = 1.33$)

A C-D nozzle is never operated at a nozzle pressure ratio below the value which will permit choking of the throat. The reason for this is that, if the throat does not choke, the exit velocity will be less than that existing at the throat, therefore reducing the maximum thrust available.

C-D Nozzle $P_{T9}/P_0 > 1.849$

If a C-D nozzle is operating on design, the exit area (A_{10}) will be such that $P_{10} = P_0$ and the exhaust gasses are completely expanded. This discharge area (A_{10}) is uniquely defined by the design nozzle pressure ratio. When a C-D nozzle is operated at nozzle pressure ratios above design, the discharge area will not be large enough to fully expand the flow within the confines of the nozzle. Similar to a converging nozzle operating supercritically, there will exist a pressure differential at the exit plane causing a force $A_{10}(P_{10} - P_0)$. The gross thrust calculated for this nozzle using (2.42) will be greater than actual. The gross thrust coefficient (C_g) will therefore decrease as (P_{T9}/P_0) gets further and further above design nozzle pressure ratio. A C-D nozzle operating above the design (P_{T9}/P_0) is termed underexpanded. The flow process up to the exit area in an underexpanded nozzle is ideally isentropic. Any nonisentropic processes (friction) will also be included in determining C_g . Figure 2.33 shows the H-S diagram for a C-D nozzle.

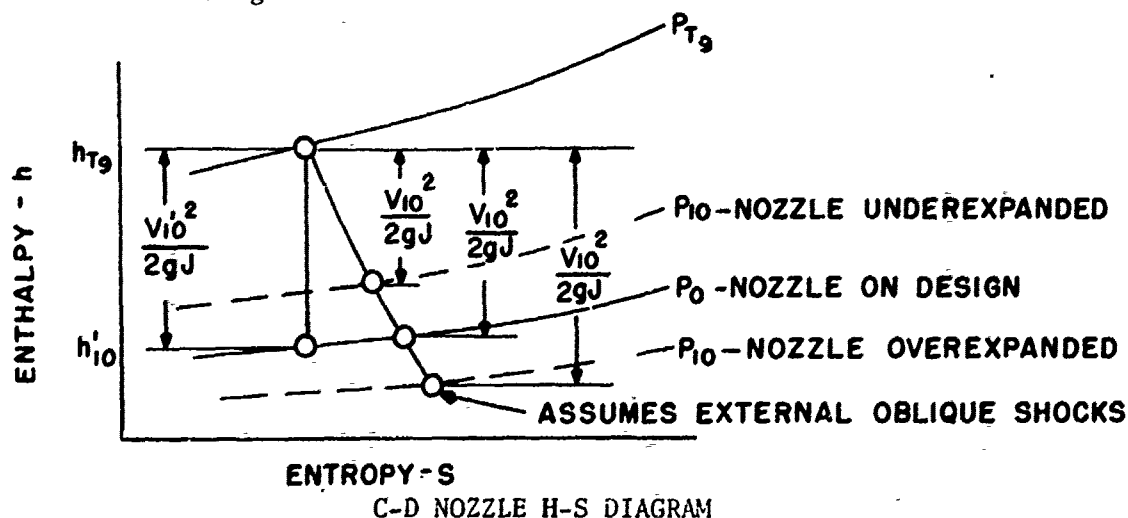


FIGURE 2.33

The operation of a C-D nozzle at pressure ratios below design but above 1.849 results in nonisentropic flow. The nozzle, by virtue of its fixed contour, overexpands (see Figure 2.33) the supersonic flow to a static pressure P_{10} less than P_0 . Thus, the gross thrust calculated from (2.42) will be greater than actual and the gross thrust coefficient will decrease with pressure ratios below design P_{T9}/P_0 . In addition to this situation, overexpansion causes a shock system to form. For pressure ratios slightly below design, the shocks are oblique and external to the nozzle. The further P_{T9}/P_0 goes below design, the stronger the shocks will be until the oblique shocks become one normal shock and attaches. Actually when the static pressure P_{10} is roughly 50% of the ambient pressure, the flow separates relieving the overexpanded condition.

NOZZLE PERFORMANCE

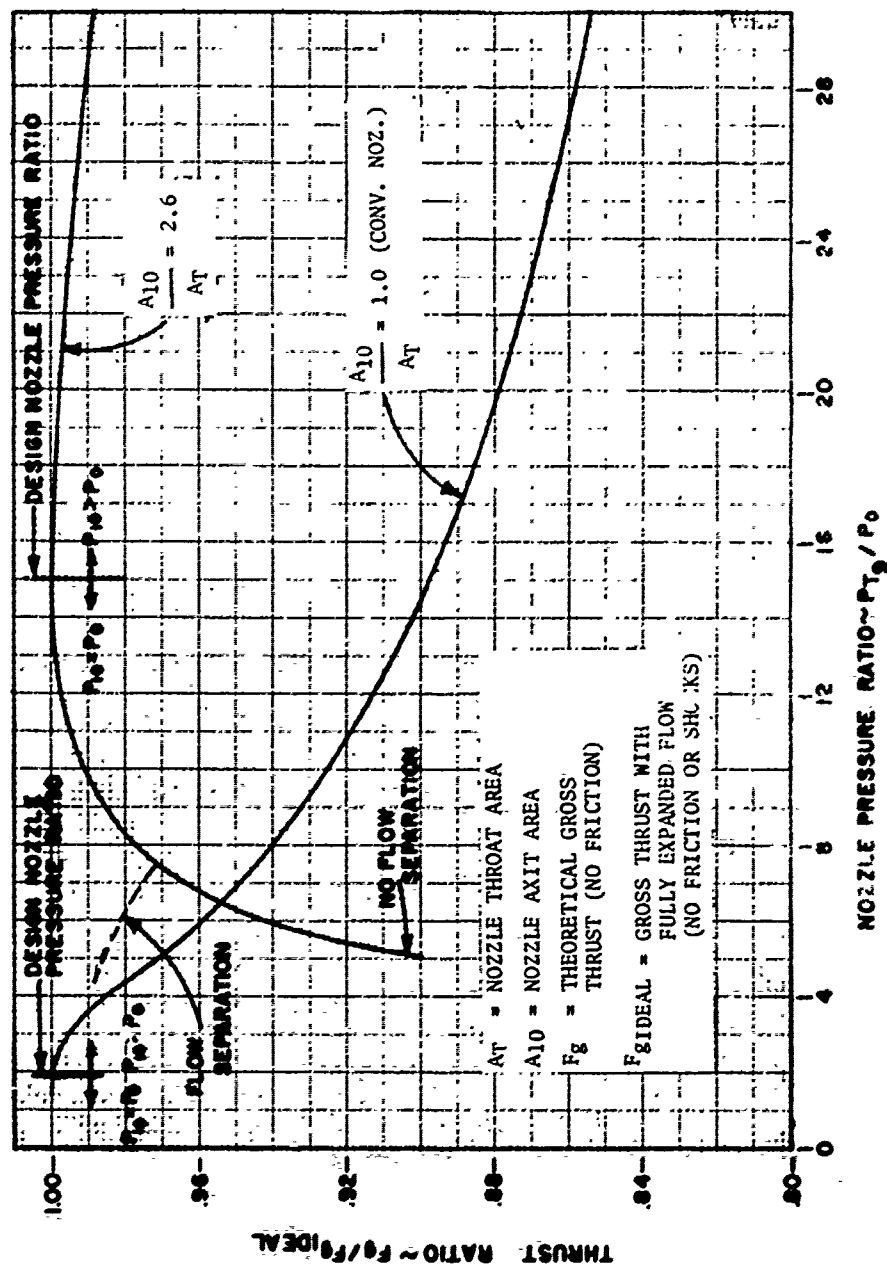


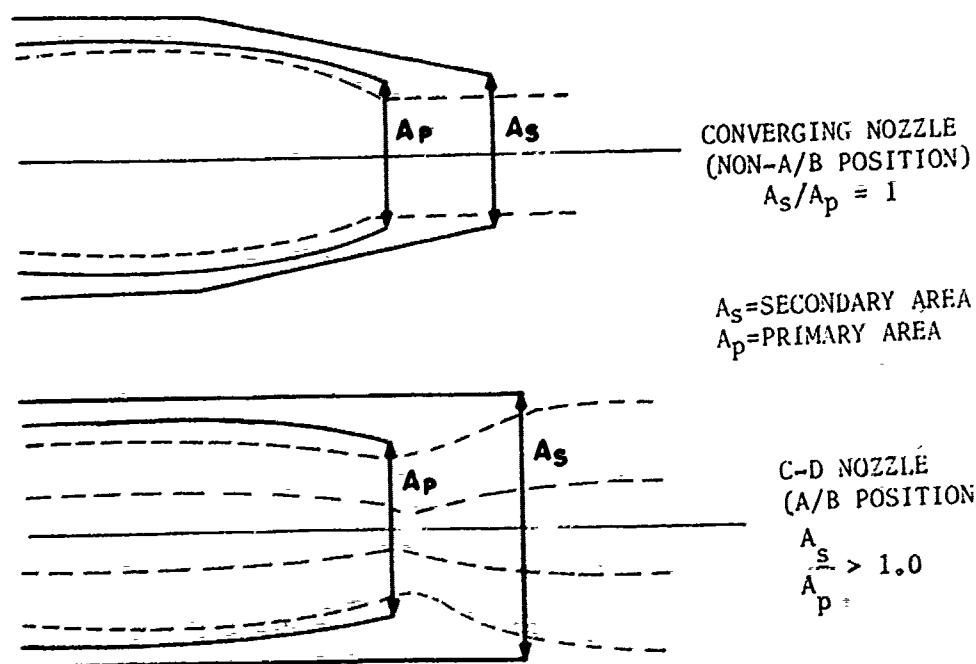
FIGURE 2.54

At this point, a summary of the pertinent facts should be made:

1. Converging nozzle - Operation below the critical pressure ratio results in complete expansion. Operation above results in a gross thrust which is less than that obtainable by complete isentropic expansion.
2. C-D nozzle - There is one nozzle pressure ratio, called design pressure ratio, which results in complete isentropic expansion and maximum thrust. Above this pressure ratio, the gross thrust is less than the maximum because of incomplete expansion ($P_{10} > P_0$), and below, overexpansion and a large negative force due to P_{10} less than P_0 reduces the thrust.

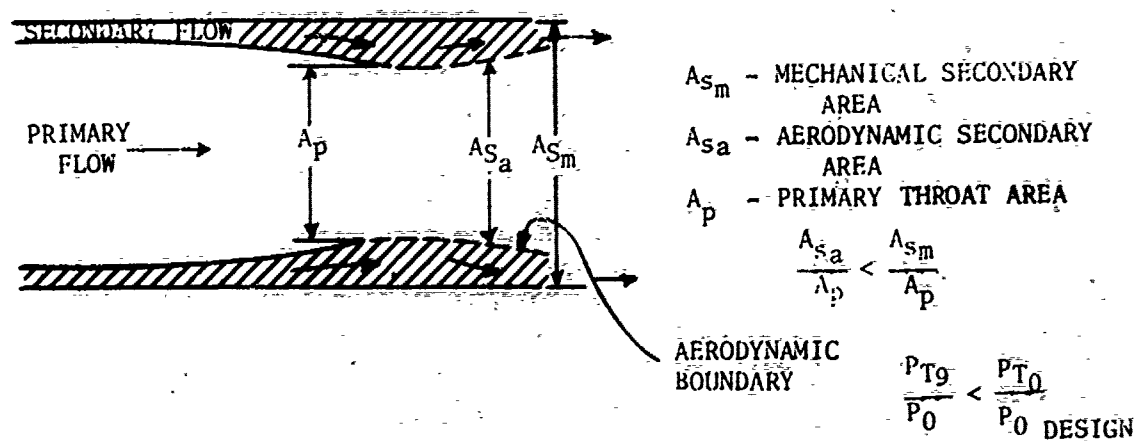
A plot representing these results is much clearer. Figure 2.34 shows, for two nozzles (Convergent, and C-D), the theoretical gross thrust ratioed to the ideal thrust. The theoretical gross thrust is that which would be measured on a thrust stand if there were no friction or measurement errors, etc. The ideal is that thrust which would result from complete isentropic expansion. Figure 2.34 shows the advantages as well as the disadvantages of convergent and C-D nozzles.

Turbojet powered aircraft that are subsonic generally do not operate at nozzle pressure ratios above 5. Aircraft which operate supersonically and at high altitude experience pressure ratios of 20 or higher. At these flight conditions, it is advantageous to "add" a C-D nozzle. Many early supersonic aircraft had two position nozzles; the "closed" or converging position was for military power or non-afterburner operation since the aircraft speeds and altitudes produced relatively low nozzle pressure ratios; the "open" C-D position produced aircraft speeds and altitudes that had relatively high nozzle pressure ratios. When going to afterburner position on the nozzle, there was a loss in maximum thrust available, depending on the nozzle pressure ratio (see Figure 2.34). As the airplane accelerated or climbed, the nozzle pressure ratio approached design P_{T_9}/P_0 . This two position nozzle was a compromise to a fully variable C-D nozzle. Figure 2.35 shows schematically a two position C-D nozzle. Notice the space shown between the primary nozzle and the secondary nozzle walls. When the nozzle is in the open or A/B position and below design pressure ratio, overexpansion causes the local static pressure prior to the discharge area to be less than ambient. If the entrance to the secondary passage is open to the free stream, a flow would result since $P_{local} < P_{ambient}$. This secondary flow aerodynamically forms a C-D nozzle with less divergence than the fixed C-D boundaries (see Figure 2.36). The further P_{T_9}/P_0 is below design, the lower will be the local static pressure, and the greater the secondary flow. This type of nozzle is called an ejector nozzle. It is seen that the secondary flow produces a somewhat fully variable C-D nozzle.



TWO POSITION C-D NOZZLE

FIGURE 2.35



EJECTOR NOZZLE OPERATING
BELOW DESIGN PRESSURE RATIO

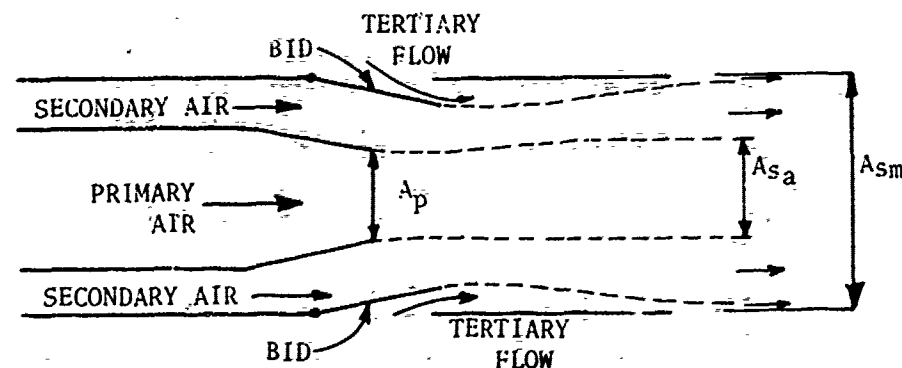
FIGURE 2.36

By introducing the secondary flow, there exists a secondary ram drag and a secondary gross thrust. Since there is no energy added to this flow, the net thrust $F_{NSEC} < 0$. The primary gross thrust of the basic engine increases due to the aerodynamically compensated nozzle with the net result that

$$F_{N_{TOTAL/EJECTOR}} > F_{N_{TOTAL/NON-EJECTOR}}$$

when (P_{T9}/P_0) is below design (P_{T9}/P_0) .

Most contemporary C-D nozzles are of the ejector type. Some designs utilize blow-in-doors. Referring to Figure 2.37, it is seen that in addition to the secondary air, tertiary air is admitted through blow-in-doors. The operating principle is the same. When the C-D nozzle is overexpanded, the local static pressure upstream of the nozzle exit will be below ambient and there will be an inward force on the doors, $[A_{DOOR}(P_{LOCAL} - P_0)]$. The doors will open and admit air as shown. The amount the doors open depends on the force applied and it should be clear that the doors will seek a position to provide an optimum aerodynamic exit area.



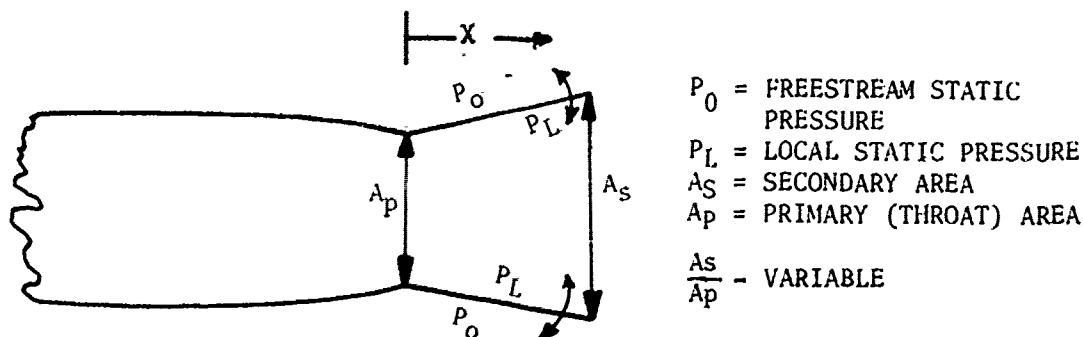
A_{s_a} = AERODYNAMIC SECONDARY AREA
 A_{s_m} = MECHANICAL SECONDARY AREA
 A_p = PRIMARY (THROAT) AREA

$$\frac{A_{s_a}}{A_p} < \frac{A_{s_m}}{A_p} \quad \left(\frac{P_{T9}}{P_0} \right) < \left(\frac{P_{T9}}{P_0} \right)_{DES}$$

BLOW-IN-DOOR EJECTOR NOZZLE

FIGURE 2.37

Some nozzles utilize a variable geometry design as shown on Figure 2.38. If the contour lines are variable, the position of the nozzle will be a function of $f(X(P_L - P_0))$ over the nozzle surface area. This feature provides an automatic schedule for the exit area as a function of the amount of overexpansion or under expansion.



VARIABLE NOZZLE CONTOURS

FIGURE 2.38

All of these concepts (Secondary Flow, Blow-In-Doors, Variable Contours) are devices which tend to increase the momentum thrust. As with any other scheme, the penalties (weight, added length, added flow friction) must be weighed not only as they affect engine thrust but, more significantly, the total aircraft performance.

What has been shown above focused on how a nozzle converts static enthalpy into kinetic energy for thrust. Basic engine operation is not concerned with the mechanisms which perform the conversion. The only parameter which affects the engine operation is airflow, or more specifically, corrected airflow. The validity of this statement will become evident in Section 3. For a non-afterburning convergent nozzle, the corrected airflow ($W_a \sqrt{\theta_{T_9}} / \delta_{T_9}$) is the same from the entrance to the nozzle to the exit. If the exit section is chosen to determine this parameter, then:

$$\frac{W_a \sqrt{\theta_{T_9}}}{\delta_{T_9}} = A_{10} \left[\frac{P_{SL}}{\sqrt{T_{SL}}} \sqrt{\frac{\gamma g}{R}} \right] \frac{M_{10}}{\left[\left(1 + \frac{\gamma-1}{\gamma} M_{10}^2 \right)^{\frac{\gamma+1}{\gamma-1}} \right]^{\frac{1}{2}}} \quad (2.44)$$

But

$$M_{10} = \left[\left(\frac{P_{T_9}}{P_{10}} \right)^{\frac{\gamma-1}{\gamma}} - 1 \right]^{\frac{1}{2}} \left[\frac{2}{\gamma-1} \right]^{\frac{1}{2}}$$

Substituting this into (2.44) and simplifying gives:

$$\frac{W_a \sqrt{\theta_{T_9}}}{\delta_{T_9}} = \frac{P_{SL}}{\sqrt{T_{SL}}} A_{10} \left(\frac{P_{10}}{P_{T_9}} \right)^{\frac{1}{\gamma}} \frac{2g \gamma}{R(\gamma-1)} \left[1 - \left(\frac{P_{10}}{P_{T_9}} \right)^{\frac{\gamma-1}{\gamma}} \right] \quad (2.45)$$

From (2.45), $W_a \sqrt{\theta T_9 / \delta T_9}$ is a function only of P_{T_9}/P_{10} because A_{10} is constant. As P_{T_9}/P_{10} increases, M_{10} increases. For all values of $P_{T_9}/P_0 \leq 1.849$ ($M_{10} \leq 1.0$), $P_{10} = P_0$. Thus, $W_a \sqrt{\theta T_9 / \delta T_9}$ will be a function of the nozzle pressure ratio P_{T_9}/P_0 . When P_{T_9}/P_0 exceeds 1.849, P_{T_9}/P_{10} remains constant at 1.849 and the nozzle is choked. If a diverging section is added, the corrected airflow is unchanged because the throat Mach number is unity. Thus, the corrected airflow of a nozzle (Convergent or C-D) is solely a function of the nozzle pressure ratio. Figure 2.39a shows this variation for two nozzle areas. For convenience, the curve on Figure 2.39a can be converted to the form of:

$$\frac{W_a \sqrt{\theta T_9}}{\delta T_9} = f \left(P_{T_9} / P_{T_2} \right) \text{ in lieu of } P_{T_9} / P_0.$$

The reason will become clear in Section 3. To do this, constant values of P_{T_2}/P_0 are selected then:

$$\frac{P_{T_9}}{P_{T_2}} = \left(\frac{P_{T_9}}{P_0} \right) \times \frac{1}{P_{T_2}/P_0}$$

If the inlet efficiency is 100%, P_{T_2}/P_0 equals P_{T_0}/P_0 and P_{T_2}/P_0 is uniquely defined by M_0 . With this information, Figure 2.39b results and is shown for one nozzle area.

NOZZLE PERFORMANCE

NOZZLE FLOW $\sim \gamma \cong 1.33$

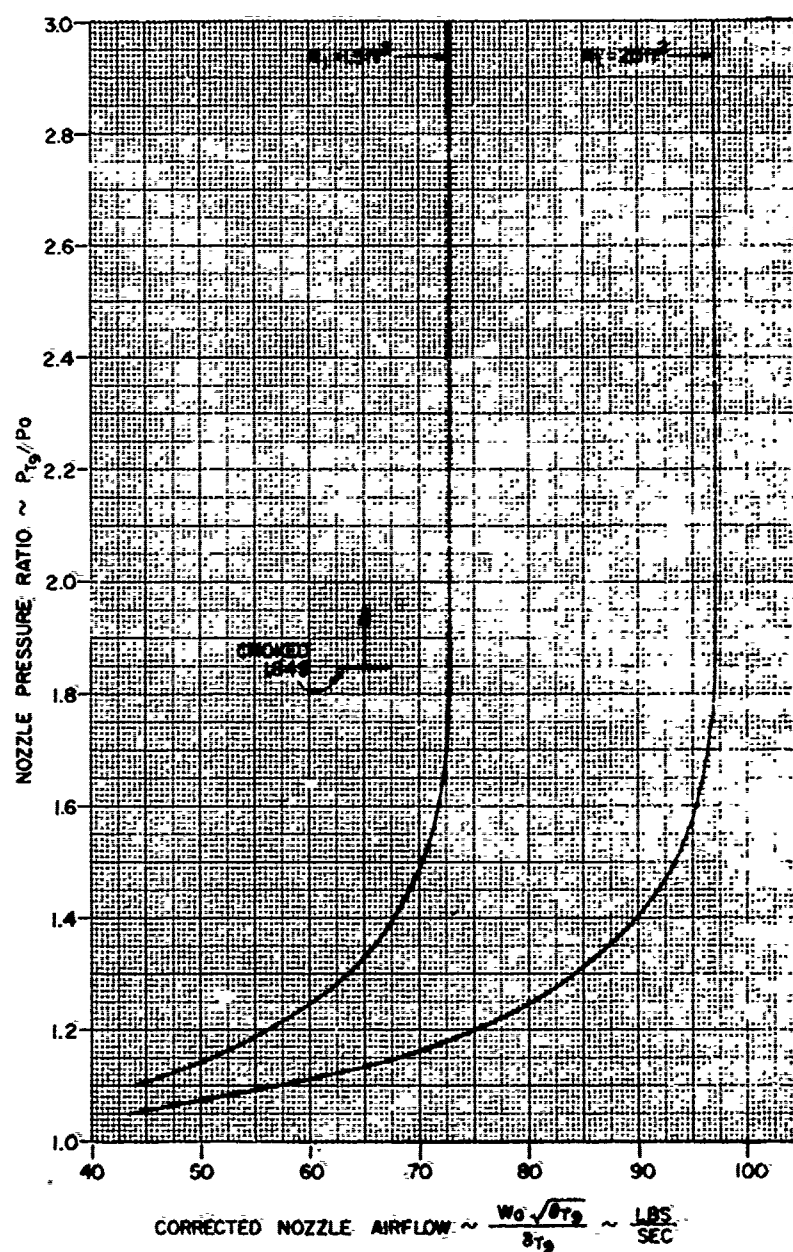


FIGURE 2.39a

NOZZLE PERFORMANCE

$$A = 1.5 \text{ ft}^2$$

$$\gamma = 1.33$$

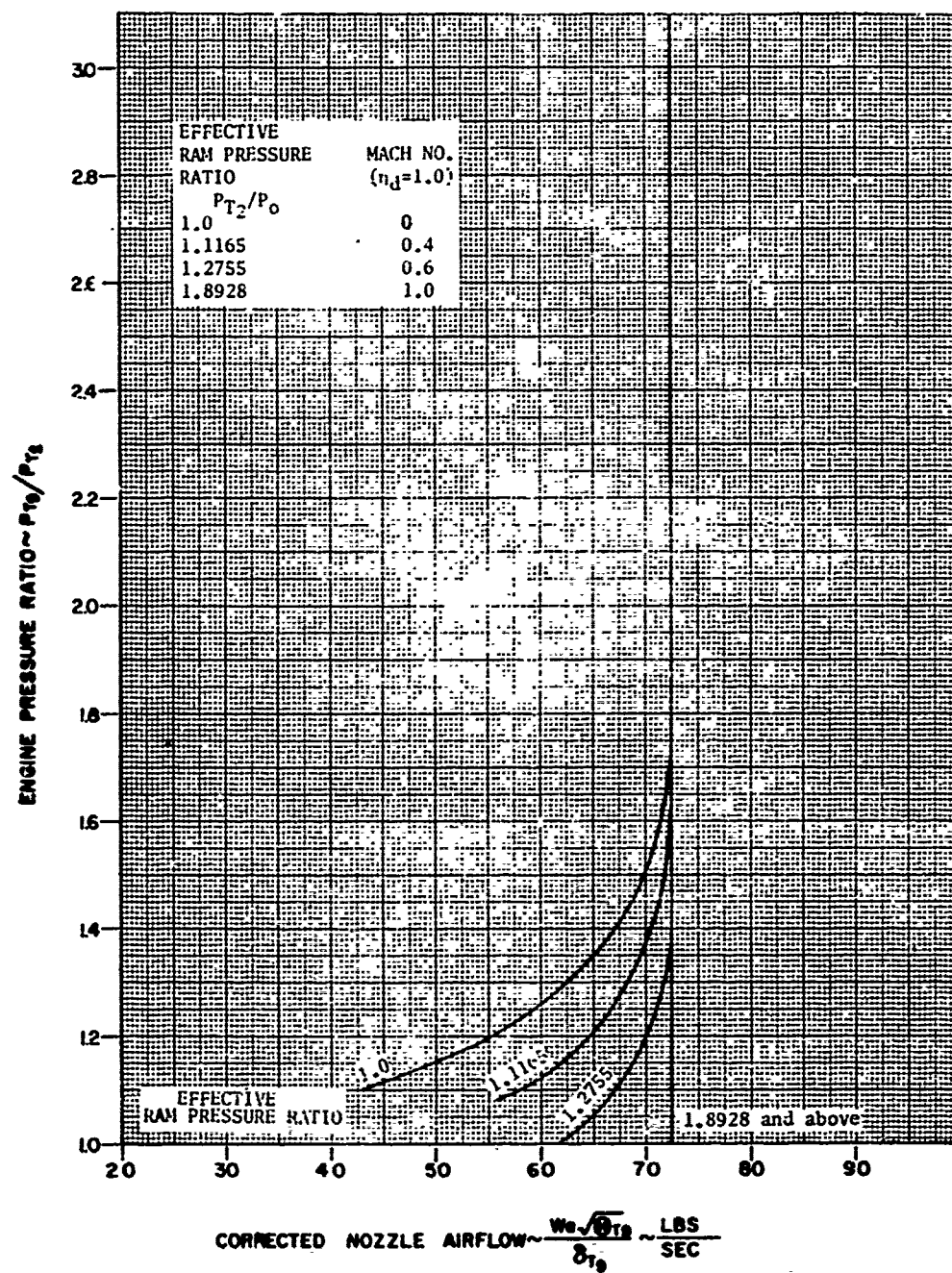


FIGURE 2.39b

SECTION 3

THE COMPLETE ENGINE

3.1 MATCHING

During steady state operation of the engine there must be a definite relationship between the compressor work, airflow and speed and the turbine work, airflow and speed while at the same time the nozzle must accept the airflow supplied to it.

In this analysis, for simplicity, it will be assumed that:

- (1) The turbine work and compressor work are equal. (Obviously the turbine work is greater than the compressor work due to friction, and the requirement to operate pumps, generators and the like.)
- (2) The compressor airflow, turbine airflow and nozzle airflow are all equal. (This assumption is invalid in so far as air may be bled from the compressor and there is the additional mass flow through the turbine due to fuel addition.)
- (3) The compressor and turbine rotational speeds are the same since they are mounted on a common shaft.

The match technique demonstrated herein will be for a single spool engine. The effects of deviations from the assumptions made in subparagraphs (1) and (2) above will be discussed in appropriate locations. Initially all component efficiencies are unity in order to simplify the analysis. The effects of non-ideal processes will be discussed as appropriate.

GAS GENERATOR MATCH

The first step in the match process is to determine where the gas generator (compressor - combustor - turbine) will function together as a unit. To do this the compressor map (in terms of turbine referred parameters) is superimposed on the turbine map. The following procedure may then be employed to obtain a match.

1. Assume a value of $N/\sqrt{\theta_{T_2}}$ on the compressor map (Figure 2.18).
2. Select corresponding values of P_{T_3}/P_{T_2} and $W_a\sqrt{\theta_{T_2}}/\delta_{T_2}$ from the map.
3. The compressor work is then obtained from



$$W_c = \frac{C_p T_{T_2}}{\eta_c} \left[\left(\frac{P_{T_3}}{P_{T_2}} \right)^{\frac{\gamma-1}{\gamma}} - 1 \right]$$

or

$$\frac{W_c}{\theta_{T_2}} = \frac{\Delta h_{T_c}}{\theta_{T_2}} = \frac{C_p T_{SL}}{\eta_c} \left[\left(\frac{P_{T_3}}{P_{T_2}} \right)^{\frac{\gamma-1}{\gamma}} - 1 \right]$$

(If the compressor efficiency is not unity it may be included here.)

$$4. \text{ Calculate } \frac{\Delta h_{T_c}}{\theta_{T_4}} = \left(\frac{\Delta h_{T_c}}{\theta_{T_2}} \right) \left(\frac{T_{T_2}}{T_{T_4}} \right)$$

(It is additionally now necessary to assume a value of T_{T_4}/T_{T_2}).

$$5. \text{ Calculate } \frac{W_{a_c} \sqrt{\theta_{T_4}}}{\delta_{T_4}} = \left(\frac{W_{a_c} \sqrt{\theta_{T_2}}}{\delta_{T_2}} \right) \left(\frac{P_{T_2}}{P_{T_4}} \right) \sqrt{\frac{T_{T_4}}{T_{T_2}}}$$

($P_{T_2}/P_{T_4} = P_{T_2}/P_{T_3}$ if $\eta_b^* = 0$, otherwise additional knowledge about the combustor is required.)

$$6. \text{ Calculate } N/\sqrt{\theta_{T_4}} = N/\sqrt{\theta_{T_2}} \sqrt{\frac{T_{T_2}}{T_{T_4}}}$$

7. Repeat process for all desired values of $N/\sqrt{\theta_{T_2}}$

8. Plot compressor map in terms of turbine referred parameters on the turbine map. (Figure 2.29).

The intersection of $(N/\sqrt{\theta_{T_4}})_{COMP}$ and $(N/\sqrt{\theta_{T_4}})_{TURB}$ are the locus of points where the compressor work, airflow and speed are equal to the turbine work, airflow and speed for the value of T_{T_4}/T_{T_2} assumed, and hence the gas generator is matched along this line. Figures 3.1a through 3.1f show the match lines for values of T_{T_4}/T_{T_2} from 2.0 to 4.5. The match lines on Figure 3.1 are for a no bleed, no accessory load match with component efficiencies of unity. If air is bled from the compressor

COMPRESSOR-TURBINE MATCH

$$T_{T4}/T_{T2} = 2.0$$

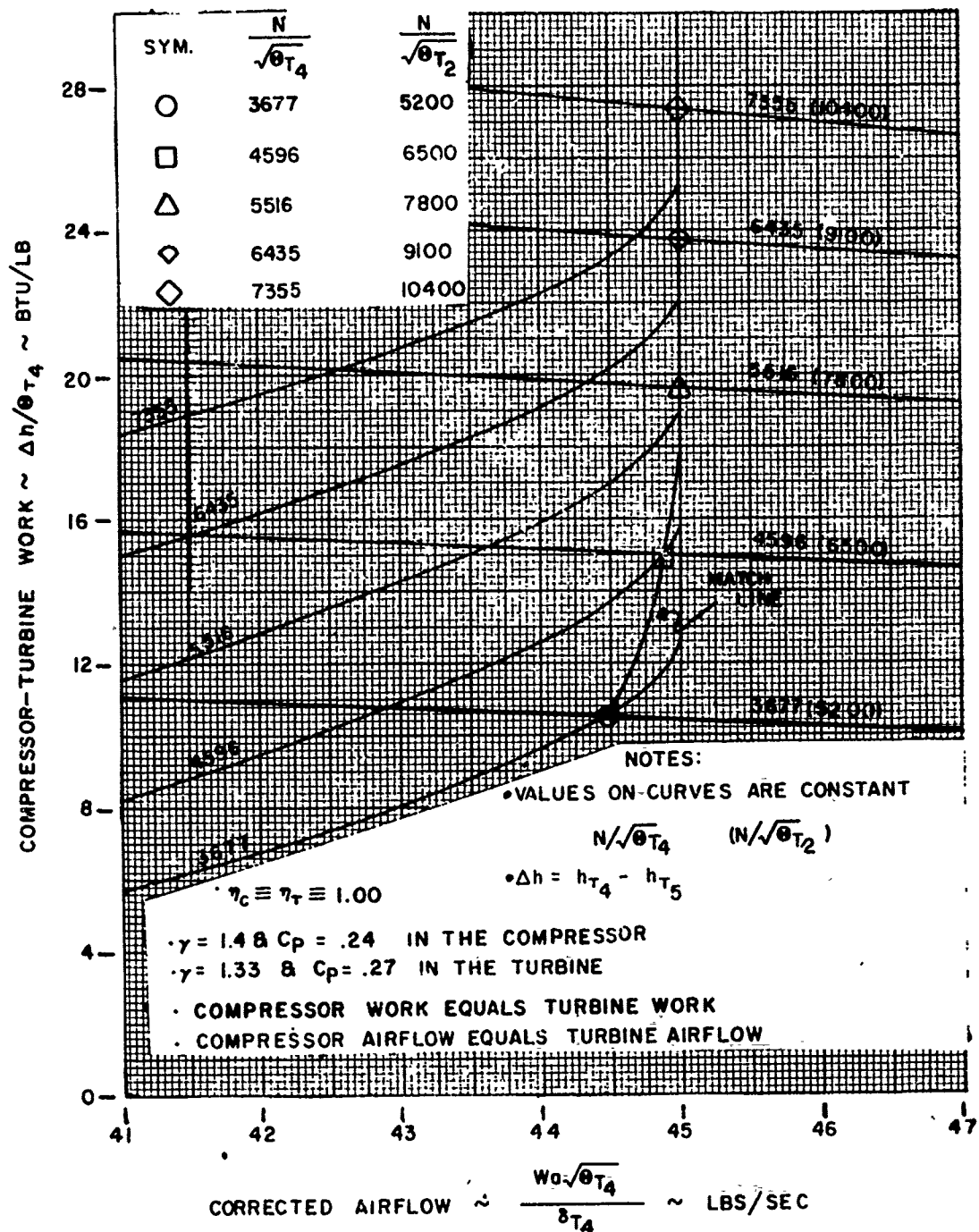


FIGURE 3.1a

COMPRESSOR-TURBINE MATCH

$$T_{T4}/T_{T2} = 2.5$$

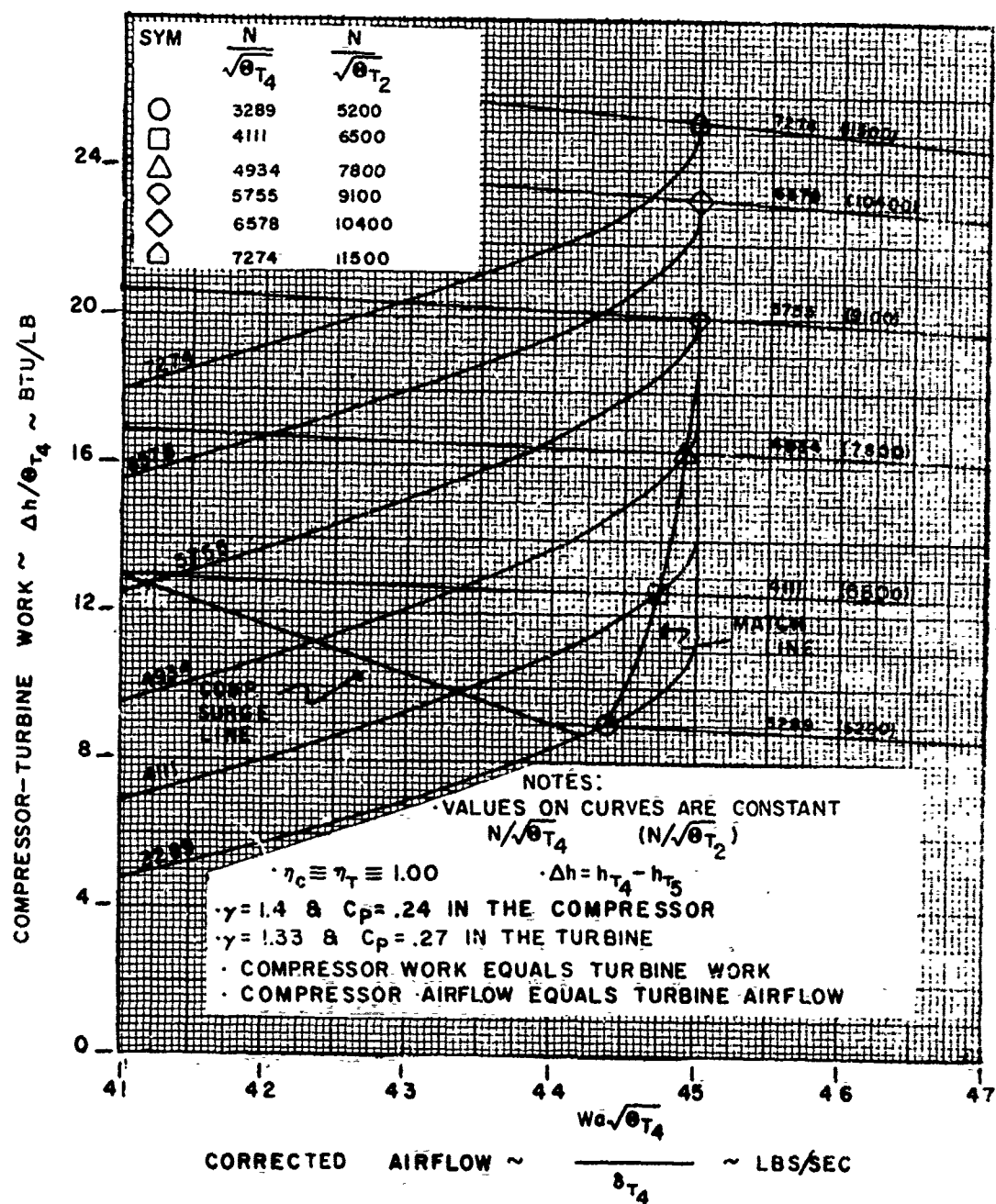


FIGURE 3.1b

COMPRESSOR-TURBINE MATCH

$$T_{T4} / T_{T2} = 3.0$$

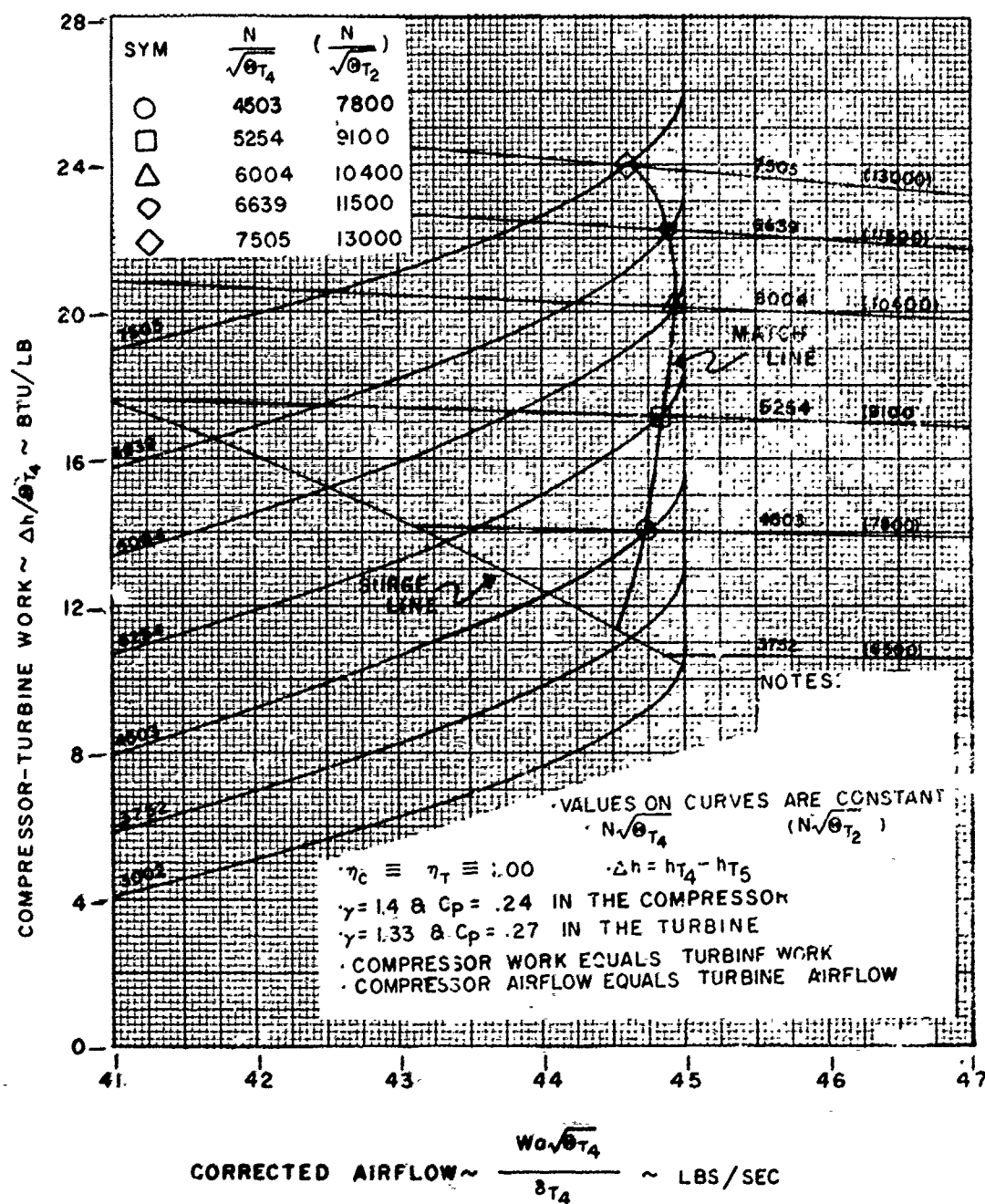


FIGURE 3.1c

COMPRESSOR-TURBINE MATCH

$$\tau_{T4}/\tau_{T2} = 3.5$$

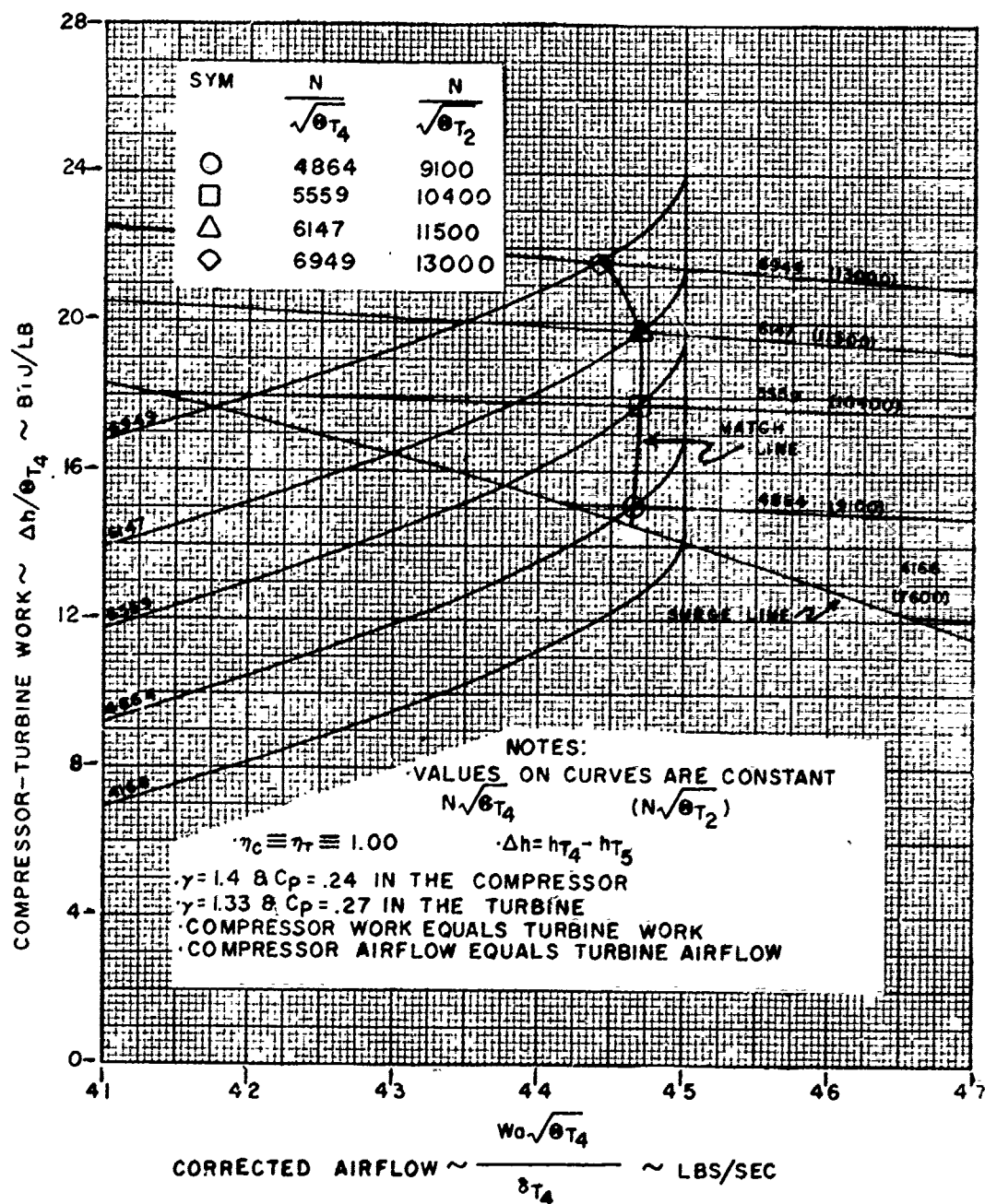


FIGURE 3.1d

COMPRESSOR-TURBINE MATCH

$$\tau_{T4} / \tau_{T2} = 4.0$$

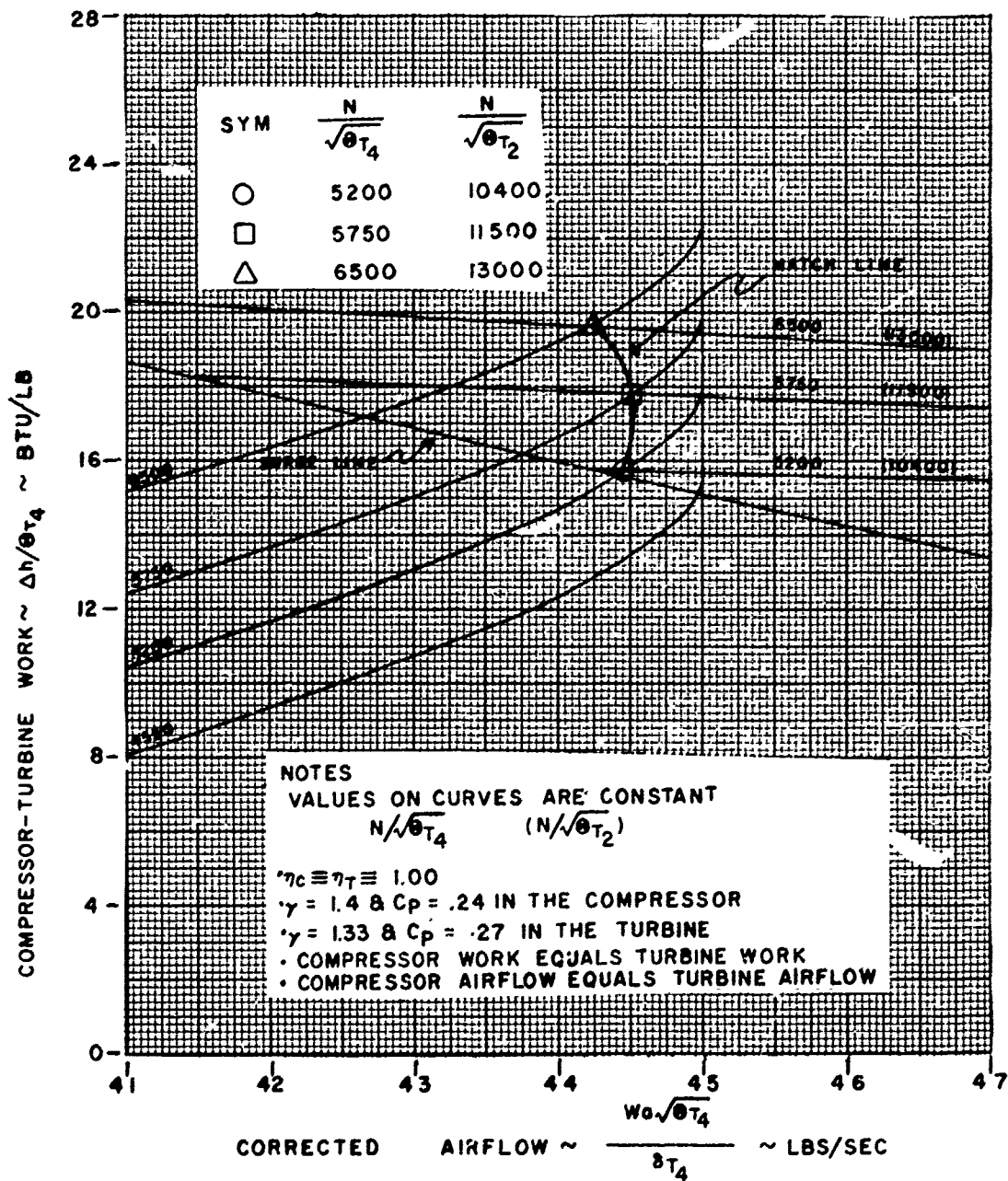


FIGURE 3.1e

COMPRESSOR-TURBINE MATCH

$$T_{T4}/T_{T2} = 4.5$$

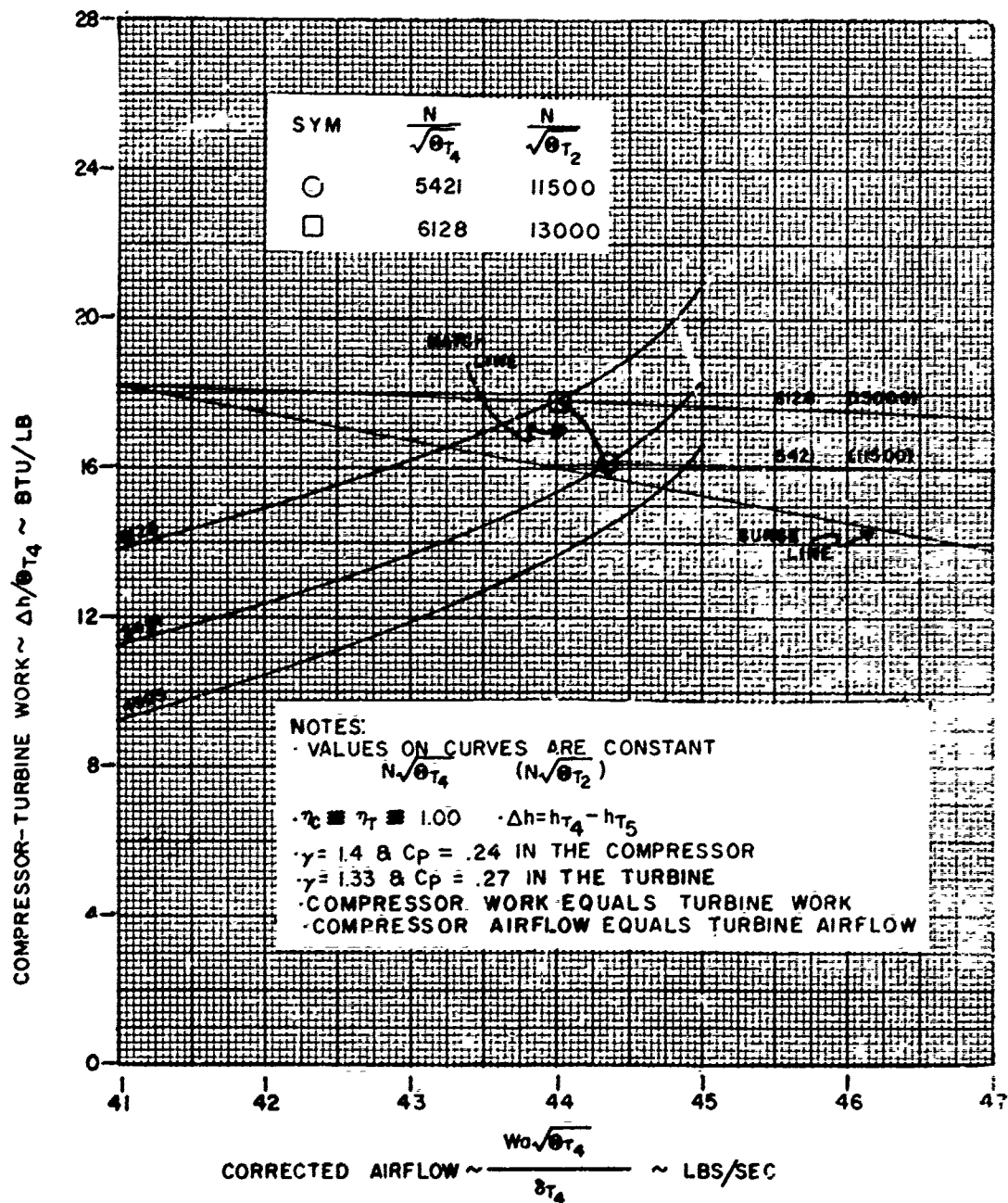


FIGURE 3.1f

then

$$\left(\frac{W_a \sqrt{\theta_{T_4}}}{\delta_{T_4}} \right)_{\text{TURB}} + \left(\frac{W_a \sqrt{\theta_{T_4}}}{\delta_{T_4}} \right)_{\text{BLEED}} = \left(\frac{W_a \sqrt{\theta_{T_4}}}{\delta_{T_4}} \right)_{\text{COMP}}$$

Increasing bleed airflow will cause the transformed compressor map to move to the left on the turbine map.

Similarly for accessory loads.

$$\frac{W_{\text{TURB}}}{\theta_{T_4}} = \frac{\Delta \dot{h}_{\text{TURB}}}{\theta_{T_4}} = \frac{W_c}{\theta_{T_4}} + \frac{W_{\text{loads}}}{\theta_{T_4}}$$

and an increase in accessory loads will move the transformed compressor map up on the turbine map.

Each of the match lines of Figure 3.1 is then plotted on the compressor map as shown in Figure 3.2. The calculation procedure required is the reverse of that outlined above.

GAS GENERATOR - NOZZLE MATCH

After the gas generator is matched, the next step in the **match** process is to add a nozzle and determine where the entire engine will function as a unit. The procedure followed is to transform the matched gas generator into nozzle referred parameters and superimpose the matched gas generator (Figure 3.2) on the nozzle map (Figure 2.39). To do this

1. Select a value of $N/\sqrt{\theta_{T_2}}$ on the compressor map.
2. Select corresponding value of $\frac{W_a \sqrt{\theta_{T_2}}}{\delta_{T_2}}$ and P_{T_3}/P_{T_2}
3. Calculate

$$\frac{W_a \sqrt{\theta_{T_4}}}{\delta_{T_4}} = \left(\frac{W_a \sqrt{\theta_{T_2}}}{\delta_{T_2}} \right) \left(\frac{P_{T_2}}{P_{T_4}} \right) \sqrt{\frac{T_{T_4}}{T_{T_2}}}$$

(If $\eta_b^* = 0$, $P_{T_2}/P_{T_4} = P_{T_2}/P_{T_3}$, otherwise additional knowledge about the combustor is required).

COMPRESSOR-TURBINE MATCH (COMPRESSOR MAP)

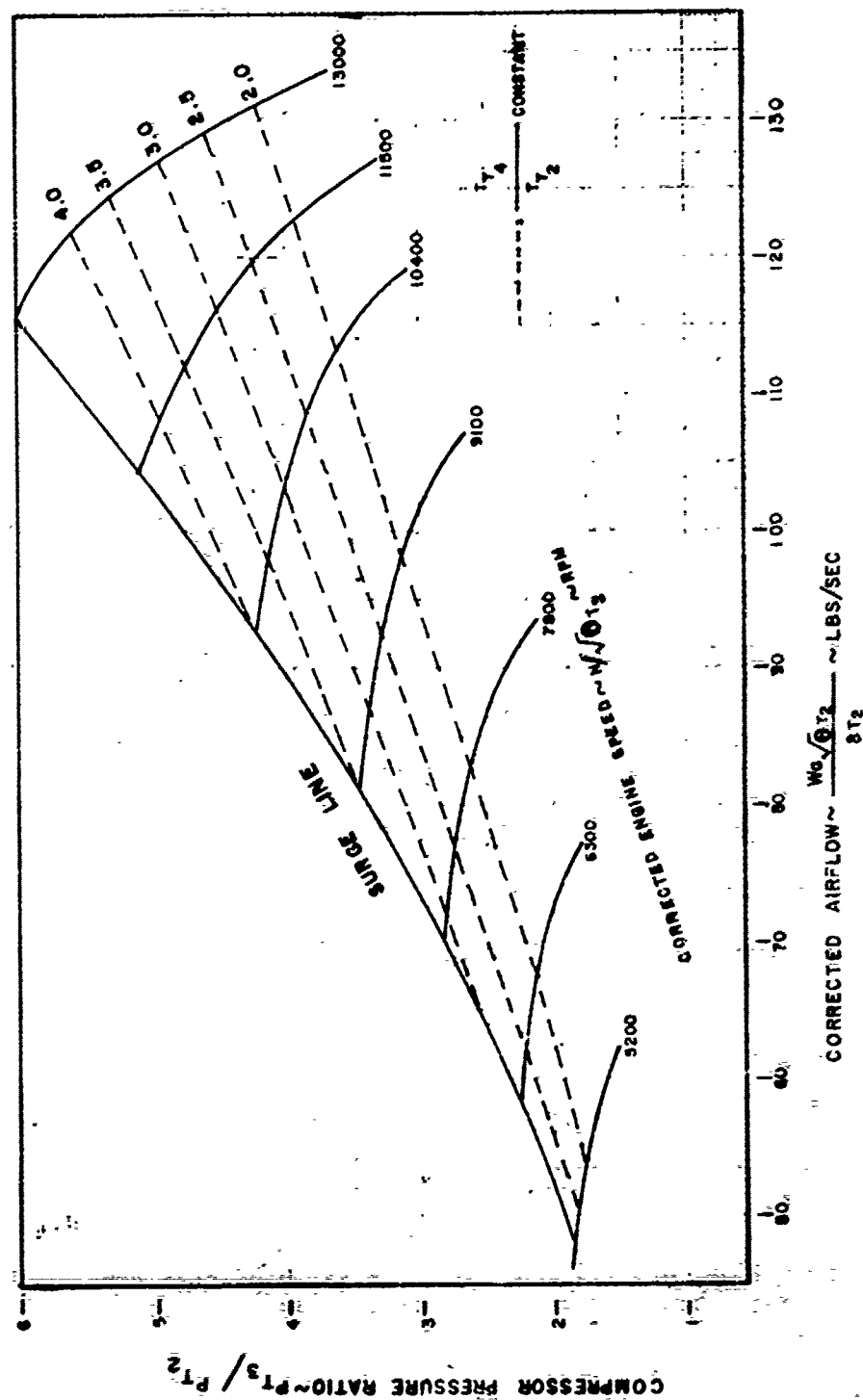


FIGURE 3.2

4. Calculate

$$\frac{h_{T_4} - h_{T_5}}{T_{T_4} \cdot \eta_T} = \frac{C_p}{\eta_c} \frac{T_{T_2}}{T_{T_4}} \left[\left(\frac{P_{T_3}}{P_{T_2}} \right)^{\frac{\gamma-1}{\gamma}} - 1 \right]$$

5. Calculate

$$\frac{P_{T_5}}{P_{T_4}} = \left[1 - \left(\frac{h_{T_4} - h_{T_5}}{C_p T_{T_4} \eta_T} \right) \right]^{\frac{\gamma}{\gamma-1}}$$

6. Calculate

$$\frac{T_{T_5}}{T_{T_4}} = 1 - \left(\frac{h_{T_4} - h_{T_5}}{C_p T_{T_4}} \right)$$

7. Calculate

$$\frac{W_a \sqrt{\theta_{T_9}}}{\delta_{T_9}} = \frac{W_a \sqrt{\theta_{T_4}}}{\delta_{T_4}} \sqrt{\frac{T_{T_4}}{T_{T_9}}} \left(\frac{P_{T_4}}{P_{T_9}} \right)$$

(If the tailpipe is isentropic $T_{T_4}/T_{T_9} = T_{T_4}/T_{T_5}$

and $P_{T_4}/P_{T_9} = P_{T_4}/P_{T_5}$, otherwise additional knowledge about the tailpipe is required.)

8. Calculate

$$\frac{P_{T_9}}{P_{T_2}} = \left(\frac{P_{T_4}}{P_{T_2}} \right) \left(\frac{P_{T_9}}{P_{T_4}} \right)$$

(If $\eta_b^* = 0$, $P_{T_4}/P_{T_2} = P_{T_3}/P_{T_2}$. If the tailpipe is frictionless $P_{T_9}/P_{T_4} = P_{T_5}/P_{T_4}$.

Flight Mach number and inlet recovery are required to determine P_{T_2} .)

9. Repeat the process for all desired values of $N/\sqrt{\theta_{T_2}}$.

For each value of $N/\sqrt{\theta_{T_2}}$ the compressor airflow and pressure ratio transformed to nozzle referenced conditions are superimposed on the nozzle map (Figure 2.39). Figure 3.3 shows the results for an exit area of 1.5 square feet if the nozzle is a converging nozzle or a throat area of 1.5 square feet if it is a C-D nozzle. The intersection of the compressor-turbine match lines with the nozzle curve represents the operating line of the engine. For a matched compressor-turbine, the operating line depends only on the exit area for a converging nozzle or throat area for a C-D nozzle.

By calculating in reverse order using the outline given for the compressor-turbine-nozzle match, the operating line is placed on the compressor map as shown in Figure 3.4.

The following useful curves can be determined from Figures 3.3 and 3.4 for the operating line.

From Figure 3.3

• Figure 3.5 $N/\sqrt{\theta_{T_2}}$ vs. P_{T_9}/P_{T_2} (Engine Pressure Ratio - EPR)

From Figure 3.4

• Figure 3.6 $N/\sqrt{\theta_{T_2}}$ vs. P_{T_3}/P_{T_2}

• Figure 3.7 $N/\sqrt{\theta_{T_2}}$ vs. $\frac{W_a \sqrt{\theta_{T_2}}}{\delta_{T_2}}$

• Figure 3.8 $N/\sqrt{\theta_{T_2}}$ vs. T_{T_4}/θ_{T_2}

$$\text{Note : } \frac{T_{T_4}}{\theta_{T_2}} = \left(\frac{T_{T_4}}{T_{T_2}} \right) \left(T_{SLS} \right)$$

From Figures 3.6 and 3.8

• Figure 3.9 $N/\sqrt{\theta_{T_2}}$ vs. T_{T_5}/θ_{T_2}

$$\text{Note : } (h_{T_4} - h_{T_5}) = \dot{W}_T = \dot{W}_c = C_p T_{T_2} \left[\left(\frac{P_{T_3}}{P_{T_2}} \right)^{\frac{\gamma-1}{\gamma}} - 1 \right]$$

$$\frac{T_{T_5}}{\theta_{T_2}} = \frac{T_{T_4}}{\theta_{T_2}} - T_{SLS} \left[\left(\frac{P_{T_3}}{P_{T_2}} \right)^{\frac{\gamma-1}{\gamma}} - 1 \right]$$

COMPRESSOR-TURBINE-NOZZLE MATCH

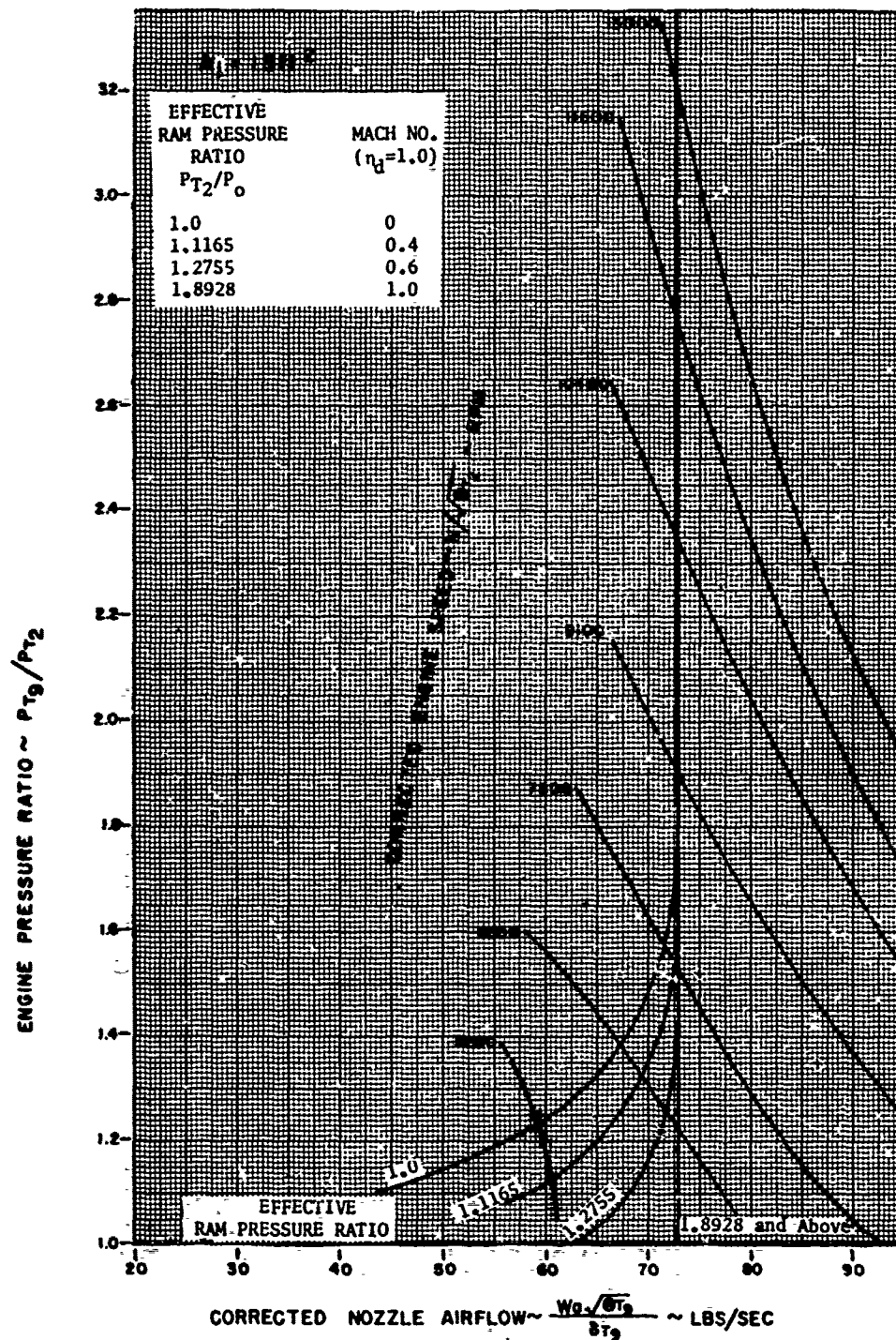
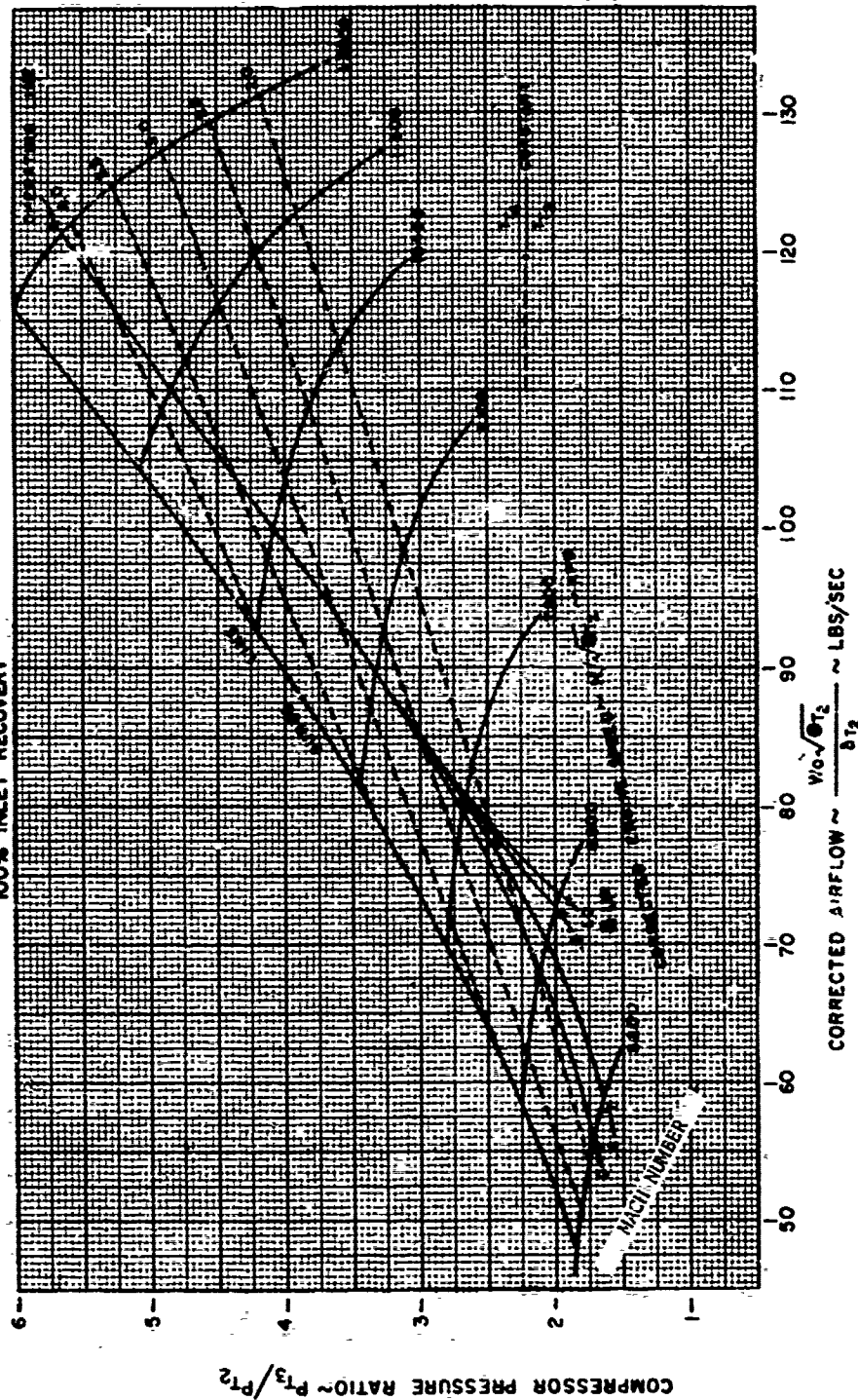


FIGURE 3.5

GENERALIZED ENGINE PERFORMANCE

$A_1 = 1.511^2$
100% INLET RECOVERY



4) 100% INLET RECOVERY

From Figures 3.7, 3.8, and 3.9

• Figure 3.10 $\frac{W_f}{\sqrt{\theta_{T_2}} \delta_{T_2}}$ vs. $N/\sqrt{\theta_{T_2}}$

Note:
$$W_f = \frac{W_a C_p (T_{T_4} - T_{T_3})}{\eta_b H.V.}$$

$$\frac{W_f \sqrt{\theta_{T_2}}}{\theta_{T_2} \delta_{T_2}} = \frac{\dot{W}_a \sqrt{\theta_{T_2}}}{\delta_{T_2} \eta_b} \left[\frac{T_{T_4}}{\theta_{T_2}} - \frac{T_{T_3}}{\theta_{T_2}} \right] \frac{C_p}{H.V.}$$

and

$$\frac{W_f}{\sqrt{\theta_{T_2}} \delta_{T_2}} = \frac{\dot{W}_a \sqrt{\theta_{T_2}}}{\eta_b \delta_{T_2}} \left[\frac{T_{T_4}}{\theta_{T_2}} - \left(\frac{P_{T_3}}{P_{T_2}} \right)^{\frac{\gamma-1}{\gamma}} T_{SLS} \right]$$

(If $\eta_c = 1.0$)

Figures 3.5 through 3.10 are called the gas generator curves (GGC).

ENGINE PRESSURE RATIO

100% INLET RECOVERY

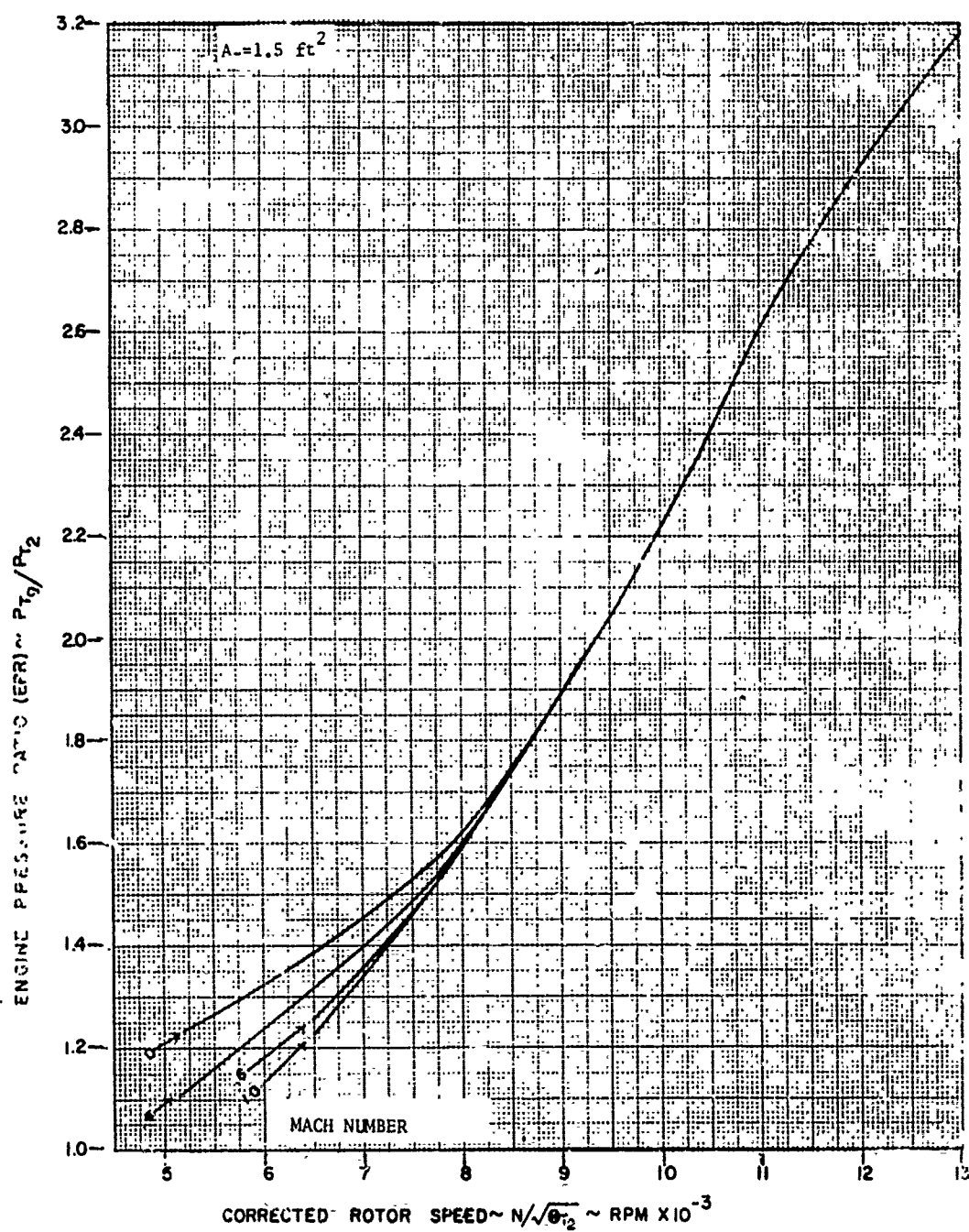


FIGURE 3.5

COMPRESSOR PRESSURE RATIO

100% INLET RECOVERY

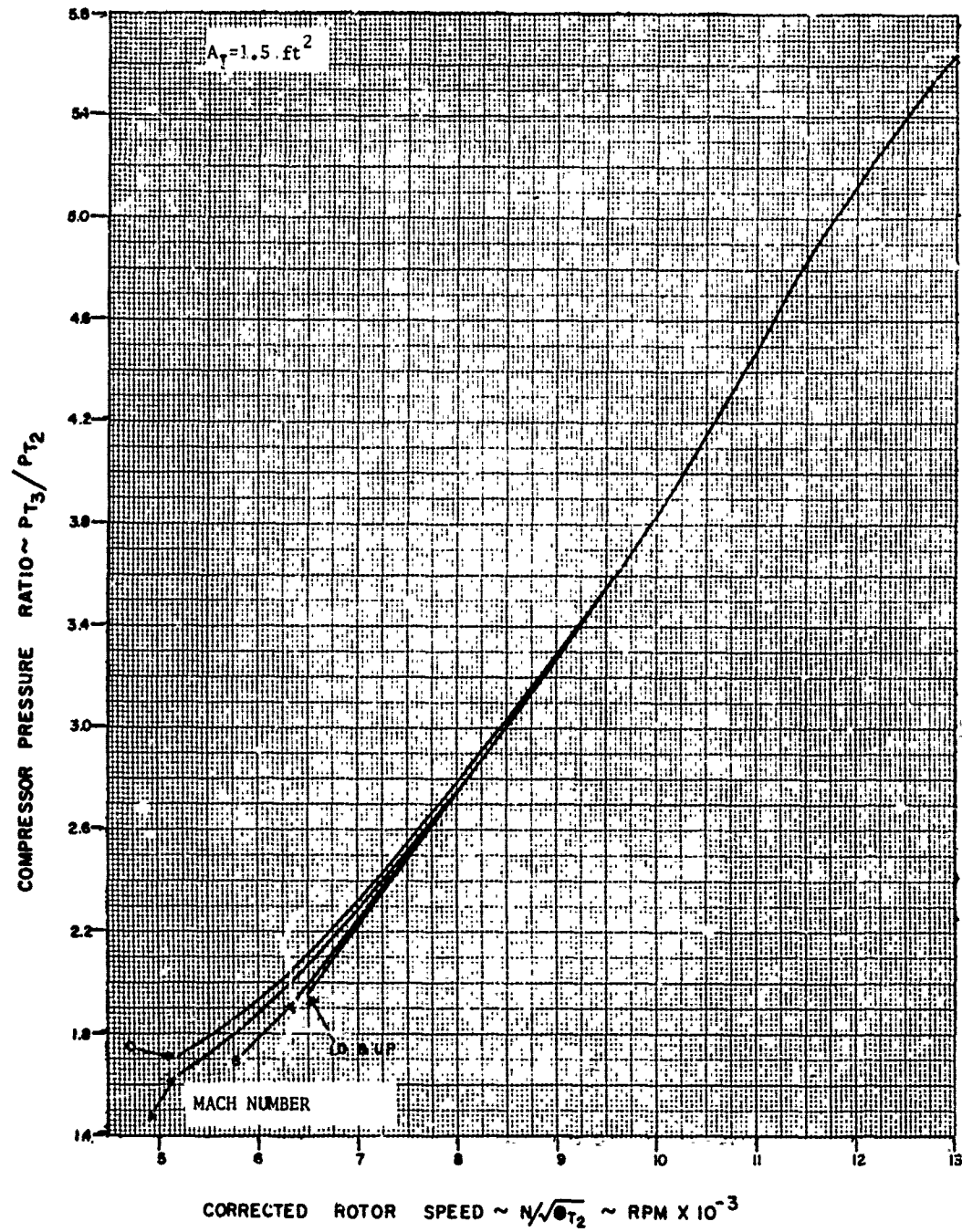


FIGURE 3.6

ENGINE AIRFLOW

100% INLET RECOVERY

$$A_T = 1.5 \text{ ft}^2$$

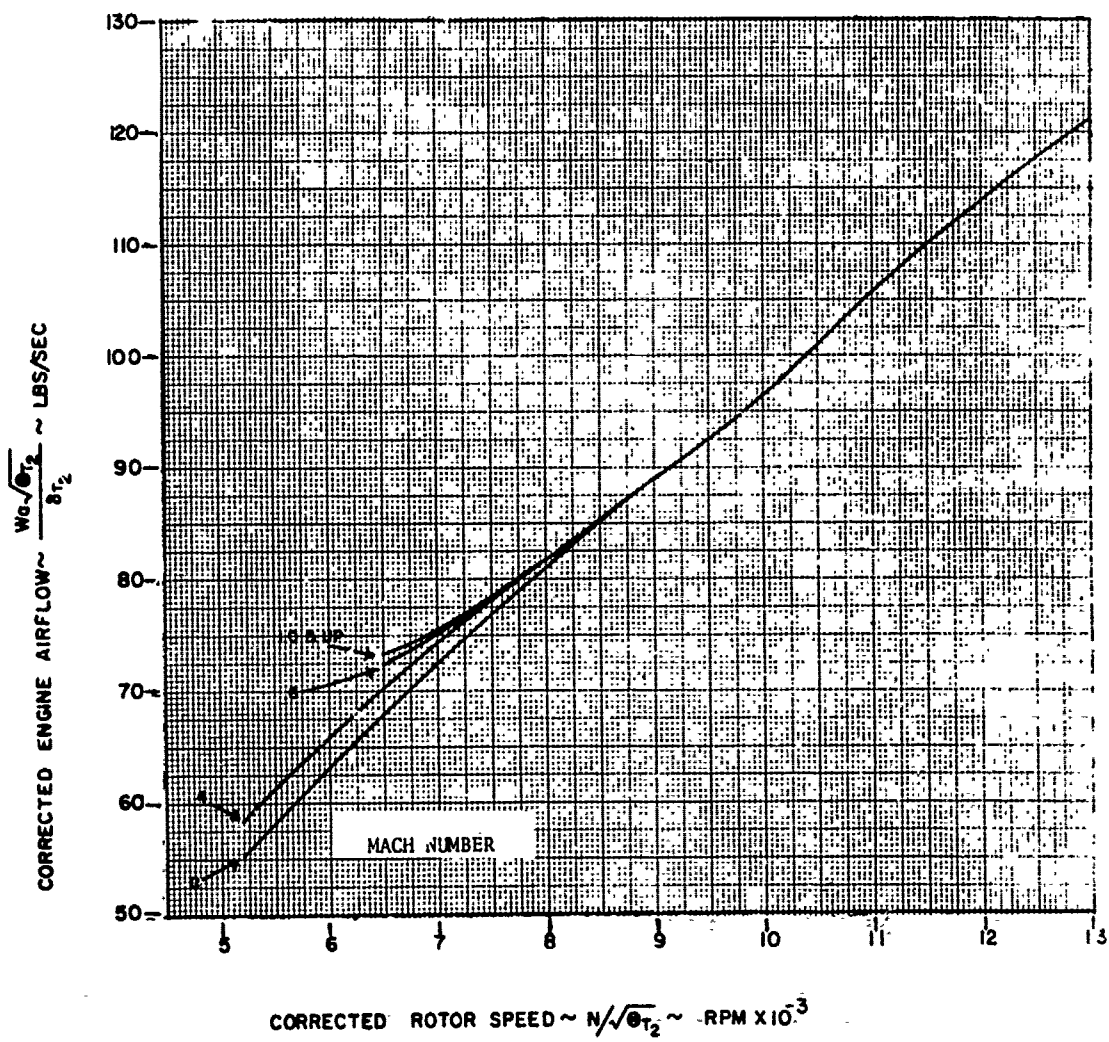


FIGURE 3-7

TURBINE INLET TEMPERATURE

100% INLET RECOVERY

$$A_T = 1.5 \text{ ft}^2$$

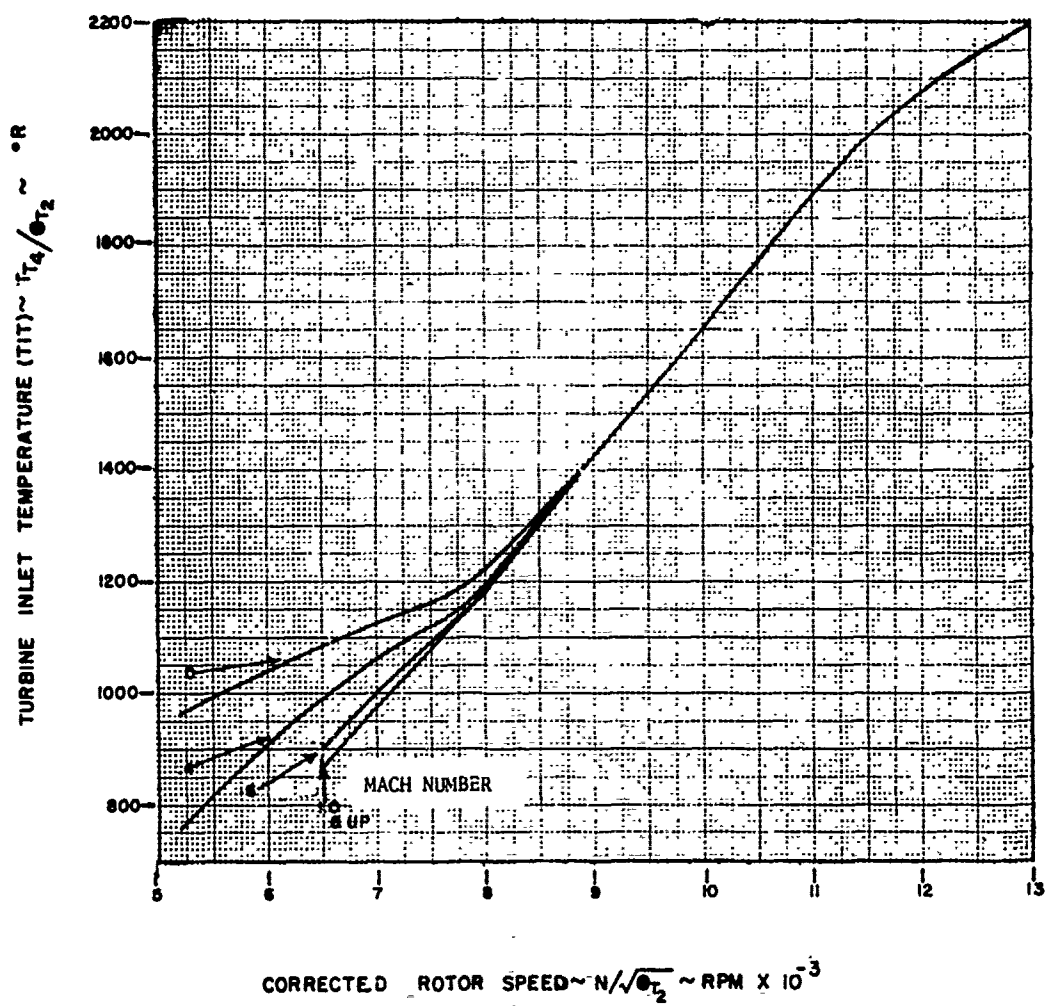


FIGURE 3.8

TAILPIPE TEMPERATURE

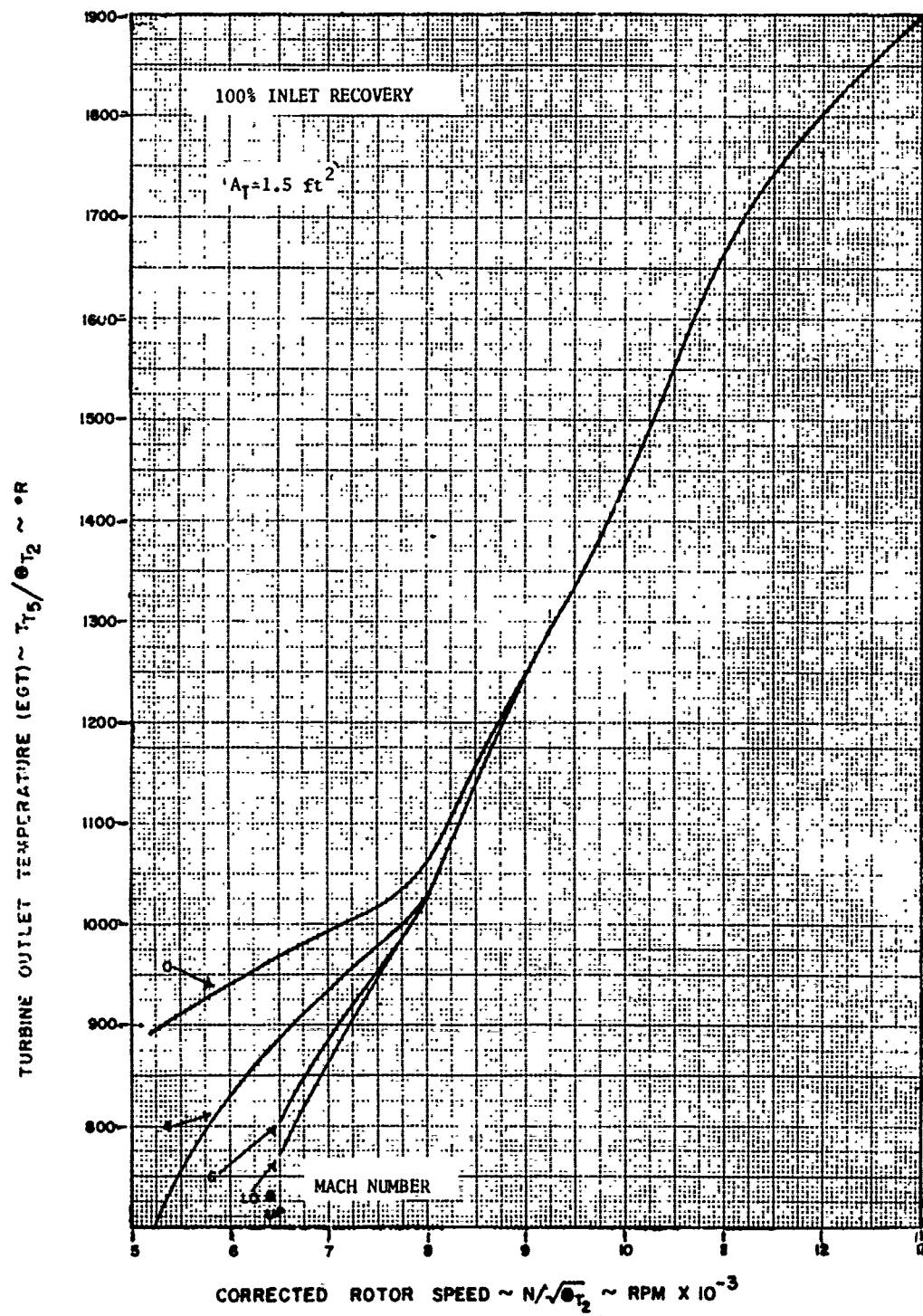


FIGURE 3.9

ENGINE FUEL FLOW

100% INLET RECOVERY

$$A_T = 1.5 \text{ ft}^2$$

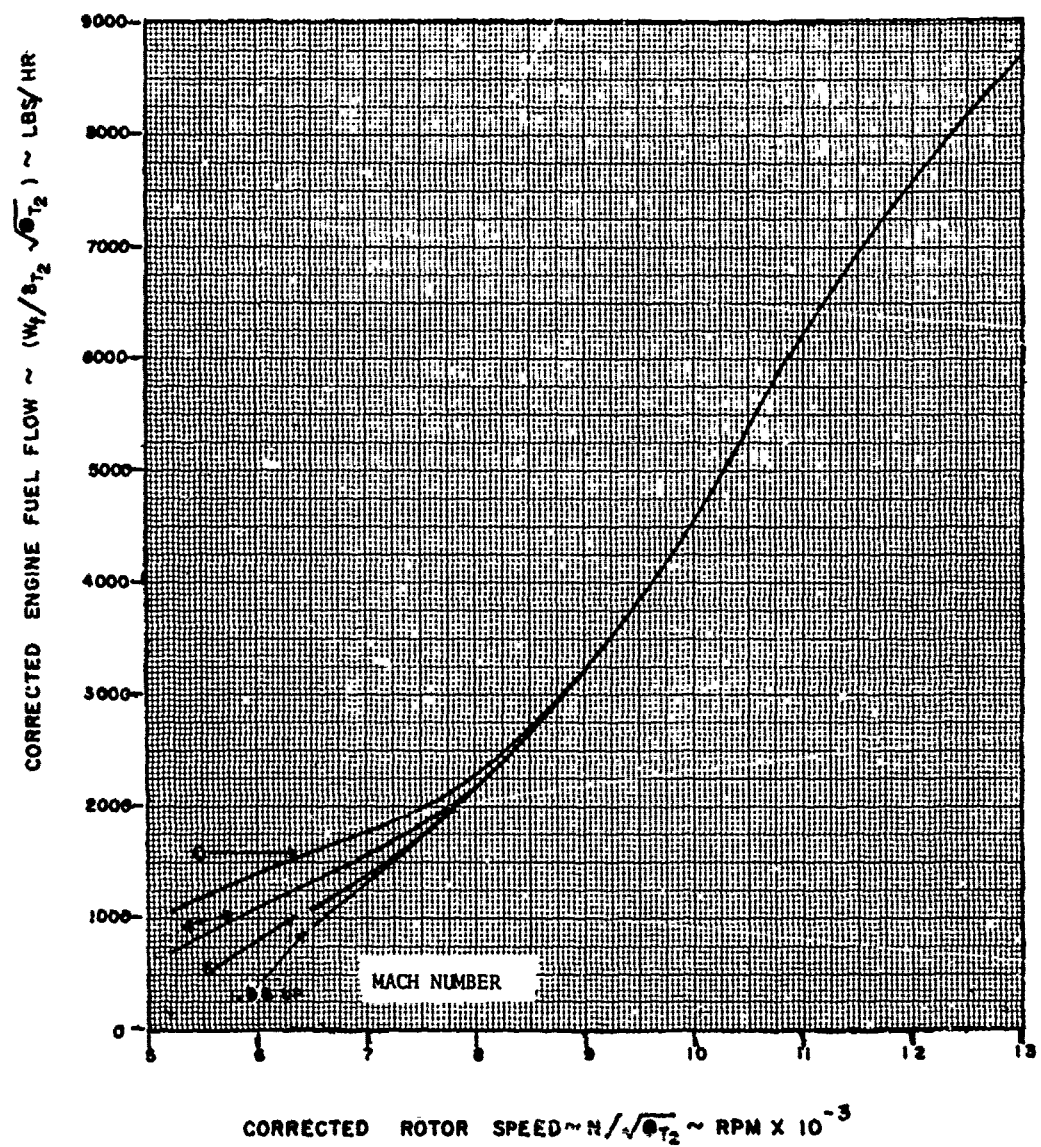


FIGURE 3.10

3.2 ENGINE PERFORMANCE

In Section 3.1 engine parameters have been shown to be a function of corrected rotor speed ($N/\sqrt{\theta_{T_2}}$), a fact that is of significant usefulness. Additionally it should be noted that with the possible exception of air flow and turbine inlet temperature, all parameters are measureable in flight.

At this point it is well to mention assumptions made during the match and assumptions concerning the fluid properties. Worthy of mention are:

1. Steady Flow - The engine match and gas generator curves were obtained during steady state operation. During testing, cruise flight conditions are definitely steady state, and climb, descent and accelerating flight at constant throttle setting are for practical purposes steady state conditions. During non-steady state conditions (engine accelerations, etc.) the engine match will be different and other gas generator curves would have to be established.
2. Nozzle Size - The engine was matched for a fixed nozzle throat area. Changes in nozzle size will change the operating line, smaller nozzle throat areas moving the operating line towards the stall line and larger nozzle throat areas moving the operating line away from the stall line. This effect is realized by considering Figures 3.3 and 2.39a.
3. Internal Engine Geometry - If variable stators or bleed valves are used in the compressor, (e.g., to relieve stall problems) the compressor map will vary as stator or bleed valve positions vary, and hence the match line will vary. If stators and bleed valves are scheduled with $N/\sqrt{\theta_{T_2}}$ then geometry effects would be self contained on a single compressor map and generalization of the gas generator curves should be obtained. Depending on the engine, it may be desirable to measure engine geometry during flight test.
4. Bleeds or Power Extraction - The bleeds referred to here are those required for anti-ice, pressurization, etc. From an analytical point of view, the gas generator curves can be developed for the no bleed condition with correction curves established enabling adjustments to be made for various air bleeds. If the GGC are developed from test, the bleed configuration must be known. Usually it is difficult to measure bleed flow accurately and to install the instrumentation required to do so. If this is the case, the extremes of bleed extraction can be tested from which the worst effect(s) determined. A similar effort is required for power extraction.

5. Component Efficiencies - It was shown, during the matching procedure, where the various component efficiencies are accounted for. If the techniques are reviewed, it will be seen that the matching procedure is iterative, when accounting for component efficiencies. The nozzle efficiency was not mentioned during the match process. The nozzle airflow curve, Figure 2.39, calculated the ideal gas flow for a given nozzle throat area (see Section 2.5). Due to the boundary layer and nozzle expansion, it is difficult to establish the effective area which will produce the desired match. Rather than attempt to manufacture a nozzle with an area calculated to yield the correct match, convergent nozzles are sometimes undersized and "cut back" to produce the correct match. C-D nozzles generally have throat areas that are adjustable so as to produce the desired operating line.

To determine the gas generator curves from test, no efficiencies need be determined.

6. Ideal Gas - An ideal gas is one which obeys the perfect gas law. This also implies that C_p is constant. The match was established using this assumption. The effect of a variable C_p on the GGC can be shown to be rather insignificant especially if the equations, which were developed assuming constant C_p , are used with a C_p based on the local temperature. To develop the curves from test, the effect of a variable C_p is inherent in the data.
7. Reynolds Number - The GGC are based on a unique compressor map. As mentioned in Section 2.2 the performance of the compressor will change as Reynolds number changes. The effects on compressor map will be determined for these conditions and applied as corrections; thus when analytically determining the GGC, altitude must be noted. (Usually the effects occur at altitudes above 40,000 feet.) Hence during flight test, the data should be coded for altitude.

The generalization of the engine performance can now be appreciated. A review of the assumptions made gives insight into how the GGC can be utilized. The operating line is established by the engine manufacturer in an attempt to yield the best overall operating conditions. Once established for a given engine design, each engine of that design is produced and adjusted by using nozzle area to repeat the desired operating line. Thus when an engine is installed in the aircraft, the gas generator curves are determined and any difference that exists from the uninstalled to the installed condition is the "installation effect" (bleeds, inlet, etc.). The magnitude of the shift is critical and must be evaluated to determine the extent of any off design operation. It is obvious now, why engine manufacturers limit the power and bleed take-offs. If the installation causes severe problems the cause must be determined and corrected. The

gas generator curves are the keys in determining installation effects and analysis of possible corrective measures.

Once the installation is complete and the installed GGC are established for each engine, any shift as a function of time gives warnings that some component of the engine has changed and if severe enough corrective action is warranted. Thus, the GGC can be looked upon as engine health curves. All engine performance that is utilized to establish aircraft performance should be evaluated by comparing it to a set of previously established GGC for that engine. If a set of data falls either high or low on these curves, the validity of thrust or fuel consumption data may be questionable.

3.3 THRUST DETERMINATION

The preceeding discussion has focused on how engine performance generalizes. The GGC represent the thermodynamic characteristics of a particular engine. Of practical use is the determination of net thrust at some particular altitude, Mach number, and throttle setting. As an example, the maximum thrust determination for an engine governed to a constant speed (N_{max}) will be described. Altitude and Mach number must be specified. To start, calculate the governing corrected rotor speed ($N_{max}/\sqrt{\theta_{T2}}$) where θ_{T2} is determined from a specified altitude and Mach number for which the thrust is desired. Enter a curve similar to Figure 3.7 for the particular engine to get the corrected airflow. The inlet recovery, previously determined and generalized as shown typically on Figure 1.9a, in conjunction with altitude and Mach number is used to compute the actual airflow from the corrected airflow. With this, the ram drag can be determined.

The nozzle pressure ratio is calculated from altitude, Mach number, and engine pressure ratio using a curve similar to Figure 3.5. The theoretical gross thrust is obtained by using the appropriate equation depending on the nozzle (convergent or C-D) and pressure ratio. Multiplying the result by the gross thrust coefficient, yields the actual gross thrust. Subtracting the ram drag from the gross thrust yields the net thrust.

The only basic information required is a knowledge of how the engine is controlled. For the engine in the above example, the fuel control simply maintained a constant engine speed. Some engines, however, may be governed in maximum power by a speed biased by total inlet temperature. Thus, for any given total inlet temperature, the fuel control will set and maintain the scheduled speed. Once the fuel control characteristics are known, it is an easy process to combine them with the GGC to get the engine performance.

3.4 AFTERBURNER OPERATION

Once the engine is designed any modification to the engine should be considered in light of the effect it will have on the GGC. An obvious modification is the installation of an afterburner. For isentropic non-afterburning operation

$$\frac{W_a \sqrt{\theta_{T_5}}}{\delta_{T_5}} = \frac{W_a \sqrt{\theta_{T_9}}}{\delta_{T_9}} = \frac{W_a \sqrt{\theta_{T_{10}}}}{\delta_{T_{10}}}$$

For A/B operation, it is desired to keep $\frac{W_a \sqrt{\theta_{T_5}}}{\delta_{T_5}}$ constant since the basic operating line of the engine would otherwise change. When the A/B is lit, the engine is generally operating at high power settings and M_{10} is unity for a convergent nozzle. Ideal A/B operation is with $P_{T_5} = P_{T_9} = P_{T_{10}}$. There is a rise in total temperature producing $T_{T_5} < T_{T_9} = T_{T_{10}}$. Since the nozzle is choked and the total pressure is constant, the airflow must decrease because $(T_{T_{10}})_{A/B} > (T_{T_{10}})_{NON A/B}$. This decrease in airflow will cause $\frac{W_a \sqrt{\theta_{T_5}}}{\delta_{T_5}}$ to decrease changing the match of the engine. If the engine

speed is held constant, the operating line may be driven past stall. To avoid this problem, the nozzle area must increase by:

$$\frac{(A_{10})_{A/B}}{(A_{10})_{NON A/B}} = \sqrt{\frac{T_{T_{10} A/B}}{T_{T_{10} NON A/B}}} = \sqrt{\frac{T_{T_9}}{T_{T_5}}}$$

Actually $(A_{10})_{A/B}$ must be slightly larger than that given by the above equation because of the A/B fuel flow. A similar result will occur if the A/B is operated in an engine installed with a C-D nozzle. The only change in the analysis is that $A_{T A/B} > A_{T NON A/B}$. Note that the divergence area ratio A_{10}/A_T remains constant for complete expansion because $(P_{T_9}/P_{T_{10}})_{A/B}$ equals $P_{T_9}/P_{T_{10}})_{NON A/B}$.

Since the nozzle area was shown to be an extremely sensitive parameter governing the match of the engine, a continuously modulating nozzle may be required in A/B to keep the match constant. Measurement of T_{T_9} is not possible, due to the high temperature. The method normally employed is to monitor compressor pressure ratio (or engine pressure ratio) and corrected engine speed. A cam is installed in the fuel control representing the desired operating line. If the sensed pressure ratio is greater than desired for a given corrected engine speed (see Figures 3.5 and 3.6) the fuel control will increase the nozzle area until the error is nulled.

Conversely, if the sensed pressure ratio is less, the fuel control will decrease the area. Any problem that arises in A/B usually can be traced to the fuel control not fulfilling its function of maintaining the engine operating line.